



**Universiteit Utrecht**

INSTITUTE FOR THEORETICAL PHYSICS

MASTER THESIS

---

# Black Hole Phase Transitions and Magnetic AdS Black Branes in $N=2$ Supergravity

---

*Author:*  
N.W.M. Plantz

*Supervisor:*  
prof. dr. S.J.G. Vandoren

*A thesis submitted in partial fulfilment of the requirements  
for the degree of Master of Science*

October 2014

# Abstract

The first part of this thesis will focus on black hole phase transitions. Using the Hawking-Page phase transition as a starting point, we obtain the framework that can generally be applied to the study of black hole phase transitions. We will review the phase structure of different black hole solutions, pointing out the influence of the addition of new fields to the theory. Furthermore, we study the similarities between the phase structure of Minkowski spacetimes in a finite cavity and that of asymptotically anti-de Sitter theories. Finally, we point out the influence of the black hole topology on the phase diagram. Using the knowledge of the black hole solutions in the first part, the second part describes the search for a new magnetic AdS black brane solution in  $N = 2$  supergravity, generalizing the one that has recently been found. After a review of this known solution, we will show the difficulties which arise in finding an analytical solution. We then proceed describe asymptotic magnetic black brane solutions, which can be used as a starting point for the method used to find numerical solutions.

# Contents

<b>Introduction</b>	<b>1</b>
<b>1 General Theory</b>	<b>2</b>
1.1 Anti-de Sitter spacetime . . . . .	2
1.2 Black hole thermodynamics . . . . .	3
1.3 Supergravity . . . . .	5
1.3.1 Supersymmetry . . . . .	5
1.3.2 N=2 supergravity . . . . .	5
1.3.3 The target manifold . . . . .	6
1.3.4 The N=2 supergravity action . . . . .	7
<b>2 The Hawking-Page Phase Transition</b>	<b>9</b>
2.1 Black hole phase transitions: a brief history . . . . .	9
2.2 The phases . . . . .	9
2.3 Thermal stability of the phases . . . . .	12
2.4 The phase transition . . . . .	13
2.5 Summary . . . . .	16
<b>3 Charged Black Hole Phase Transitions</b>	<b>18</b>
3.1 The black hole solution . . . . .	19
3.2 The grand canonical ensemble . . . . .	20
3.2.1 The phases . . . . .	20
3.2.2 Thermal stability of the phases . . . . .	22
3.2.3 The phase diagram . . . . .	23
3.3 The canonical ensemble . . . . .	25
3.3.1 The phases . . . . .	25
3.3.2 Thermal stability of the phases . . . . .	27
3.3.3 The phase diagram . . . . .	29
3.4 Summary . . . . .	32
<b>4 Black Hole Phase Transitions in a Minkowski Box</b>	<b>34</b>
4.1 The York formalism . . . . .	35
4.2 The black hole solutions . . . . .	37
4.3 The Schwarzschild black hole . . . . .	38

4.4	The Reissner-Nordström black hole in the grand canonical ensemble . . . . .	42
4.4.1	The stable phases . . . . .	42
4.4.2	The phase diagram . . . . .	44
4.5	The Reissner-Nordström black hole in the canonical ensemble . . . . .	46
4.5.1	The stable phases . . . . .	46
4.5.2	The phase diagram . . . . .	47
4.6	Summary . . . . .	51
<b>5</b>	<b>Black Brane Phase Transitions and Holographic Superconductivity</b>	<b>52</b>
5.1	Black brane solutions . . . . .	52
5.1.1	The black brane temperature . . . . .	55
5.2	The Schwarzschild black brane . . . . .	55
5.3	The grand canonical ensemble . . . . .	57
5.3.1	The phases . . . . .	57
5.3.2	The phase diagram . . . . .	58
5.4	The canonical ensemble . . . . .	58
5.4.1	The phases . . . . .	59
5.4.2	The phase diagram . . . . .	59
5.5	Summary . . . . .	60
5.6	Black brane solutions with a complex scalar field . . . . .	61
5.6.1	The phases . . . . .	62
5.6.2	The phase diagram . . . . .	64
5.7	Holographic superconductivity . . . . .	66
5.8	Summary . . . . .	68
<b>6</b>	<b>Topological Black Hole Phase Transitions</b>	<b>69</b>
6.1	The topological black hole solution . . . . .	70
6.2	Topological black hole thermodynamics . . . . .	72
6.2.1	The grand canonical ensemble . . . . .	72
6.2.2	The canonical ensemble . . . . .	75
6.3	The hyperbolic black hole . . . . .	76
6.3.1	The temperature . . . . .	76
6.3.2	The heat capacity . . . . .	77
6.3.3	The thermodynamic potentials . . . . .	77
6.4	Summary . . . . .	77
	<b>Intermission</b>	<b>80</b>
<b>7</b>	<b>Magnetic Black Holes in <math>N = 2</math> <math>D = 4</math> Supergravity</b>	<b>81</b>
7.1	The supergravity theory . . . . .	82
7.1.1	The equations of motion . . . . .	82
7.2	The 1/4 BPS solution . . . . .	83
7.3	Constant scalars . . . . .	84
7.4	The deformed BPS solution . . . . .	85
7.5	Searching for a new analytical solution . . . . .	86

*CONTENTS*

iv

7.5.1	Small deformations of the known solution . . . . .	86
7.5.2	A new solution? . . . . .	87
7.5.3	Asymptotic solutions . . . . .	90
7.6	Summary . . . . .	92
<b>Conclusion and Outlook</b>		<b>93</b>
<b>A Mass in general relativity</b>		<b>95</b>
<b>B Calculation of thermodynamic potentials</b>		<b>98</b>
<b>Acknowledgements</b>		<b>104</b>

# Introduction

Ever since the AdS/CFT correspondence was conjectured [2], anti-de Sitter black hole solutions experienced a thousandfold increase of attention. The fact that Maldacena's celebrated paper on this correspondence has recently been cited for the ten thousandth time proves this. In particular, the thermodynamics of anti-de Sitter black holes received a lot of attention over the past few years.

However, the birth of black hole thermodynamics occurred long before the AdS/CFT correspondence existed. Already in 1983, the classic paper by S.W. Hawking and D.N. Page on black hole phase transitions appeared [7]. As a negative cosmological constant has a stabilizing effect on black hole solutions, this paper dealt black holes in an asymptotically anti-de Sitter spacetime. This is not a spacetime we live in, however. For this reason, subsequent papers on black hole phase transitions mainly focused on Minkowski spacetime [22] [23]. A generalization on the Hawking-Page phase transition appeared in 1999, sixteen years after Hawking's and Page's paper. This paper dealt with charged black holes in anti-de Sitter spacetime [13]. Starting around this time, the number of papers on black hole phase transitions diverged.

This thesis will at first be focused on black hole phase transitions as well. We will first investigate the framework used to describe the Hawking-Page phase transition and subsequently use this to study other types of black holes. In particular, we will review what happens when we add a charged gauge field to the theory [13]. We then quickly show that similar results can be obtained using Minkowski spacetime with a radial cut-off [22][33]. Afterwards, returning to anti-de Sitter, we consider different black hole topologies. In particular, we consider planar and hyperbolic black holes and point out the influence of the topology on their phase structure [44][43]. We also consider the addition of a complex scalar field to a black brane theory [34].

We then turn to magnetic black brane solutions in  $N = 2$  supergravity. Also supergravity anti-de Sitter solutions have gained a lot of interest since Maldacena's conjecture. Indeed, the application of AdS/CFT requires that the bulk theory can be embedded in string theory, or in particular in supergravity as a low-energy limit of string theory. We can use the same framework of black hole thermodynamics described in the first part of this thesis to study the thermodynamics of supergravity solutions. However, our goal is to first of all find a new magnetic black brane solution in  $N = 2$  supergravity. We expect that it should be possible to generalize a solution that has recently been found [47]. After explaining the search for an analytic expression for such a solution, we will discuss the possibility of a numerical solution.

# Chapter 1

## General Theory

Here we will shortly review some general concepts which are necessary to understand the rest of the thesis. This chapter will very briefly cover anti-de Sitter spacetime, black hole thermodynamics and very incomplete review of supergravity.

### 1.1 Anti-de Sitter spacetime

The  $d$ -dimensional Anti-de Sitter spacetime, often denoted by  $\text{AdS}_d$ , is a solution of the vacuum Einstein equations with a negative cosmological constant  $\Lambda$ . These equations follow from the Einstein Hilbert action

$$S = \frac{1}{16\pi} \int d^d x \sqrt{g} (R - 2\Lambda) \quad (1.1)$$

where  $g = |\det(g_{\mu\nu})|$ .

The AdS solution can be written in many different coordinate systems; here we will list the ones most commonly used. First of all, AdS spacetime is a maximally symmetric spacetime with a negative Ricci curvature and hence can be embedded in a  $d + 1$ -dimensional spacetime using the *embedding coordinates*  $\{X_1, X_2, \dots, X_{d+1}\}$  such that [1]

$$ds^2 = -dX_1^2 - dX_{d+1}^2 + \sum_{i=2}^d dX_i^2. \quad (1.2)$$

The embedding is given by a the hyperboloid

$$-X_1^2 - X_{d+1}^2 + \sum_{i=2}^d X_i^2 = -L^2. \quad (1.3)$$

As such, the quantity  $L$  is often called the *AdS radius*, related to the cosmological constant by

$$L^2 = \frac{(d-1)(d-2)}{-2\Lambda}. \quad (1.4)$$

Another coordinate system is the *global coordinate system* given by

$$ds^2 = - \left( 1 + \frac{r^2}{L^2} \right) dt^2 + \frac{dr^2}{\left( 1 + \frac{r^2}{L^2} \right)} + r^2 d\Omega_{d-2}^2, \quad (1.5)$$

where  $d\Omega_{d-2}^2$  denotes the standard spherical metric in  $d - 2$  dimensions and  $r > 0$ . These coordinates cover the entire spacetime.

Furthermore, the Poincaré coordinate system is given by

$$ds^2 = -\frac{r^2}{L^2} dt^2 + \frac{L^2}{r^2} dr^2 + \frac{r^2}{L^2} d\mathbf{x}_{d-2}^2 \quad (1.6)$$

with  $\mathbf{x}^{d-2} \in \mathbb{R}^{d-2}$ . This is also often written in terms of the coordinate  $z = 1/r$  as

$$ds^2 = \frac{L^2}{z^2} \left( -dt^2 + dr^2 + d\mathbf{x}_{d-2}^2 \right). \quad (1.7)$$

A peculiar feature in AdS is that the boundary  $r = \infty$  can be reached by lightlike geodesics in a finite coordinate time. From Eq.(1.7) it is clear that this boundary is conformally related to Minkowski spacetime in  $d - 1$  dimensions. In contrast to lightlike geodesics, timelike geodesics are confined to the spacetime and can never escape towards infinity.

When the AdS/CFT correspondence was conjectured in 1997 [2], the interest in asymptotically AdS spacetimes exploded. Even today the paper still has a huge influence on black hole physics, having recently been cited for the ten thousandth time. The AdS/CFT conjecture states that there can be a correspondence between an  $n + 1$ -dimensional asymptotically AdS classical supergravity theory and a strongly coupled conformal field theory on the  $n$ -dimensional boundary of this spacetime. As this thesis will almost exclusively focus on the AdS side of the correspondence, we refer the reader to [3] for more information.

## 1.2 Black hole thermodynamics

Arguably one of the most beautiful correspondences in theoretical physics is the analogy between black hole mechanics and thermodynamics. Before 1973, black hole physics and thermodynamics were two completely different fields in physics. At that time, black hole mechanics was described by four laws[4]:

- The surface gravity  $\kappa$  of a black hole is constant over its event horizon.
- Upon changing the area  $A$ , angular momentum  $J$  or the charge  $Q$  of a black hole, the corresponding change in the mass  $M$  is given by

$$dM = \frac{\kappa}{8\pi} dA + \Omega dJ + \Phi dQ. \quad (1.8)$$



Here,  $J$  and  $\Phi$  are related to the angular momentum and the electrostatic potential difference with infinity respectively.

- The area of a black hole never decreases.
- The surface gravity of a black hole cannot be brought to zero by only a finite number of operations.

There was no reason whatsoever to speak of quantities like temperature or entropy when dealing with the physics of black holes.

This changed in 1973, when Bekenstein published his famous paper 'Black holes and Entropy' [4]. In this paper he noticed the similarity between the above four laws and the four laws of thermodynamics. To draw this analogy, he connected the area of a black hole with the thermodynamic entropy and the surface gravity with temperature. Black hole thermodynamics was born. However, this was only meant as an analogy. Indeed: a black hole could not possibly have a nonzero temperature, for if it were in equilibrium with a body of temperature  $T$ , it would absorb the blackbody radiation emitted by this body. Since radiation cannot escape the black hole, the black hole will only absorb radiation and emit nothing, making thermodynamic equilibrium impossible.

In 1975 however, Hawking published his celebrated paper on Hawking radiation [5]. By including quantum mechanical aspects, he showed that black holes *can* radiate, thereby enabling the possibility of a black hole in thermal equilibrium. With this, the analogy described above became a real correspondence. Moreover, Hawking showed that the entropy of a black hole is given by

$$S = k_B \frac{c^3 A}{4\hbar G} \quad (1.9)$$

from which the Hawking temperature

$$T = \frac{\kappa}{2\pi} \quad (1.10)$$

followed.

Applying black hole mechanics, one often wishes to compute more thermodynamic quantities. Knowledge of the thermodynamic potential of the theory enables us to calculate all of these. In this thesis, we will often use the zero-loop approximation to calculate thermodynamic potentials. This uses the fact that the partition function can be written in the path integral formulation as

$$Z = \int \mathcal{D}\phi e^{iS[\phi]} \quad (1.11)$$

where the path integral is over all the fields in the theory, including the metric tensor. The zero loop approximation then amounts to approximating the action by its value at a classical solution. In Euclidean signature with imaginary time  $\tau = it$ , this yields

$$\beta F = -\log Z = S_E, \quad (1.12)$$

with  $S_E$  the Euclidean action.

## 1.3 Supergravity

In this section, we will give a very basic outline of supergravity in four dimensions. By no means do we intend to give the reader a thorough review of supergravity. Rather, we will try to list just enough ingredients needed to be able to understand the rest of this thesis. For a more thorough review of supergravity the reader is referred to [6].

### 1.3.1 Supersymmetry

To understand supergravity, one must first know what supersymmetry is. In general, supersymmetry relates bosons to fermions. To describe this symmetry, one uses a Grassmann parameter  $\epsilon$ . A supersymmetry transformation then transforms bosons into fermions and vice versa. The generator of such a transformation is known as a *supercharge*, which is a constant spinor  $Q_\alpha$ . These supercharges are contained in the supersymmetry algebra, which next to the supercharges also contains for example the Poincaré algebra. Representations of such an algebra are called *supermultiplets*, which contain bosons and their fermionic counterparts. The particle content of such a multiplet is exactly such that the number of bosonic degrees of freedom is equal to the number of fermionic degrees of freedom. We will see examples of such multiplets later, when we concentrate on a specific type of supergravity.

As a generalization, one can also consider *extended supersymmetry*. This just means that there are more than one different supersymmetry transformations. The supergravity theory that we consider in this thesis has two supersymmetry transformations. In this case, the theory is said to exhibit  $N = 2$  supersymmetry, with two associated supercharges  $Q_\alpha^1$  and  $Q_\alpha^2$ .

### 1.3.2 N=2 supergravity

As the above explanation used constant spinors  $Q_\alpha^i$ , the supersymmetry described there is a global symmetry. A theory of supergravity is a theory of general relativity exhibiting *local* supersymmetry. Consequently, such a theory also has gauge fields corresponding to the gauge symmetries. These gauge fields are the two *gravitinos*, which are the two fermionic counterparts of the graviton.

#### The particle content

For the purpose of understanding this thesis, the most important thing to know about  $N = 2$  supergravity is its particle content. This follows from the supermultiplets associated to the supersymmetry algebra. One can distinguish between three kinds of supermultiplets. First of all, the gauge multiplet is the one containing the graviton. Secondly, there are a number  $n_V$  of vector multiplets, containing gauge fields. Here we only consider abelian gauge groups, which implies that each of these gauge fields yields a  $U(1)$  charge. Lastly, there can also be a number  $n_H$  of hypermultiplets. Since we do not consider these in this thesis, we will always choose  $n_H = 0$ .

We will now give an enumeration of the particle content, in which we denote the spacetime index by  $\mu \in \{0, 1, 2, 3\}$  and the flat spacetime index by  $a \in \{0, 1, 2, 3\}$ . Moreover, the index  $A \in \{1, 2\}$  for  $N = 2$  supergravity and the index  $i \in \{1, \dots, n_V\}$  denotes the vector multiplet index. We omit spinor indices for the fermions.

- The gauge multiplet
  - The graviton, denoted by the vielbein  $e_\mu^a$ .
  - The two gravitini  $\Psi_\mu^A$  are the fermionic counterparts of the graviton.
  - The graviphoton  $A_\mu^0$ , a massless gauge field.

Notice that the graviphoton must be included to ensure that the number of bosonic and fermionic degrees of freedom coincide. Indeed, the gravitini with spin  $3/2$  each have two fermionic degrees of freedom, whereas the graviton and the graviphoton both have two bosonic degrees of freedom.

- The  $n_V$  vector multiplets
  - A massless gauge field  $A_\mu^i$ .
  - Two gaugini  $\lambda^{i,A}$ , which are the fermionic counterparts of the gauge boson.
  - A complex scalar field  $z^i$ .

Again, the complex scalar field enforces the number of bosonic and fermionic degrees of freedom to be equal. Indeed, the two gaugini with spin  $1/2$  each have two fermionic degrees of freedom, whereas the gauge field and the complex scalar field each have two bosonic degrees of freedom.

As the gauge fields all correspond to an abelian gauge group, the total gauge group is  $U(1)^{n_V+1}$ . The corresponding gauge fields are denoted by  $A_\mu^\Lambda$ , where  $\Lambda \in \{0, 1, \dots, n_V\}$ .

### 1.3.3 The target manifold

The scalar fields  $z^i$  form a coordinate system on a scalar manifold  $M_V$ , which is also known as the *target manifold*.  $M_V$  is a Hermitian manifold with real dimension  $2n_V$ , which means that it admits a Hermitian metric  $g_{i\bar{j}}$ . Moreover,  $M_V$  is a *Kähler manifold*. For our purposes we can avoid the exact mathematical definition and just use that this implies that there exists a so-called real-valued Kähler potential  $\mathcal{K}(z^i, \bar{z}^i)$  such that the metric on  $M_V$  can be written as

$$g_{i\bar{j}} = \partial_i \partial_{\bar{j}} \mathcal{K}(z^k, \bar{z}^k). \quad (1.13)$$

Furthermore,  $M_V$  is *special Kähler*. For our purposes it is enough to know that this implies that there exist  $n_V + 1$  complex functions  $X^\Lambda$  and a holomorphic function  $F(X^\Lambda)$  called the

prepotential, such that the Kähler potential can be written as<sup>1</sup>

$$\mathcal{K} = -\ln \left( i \left( \bar{X}^\Lambda \frac{\partial F}{\partial X^\Lambda} - X^\Lambda \frac{\partial F}{\partial \bar{X}^\Lambda} \right) \right). \quad (1.14)$$

The functions  $X^\Lambda$  are related to the scalar fields by

$$z^i = \frac{X^i}{X^0}. \quad (1.15)$$

The prepotential  $F$  determines the geometry of the scalar manifold. Consequently it has a big influence on the physics of our supergravity theory; for example, it determines how the scalars couple to the other fields in the theory. This will become clear when we give the supergravity action that we will consider. The choice of the prepotential follows directly from the choice of a string theory compactification.

There are a few more Kähler quantities that we need to define, because they will appear in our supergravity Lagrangian. First of all we define

$$L^\Lambda = e^{\mathcal{K}/2} X^\Lambda, \quad (1.16)$$

$$M_\Lambda = e^{\mathcal{K}/2} \frac{\partial F}{\partial X^\Lambda} \quad (1.17)$$

and

$$f_i^\Lambda = \left( \partial_i + \frac{1}{2} \partial_i \mathcal{K} \right) L^\Lambda. \quad (1.18)$$

The period matrix  $\mathcal{N}_{\Lambda\Sigma}$  is defined by

$$M_\Lambda = \mathcal{N}_{\Lambda\Sigma} L^\Sigma \quad (1.19)$$

and we denote its real and imaginary part by  $R_{\Lambda\Sigma}$  and  $I_{\Lambda\Sigma}$  respectively. The above Kähler quantities are all we need to be able to read our supergravity action, which we will discuss next.

### 1.3.4 The N=2 supergravity action

In our theory, we will use Fayet-Iliopoulos (FI) gauging. This implies that we gauge the  $U(1)^{n_V+1}$  symmetry in such a way that the gravitini acquire electric charges  $e_\Lambda$  and  $-e_\Lambda$  respectively, where

$$e_\Lambda = g \xi_\Lambda. \quad (1.20)$$

Note that a gravitino has two  $n_V + 1$  electric charges, one for each gauge field. Here the  $\xi^\Lambda$  are the so-called FI parameters and  $g$  is a coupling constant. All other fields remain neutral in this gauge.

---

<sup>1</sup>A bit more precisely, the functions  $X^\Lambda$  and  $\frac{\partial F}{\partial X^\Lambda}$  are sections of an  $\mathrm{Sp}(2(n_V + 1), \mathbb{R})$ -bundle over  $M_V$ .

We will consider only the bosonic part of the action, i.e. we will set all the fermions to zero. With the FI gauging procedure described above, the action then becomes<sup>2</sup>

$$S = \int d^4x e \left( \frac{R}{2} - g_{i\bar{j}} \partial^\mu z^i \partial_\mu \bar{z}^{\bar{j}} + I_{\Lambda\Sigma} F_{\mu\nu}^\Lambda F^{\Sigma,\mu\nu} + \frac{1}{2} R_{\Lambda\Sigma} \epsilon^{\mu\nu\rho\sigma} F_{\mu\nu}^\Lambda F_{\rho\sigma}^\Sigma - g^2 V(z^i, \bar{z}^{\bar{i}}) \right). \quad (1.21)$$

Here,  $e$  is the determinant of the spacetime metric,  $R$  is the Ricci scalar<sup>3</sup> and the Levi-Civita symbol is defined with  $\epsilon^{0123} = 1^4$ . The potential  $V(z^i, \bar{z}^{\bar{i}})$  is given by

$$V(z^i, \bar{z}^{\bar{i}}) = \left( g^{i\bar{j}} f_i^\Lambda \bar{f}_{\bar{j}} - 3\bar{L}^\Lambda L^\Sigma \right) \xi_\Lambda \xi_\Sigma. \quad (1.22)$$

As this form of the potential follows from the FI gauging procedure, it is such that only the gravitini are electrically charged and the other particles are neutral. Moreover, by demanding that asymptotically the scalar fields will minimize the potential, the theory becomes asymptotically anti-de Sitter [47].

---

<sup>2</sup>One should not confuse the target metric  $g_{i\bar{j}}$  with the spacetime metric  $g_{\mu\nu}$  or the coupling constant  $g$ .

<sup>3</sup>Here we use the convention of [47], where Newton's constant is chosen in such a way that the Ricci scalar acquires a prefactor  $\frac{1}{2}$ . Infinitely many different conventions exist and can be obtained by choosing different values for Newton's constant or the coupling constant for the  $F^2$  term.

<sup>4</sup>Here 0,1,2 and 3 are flat indices.

## Chapter 2

# The Hawking-Page Phase Transition

### 2.1 Black hole phase transitions: a brief history

One of the most astounding findings in black hole physics is the equivalence between black holes and thermodynamic systems, which was outlined in section 1.2. In many thermodynamic systems, phase transitions can occur. Therefore, the abovementioned correspondence might suggest that black holes can also undergo phase transitions. Considering the title of this thesis, it will not be surprising that this has indeed been predicted theoretically. The classic paper on this topic was published in 1983 by Stephen Hawking and Don Page. Therefore, the phase transition considered in this paper is known as the Hawking-Page phase transition [7]. As this is the prime example of a black hole phase transition, we will give a detailed outline in this chapter.

### 2.2 The phases

The Hawking-Page phase transition describes the transition between phases which are static spherically symmetric vacuum solutions of the Einstein equations with a negative cosmological constant  $\Lambda$ . We consider only four-dimensional spacetimes that are asymptotically anti-de Sitter (AdS). Here and in the remaining of this thesis we will express the cosmological constant in terms of the so-called AdS radius  $L = \sqrt{\frac{3}{-\Lambda}}$ .

Due to spherical symmetry, we can write a general solution to the Einstein equations as

$$ds^2 = -f(r)dt^2 + \frac{1}{f(r)}dr^2 + r^2d\Omega_2^2 \quad (2.1)$$

with  $d\Omega_2^2 = d\theta^2 + \sin^2\theta d\phi^2$ . Here the coordinates  $\{t, r, \theta, \phi\}$  are the same standard spherical coordinates as in the (pure) AdS solution Eq. (1.5), where  $f(r) = 1 + \frac{r^2}{L^2}$ . Besides the AdS

solution, other vacuum solutions are given by

$$f(r) = 1 + \frac{r^2}{L^2} - \frac{2M}{r}. \quad (2.2)$$

for each  $M > 0$ . Given  $M$ , the solution has a unique<sup>1</sup> event horizon  $r_h > 0$  given by  $f(r_h) = 0$ . We will refer to this black hole solution as the Schwarzschild anti-de Sitter (SAdS) solution. The above solutions are the only static spherically symmetric vacuum solutions to the Einstein equations with a negative cosmological constant [8].

To study the thermodynamics of this black hole, we will work in an ensemble with a fixed temperature. Therefore, we must first investigate which solutions exist at a given Hawking temperature  $T$ . To this end we perform a Wick rotation on the general solution (2.1) to Euclidean time  $\tau = it$ , yielding

$$ds^2 = f(r)d\tau^2 + \frac{1}{f(r)}dr^2 + r^2d\Omega_2^2. \quad (2.3)$$

We then compactify the imaginary time  $\tau$  so that we can identify the inverse Hawking temperature  $\beta_H = T_H^{-1}$  of the solution with the period of  $\tau$  [9]. For the (pure) AdS solution, this just means we introduce states corresponding to pure thermal radiation with Hawking temperature  $T_H$ . There are no restrictions to the period of imaginary time, so we can create thermal states at any  $T_H$ .

For the SAdS solution, there are restrictions to the period of  $\tau$ . To see this, we study the solution just outside the black hole, where we can write the metric tensor to leading order in  $r - r_h$  as

$$ds^2 \approx f'(r_h)(r - r_h)d\tau^2 + \frac{dr^2}{f'(r_h)(r - r_h)} + r_h^2d\Omega_2^2. \quad (2.4)$$

In terms of the coordinate  $R$  defined by  $R^2 = \frac{4(r - r_h)}{f'(r_h)}$ , such that  $R \rightarrow 0$  as we approach the black hole from the outside, the metric reads

$$ds^2 = \frac{f'(r_h)^2}{4}R^2d\tau^2 + dR^2 + r_h^2d\Omega_2^2. \quad (2.5)$$

Ignoring the 2-sphere, we see that the result is just a conical metric  $ds^2 = r^2d\phi^2 + dR^2$ , upon identifying the angle  $\phi$  with  $\frac{\tau f'(r_h)}{2}$ . This means that we also have conical singularities<sup>2</sup> unless we require that  $\phi \in [0, 2\pi]/ \sim [10]$ , in which case our metric just describes flat space in polar coordinates. Here the  $\sim$  denotes that we identify the end points of the interval as the same point. Therefore, in order to avoid conical singularities for our solution, we must now require that  $\tau \in \left[0, \frac{4\pi}{f'(r_h)}\right] / \sim$ . From this it follows that the Hawking temperature of the black hole is given

---

<sup>1</sup>This follows from elementary analysis:  $f$  is a continuous strictly increasing function with  $f(r \downarrow 0) \rightarrow -\infty$  and  $f(r \rightarrow \infty) \rightarrow \infty$ .

<sup>2</sup>To see this, suppose  $\phi \in [0, \alpha]/ \sim$  and  $\alpha = \pi$ . The resulting spacetime then looks like a half-plane, say  $\{(x, y) \in \mathbb{R}^2 | y \geq 0\}$ , with the rays  $x > 0$  and  $x < 0$  glued together. Due to this gluing, the point  $(0, 0)$  will look like the apex of a cone. Such a singularity occurs for any  $\alpha \neq 2\pi$ . Manifolds with such conical singularities are sometimes called *conifolds*.

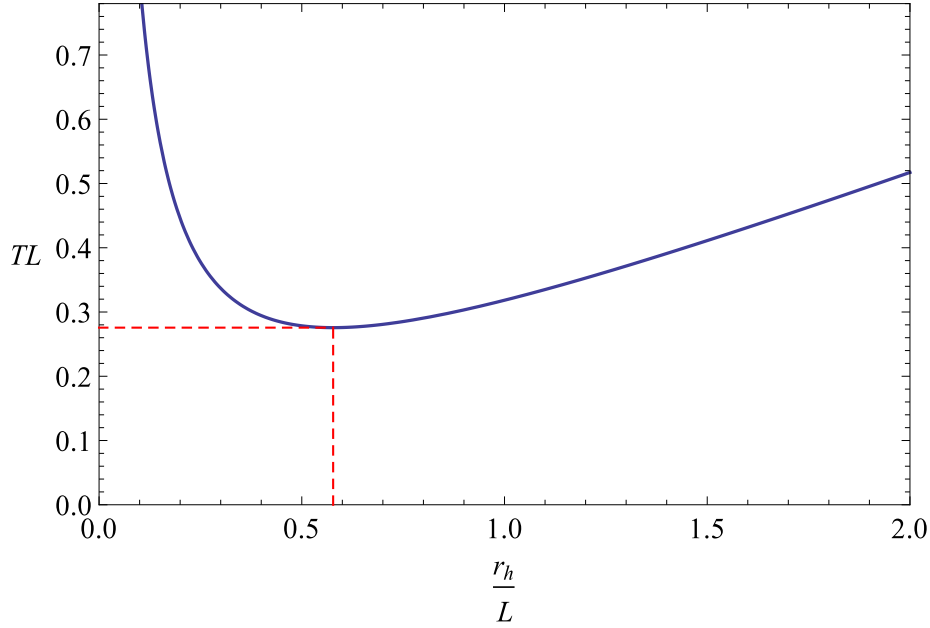


**Figure 2.1:** The temperature of the SAdS black hole as a function of its radius. The red dashed line pieces mark the positions of  $r_{min}$  and  $T_{min}$ .

by

$$T_H = \frac{f'(r_h)}{4\pi} = \frac{1}{4\pi r_h} \left( 1 + \frac{3r_h^2}{L^2} \right). \quad (2.6)$$

Notice that the Hawking temperature has a minimum at  $r_{min} = \frac{L}{\sqrt{3}}$  given by

$$T_{min} = \frac{\sqrt{3}}{2\pi L}. \quad (2.7)$$

Hence *the Schwarzschild black hole cannot exist at temperatures lower than  $T_{min}$ .*

From  $f(r_h) = 0$ , it follows that the mass of the black hole is given by

$$M = \frac{r_h}{2} \left( 1 + \frac{r_h^2}{L^2} \right). \quad (2.8)$$

Note that the First Law<sup>3</sup>  $dM = TdS$  is indeed satisfied by this expression. Moreover, the mass is a strictly increasing function of  $r_h$ , so it is one-to-one. Therefore, rather than expressing thermodynamic quantities as a function of the mass, we can equivalently express them as a function of the black hole radius, as we did in Eq. (2.6). In other words, an SAdS solution can be characterized by the parameter  $M$  or equivalently by the parameter  $r_h$ .

---

<sup>3</sup>While we refer to this as the First Law of thermodynamics, it is actually the fundamental thermodynamic relation which follows from the First and Second Law.



The Hawking temperature is plotted in Fig. 2.1 as a function of  $r_h$ . From this it follows that for each Hawking temperature above  $T_{min}$ , there are exactly two possible black hole solutions.

Summarizing, for a given Hawking temperature  $T$  we have the following possible phases.

- For  $T < T_{min}$ , the only possible phase is the pure thermal AdS solution.
- For  $T = T_{min}$ , the possible phases are pure thermal AdS and one Schwarzschild AdS solution.
- For  $T > T_{min}$ , the possible phases are pure thermal AdS and two Schwarzschild AdS solutions.

To find out whether a phase transition actually occurs, we will calculate the free energies corresponding to the solutions and see which phase is thermodynamically favored. However, we first investigate whether the above solutions are actually stable.

### 2.3 Thermal stability of the phases

The thermal stability of black hole solution follows from the heat capacity  $C$ , which is given by

$$C = T \frac{\partial S}{\partial T} = \frac{\partial M}{\partial T}, \quad (2.9)$$

where we used the First Law for the last equality. A thermally stable solution corresponds to a positive heat capacity. This is a well-known result from thermodynamics. Moreover, to see this, suppose that at some point, due to thermal fluctuations, the black hole absorbs more radiation than it emits. This means the mass of the black hole increases. If  $C < 0$ , its temperature will then drop. Consequently, the black hole will emit less radiation. The rate of absorption will therefore be higher than the rate of emission, which again causes the mass of the black hole to increase. It follows that if due to thermal fluctuations the mass of the black hole increases, the black hole will continue to grow indefinitely. Conversely, if due to thermal fluctuations, the black hole emits more radiation than it absorbs, a similar argument shows that the mass will decrease until the black hole disappears completely. Thus a black hole with a negative heat capacity is in an unstable thermal equilibrium and will decay to a stable solution.

Since Eq. (2.8) tells us that  $\frac{\partial M}{\partial r_h} > 0$ , the sign of the heat capacity is equal to the sign of  $\frac{\partial T}{\partial r_h}$ . Consequently, from Fig. 2.1 it follows that  $C < 0$  for  $r_h < r_{min}$  and  $C > 0$  for  $r_h > r_{min}$ . Thus given a temperature  $T > T_{min}$ , there are two possible black hole solutions, but only the bigger black hole solution is thermally stable.

Including the gravitational effect of thermal radiation, one can show that at some very high temperature  $T_{max}$  the radiation would become unstable and collapse to a black hole [7]. Hence the pure AdS solution is only stable at temperatures  $T < T_{max}$ . Above  $T_{max}$ , the big black hole solution is the only stable configuration.

To summarize, we have the following possible stable phases.

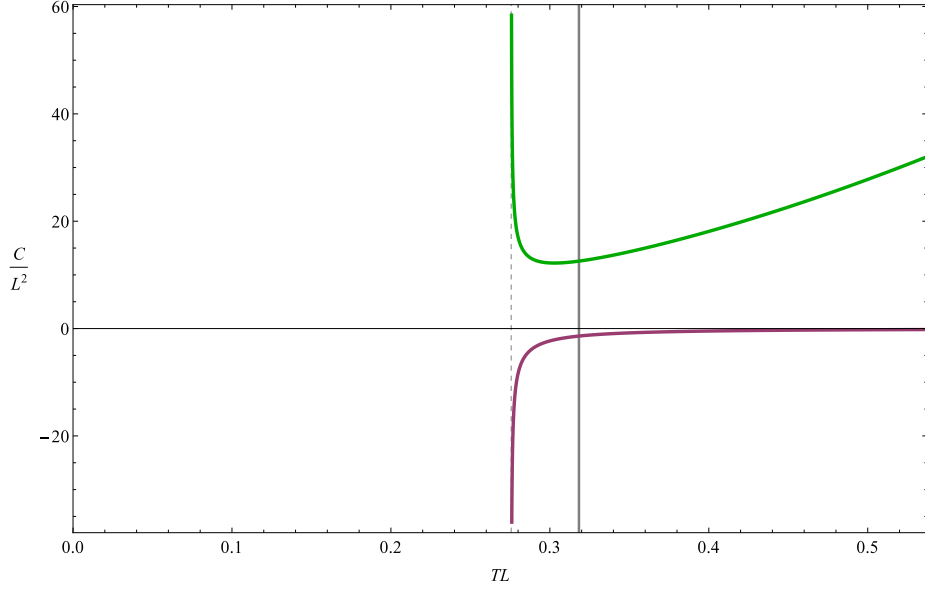


**Figure 2.2:** The heat capacities of the SAdS black holes as a function of the Hawking temperature. The green curve corresponds to the big black hole solution, which is stable. The purple curve corresponds to the small black hole solution, which is unstable. The vertical gray line denotes the temperature of the Hawking-Page phase transition.

- For  $T < T_{min}$ , the only stable phase is the pure thermal AdS solution.
- For  $T_{min} \leq T < T_{max}$ , the stable phases are pure thermal AdS and the big Schwarzschild AdS solution.
- For  $T > T_{max}$ , the only stable phase is the big Schwarzschild AdS solution.

In Fig. 2.2 the heat capacity of the two black hole solutions is plotted as a function of the Hawking temperature. The heat capacity diverges at the point  $r$  where the one branch ends and the other branch begins, which corresponds to the Hawking temperature  $T_{min}$ . This is mathematically unsurprising. In fact, the existence of more than one branch *must* yield a divergent heat capacity if the temperature is a smooth function of  $r_+$ , which it is because  $f$  is smooth. Physically, a diverging heat capacity could signal a second order phase transition or a critical point. Here, this is not the case. The diverging heat capacity merely signals the point at which a black hole can start to exist in a (meta)stable equilibrium. At this point, it is however not the thermodynamically preferred state. As we will show next, the Hawking-Page phase transition occurs at a higher temperature, which is also marked in the plot.

## 2.4 The phase transition

In the previous section we outlined the possible stable phases for a given Hawking temperature. In curved spacetimes, fixed quantities corresponding to a thermodynamic ensemble are boundary

values [11]. Therefore, to compare the free energies of two states we must make sure that the boundary values of their *physical* temperatures coincide, rather than their Hawking temperatures.<sup>4</sup> The locally measured physical temperature experiences gravitational redshift [12]. In terms of the Hawking temperature  $T_H$  it is given by

$$T_{phys}(r) = \frac{T_H}{\sqrt{g_{\tau\tau}(r)}}. \quad (2.10)$$

To see where the phase transition occurs, we calculate the Helmholtz free energy difference between the phases with the same asymptotic physical temperature to see which phase is thermodynamically favorable. In the zero-loop approximation, this amounts to calculating the difference between the on-shell actions, see Eq. (1.12).

Substituting one of the classical solutions in the Euclidean Einstein-Hilbert action

$$S = -\frac{1}{16\pi} \int d^4x \sqrt{g} (R - 2\Lambda) \quad (2.11)$$

will lead to a divergence. However, if we introduce a cut-off  $K$  for the coordinate  $r$ , we can calculate the action difference  $\Delta S = S_{SAdS} - S_{AdS}$  between the two solutions as a function of  $K$ . Afterwards we show that their difference does converge as  $K \rightarrow \infty$ .<sup>5</sup> Using that for on-shell solutions we have  $R = 4\Lambda$ , which follows immediately from contracting the Einstein equations, we get for the SAdS solution that

$$S_{SAdS} = \frac{3}{8\pi L^2} \int_0^{\beta_H} d\tau \int_{r_h}^K dr r^2 \int d\Omega_2 = \frac{\beta_H}{2L^2} (K^3 - r_h^3) \quad (2.12)$$

where  $\beta_H$  is the inverse black hole Hawking temperature and  $d\Omega_2 \equiv \sin\theta d\theta d\phi$ . The AdS solution yields

$$S_{AdS} = \frac{3}{8\pi L^2} \int_0^\beta d\tau \int_0^K dr r^2 \int d\Omega_2 = \frac{\beta}{2L^2} K^3 \quad (2.13)$$

where  $\beta$  is the inverse temperature of the thermal state. Using Eq. (2.10), equating the asymptotic physical temperatures of the phases yields

$$\beta \sqrt{1 + \frac{K^2}{L^2}} = \beta_H \sqrt{1 - \frac{2M}{K} + \frac{K^2}{L^2}} \quad (2.14)$$

so that for large  $K$  we can write

$$\beta \approx \left( 1 - \frac{ML^2}{KL^2 + K^3} \right) \beta_H. \quad (2.15)$$

---

<sup>4</sup>Note that using a coinciding Hawking temperature could yield ambiguities since the Hawking temperature depends on the choice of normalization of the timelike coordinate.

<sup>5</sup>Alternatively, we could choose not to ignore the Gibbons-Hawking-York boundary term to regularize the action. However, when calculating the free energy difference, the boundary terms coincide for the two solutions, as both are asymptotically AdS.

Substituting this in equation (2.13), the difference in the actions becomes

$$S_{SAdS} - S_{AdS} = \frac{\beta_H}{2L^2} \left( -r_h^3 + \frac{ML^2}{KL^2 + K^3} K^3 \right) \quad (2.16)$$

and as  $K \rightarrow \infty$  this yields

$$S_{SAdS} - S_{AdS} = \frac{\beta_H}{2L^2} \left( -r_h^3 + ML^2 \right) = \frac{r_h \beta_H}{4} \left( 1 - \frac{r_h^2}{L^2} \right). \quad (2.17)$$

where we used (2.8). Notice that the result is equal to  $\beta_H(M - TS)$ , as expected.<sup>6</sup> We see that  $\Delta F < 0$  if and only if  $r_h > L$ . For the small and unstable black hole solution,  $r_h < r_{min} < L$ , so this solution is never thermodynamically favorable over the pure AdS solution. For the big and stable black hole,  $r_h > L$  corresponds to a temperature  $T > T_c$  with

$$T_c = \frac{1}{\pi L}. \quad (2.18)$$

Hence at  $T = T_c$  a phase transition occurs. This is the Hawking-Page phase transition. For  $T > T_c$ , the SAdS solution is the solution with the lowest free energy, so the Schwarzschild black hole is preferred over thermal radiation. For  $T_{min} \leq T < T_c$ , thermal radiation is the energetically favorable solution, even though a stable black hole can exist. Thus for these temperatures the black hole is a metastable state. For  $T < T_{min}$ , thermal radiation is the only possible solution.

In Fig. 2.3 the free energy of both black hole solutions is plotted as function of their temperature. With these results we can plot the diagram in Fig. 2.4. Here, the blue curve denotes the energetically favorable state while the dashed curves denote metastable states. The mass of the black hole is an order parameter. At the critical temperature  $T_c$ , the energetically favorable mass jumps to a nonzero value. According to the Ehrenfest classification, this implies that the Hawking-Page phase transition is a first-order phase transition.<sup>7</sup> From the Fig. 2.4 we draw the following conclusions:

- For all temperatures at which the unstable black hole exists, it is thermodynamically unfavorable.
- For temperatures  $T < T_{min}$  with  $T_{min}$  given by (2.7), the Schwarzschild black hole cannot exist, so AdS spacetime filled with pure thermal radiation is the only possible solution.
- For temperatures  $T \in [T_{min}, T_c)$  with  $T_c$  given by (2.18), pure thermal radiation is the energetically favorable solution and the Schwarzschild black hole is a metastable state.
- At the temperature  $T = T_c$  the Hawking-Page phase transition takes place.
- For temperatures  $T \in (T_c, T_{max}]$ , the stable Schwarzschild black hole is the energetically favorable solution and pure thermal radiation is a metastable state.

<sup>6</sup>For this we used the Hawking entropy  $S = \pi r_h^2$ . It is however not trivial that the parameter  $M$  is really the mass of the black hole. See Appendix A for more details.

<sup>7</sup>Indeed, we have a discontinuity in a *first* derivative of the free energy  $S = -\frac{\partial F}{\partial T} = \pi r_h^2$ , which is discontinuous since  $r_h$  is.

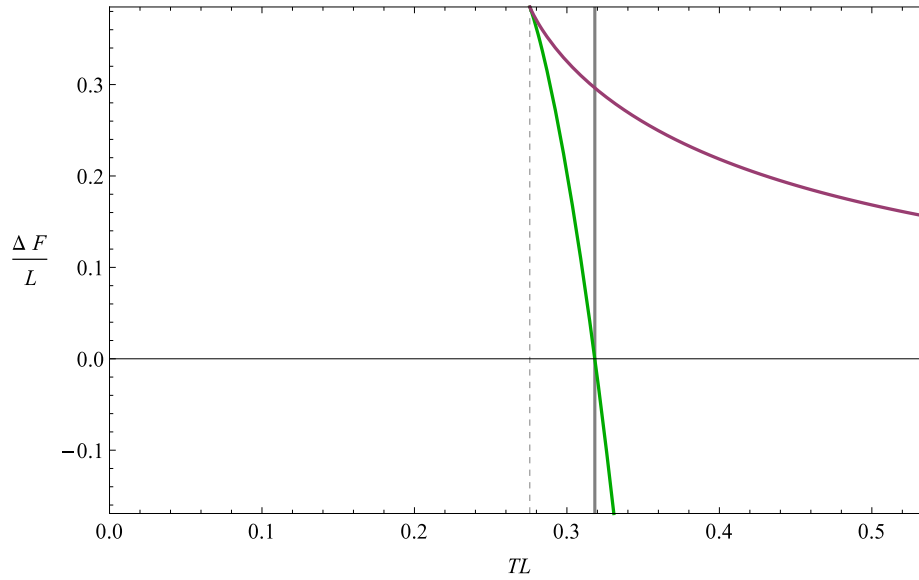


**Figure 2.3:** The Helmholtz free energies of the SAdS black holes as a function of the Hawking temperature. The green curve corresponds to the big black hole solution, whereas the purple curve corresponds to the small black hole solution. The vertical gray line denotes the temperature of the Hawking-Page phase transition.

- For temperatures  $T > T_{max}$ , pure thermal radiation collapses to a black hole, so the Schwarzschild black hole is the only possible solution.

If the spacetime is in a metastable state, it will want to decay to the thermodynamically favorable state. The unstable black hole then acts as a free energy barrier. The higher the free energy of the unstable black hole, the smaller the probability that a metastable state will tunnel to the thermodynamically preferred state. This is similar to classical nucleation theory.

## 2.5 Summary

In this chapter we described the Hawking-Page phase transition: a first-order phase transition between the thermal AdS solution and a Schwarzschild black hole. Above the critical temperature  $T_c$ , the stable black hole is the preferred solution, whereas below  $T_c$  thermal AdS is preferred. There is also an unstable black hole solution acting as a free energy barrier between the stable black hole and the thermal AdS solution.

In the AdS/CFT correspondence, the Hawking-Page phase transition is often used to describe a confinement-deconfinement phase transition. For example, at temperatures below some critical temperature  $T_c$ , quarks are confined to be grouped together in pairs or triples, whereas at higher temperatures they are in a deconfined phase, occurring freely in a quark-gluon plasma. However, at the time when the paper of the Hawking-Page phase transition was published, the AdS/CFT correspondence had not yet been conjectured. For this reason AdS spacetime was not as interest-

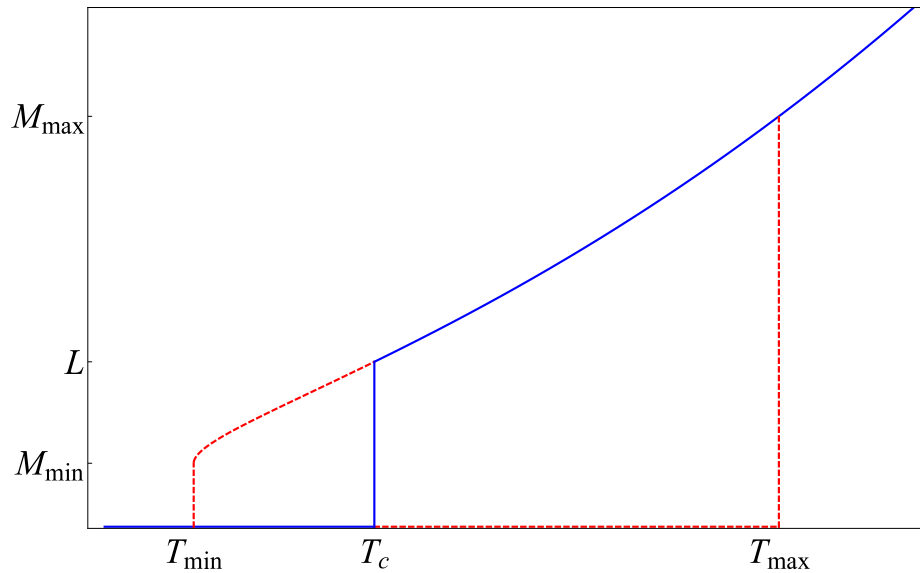


**Figure 2.4:** The order parameter for the Hawking-Page phase transition. The blue curve represents the energetically favorable solution, whereas the dashed curves denote a metastable solution.

ing then as it is now. Therefore, in the few years right after 1983 most of the papers on black hole phase transitions were about asymptotically flat spacetimes. We will see what happens there in chapter 4. However, in the next chapter we will first consider a natural extension the Hawking-Page phase transition. As we are now armed with the framework on how should deal with black hole thermodynamics, we will apply this in the next chapter again, but to *charged* black holes. We will see that these yield a much richer phase structure. Naturally, this phase structure reduces to the one obtained in this chapter in the limit of zero charge.

## Chapter 3

# Charged Black Hole Phase Transitions

In this chapter we investigate the thermodynamics of an electrically charged spherically symmetric black hole in a four-dimensional spacetime which is asymptotically AdS. The procedure will very much resemble the one in the previous chapter:

- First of all, we give the form of the solutions to the Einstein Equations and calculate their corresponding Hawking temperature.
- Secondly, we will outline what phases exist at a given temperature.
- Subsequently, we will check the thermal stability of the solutions.
- Finally, we will investigate the phase diagram by calculating the relevant thermodynamic potential.

Nevertheless, there are some important differences with the previous chapter. Firstly, the solutions we consider are not vacuum solutions, unless the charge is put to zero. Moreover, to describe the thermodynamics we must now specify the thermodynamic ensemble. In the previous chapter it sufficed to consider a fixed temperature. However, in this chapter we must also choose whether we fix the electric charge or its conjugate variable, the electrostatic potential. The former corresponds to the canonical ensemble, while the latter corresponds to the grand canonical ensemble. As we shall see, both ensembles give rise to different phase structures. Most of the material here was published in [13][14].

### 3.1 The black hole solution

The action we are considering in this Chapter is the Einstein-Hilbert-Maxwell action, given by [13]<sup>1</sup>

$$I = \frac{1}{16\pi} \int_M d^4x \sqrt{g} \left( R - F_{\mu\nu} F^{\mu\nu} + \frac{6}{L^2} \right). \quad (3.1)$$

Here, the electromagnetic field tensor  $F = dA$  is purely electric, i.e. the four-potential which solves the covariant Maxwell equations is given by

$$A = \left( -\frac{Q}{r} + \Phi \right) dt. \quad (3.2)$$

Clearly,  $\Phi$  is the electrostatic potential at  $r = \infty$ . In case we are dealing with a black hole solution with outer event horizon  $r_+$ , we fix the gauge by setting

$$\Phi = \frac{Q}{r_+}. \quad (3.3)$$

In this way the the four potential vanishes at the event horizon, which prevents the divergence of the norm of the gauge field  $g^{tt} A_t^2$  on the event horizon.

The Euclidean metric which solves the equations of motion following from (3.1) is given by equation

$$ds^2 = -f(r)dt^2 + \frac{1}{f(r)}dr^2 + r^2 d\Omega_2^2 \quad (3.4)$$

with in this case

$$f(r) = 1 - \frac{2M}{r} + \frac{Q^2}{r^2} + \frac{r^2}{L^2}. \quad (3.5)$$

As usual, the event horizons follow from  $f(r) = 0$ . Depending on the values of  $M$  and  $Q$ , this yields either 0 or 2 positive solutions that may coincide. We denote these positive solutions by  $r_+$  and  $r_-$ . Here  $r_+ \geq r_-$ , which implies that

$$r_+^2 \geq \frac{L^2}{6} \left( \sqrt{1 + 12\frac{Q^2}{L^2}} - 1 \right) \equiv r_e \quad (3.6)$$

where we eliminated  $M$  using  $f(r_+) = 0$ , i.e.

$$M = \frac{r_+}{2} \left( 1 + \frac{Q^2}{r_+^2} + \frac{r_+^2}{L^2} \right). \quad (3.7)$$

Notice how this reduces to the familiar asymptotically flat case  $r_+ = 2M$  when  $Q = \Lambda = 0$ . If  $r_+ = r_e$ , the two solutions coincide and the black hole is extremal. The inequality (3.6) must hold in order to prevent a naked singularity.<sup>2</sup>

<sup>1</sup>Note that the absence of the minus sign compared to Eq. (2.11) is because Eq. (2.11) is the Euclidean action, whereas here a Minkowskian signature is used.

<sup>2</sup>Eq. (3.6) follows from the equations  $f(r_e) = f'(r_e) = 0$ .



Using the exact same steps as in Section 4, requiring the absence of a conical singularity at  $r_+$  in the Euclidean metric yields a Hawking temperature

$$T_H = \frac{f'(r_+)}{4\pi} = \frac{1}{4\pi r_+} \left( 1 + \frac{3r_+^2}{L^2} - \frac{Q^2}{r_+^2} \right). \quad (3.8)$$

Comparing this to Eq. (2.6), we see that there is one additional term. The effect of this term depends on the thermodynamic ensemble we work in and will be discussed in the relevant sections. Furthermore, note that since  $f'(r_e) = 0$ , it follows that the limit of an extremal black hole has zero temperature, as expected.

As stated before, the phase structure depends on the chosen thermodynamic ensemble. We will start treating the grand canonical ensemble, as the results in this ensemble are more similar to the Hawking-Page phase transition.

Notice that the on-shell action does not depend on the sign of  $Q$ . Hence without loss of generality, we will only consider solutions with  $Q \geq 0$ .

## 3.2 The grand canonical ensemble

In the grand canonical ensemble, we fix the temperature  $T$  and the gauge field at spatial infinity  $A(\infty) = \Phi dt$ . The relevant thermodynamic potential is the grand potential, defined by

$$\Omega(T, \Phi) = M - TS - \Phi Q. \quad (3.9)$$

Note that the quantities  $M$ ,  $S$  and  $Q$  are *macroscopic* quantities. A quantum theory of gravity would include microscopic fluctuations, so that the quantities which are not fixed in the ensemble should be interpreted as expectation values.

### 3.2.1 The phases

In the grand canonical ensemble, one of the phases is the pure thermal AdS solution with  $f(r) = 1 + \frac{r^2}{L^2}$  together with the constant gauge field  $A_t = \Phi$ . As stated before, this solution exists at any temperature. It also exists at any value of the electrostatic potential  $\Phi$ . Indeed, neither the metric tensor nor the grand potential depend on  $\Phi$ , since the field tensor  $F_{\mu\nu}$  vanishes for any  $\Phi$ .

Now let us investigate the black hole solutions. Using Eq. (3.8) and Eq. (3.3) we can write the Hawking temperature as

$$T_H = \frac{1}{4\pi r_+} \left( 1 + \frac{3r_+^2}{L^2} - \Phi^2 \right). \quad (3.10)$$

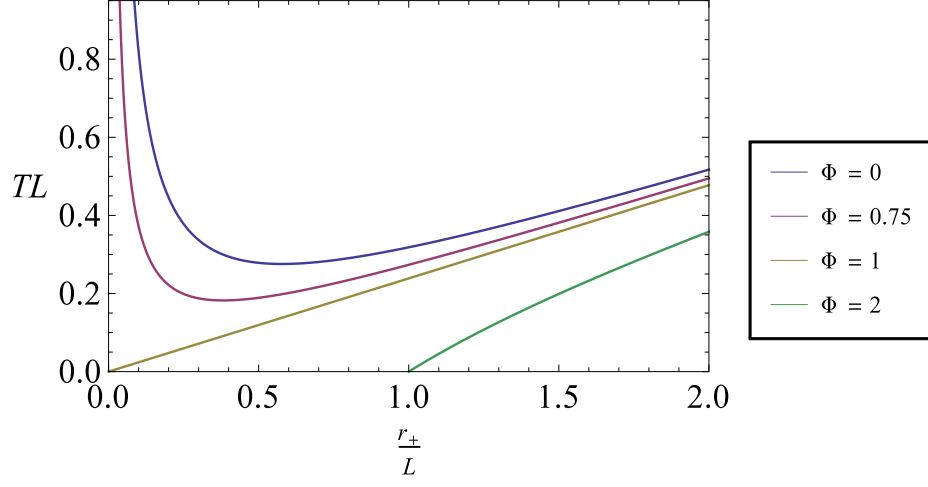


**Figure 3.1:** The temperature of the black hole solution for different values of  $\Phi$ .

This is plotted in Fig. 3.1 for several values of  $\Phi$ . One clearly sees the effect of the additional term in the temperature. If  $\Phi \geq 1$ , this term is big enough to cancel the divergence in the temperature at  $r_+ = 0$ . In this case, the black hole solution can exist at any temperature. As opposed to this, for a fixed  $\Phi < 1$  the temperature has a minimum at  $r_+ = \frac{L}{\sqrt{3}}\sqrt{1 - \Phi^2}$  given by

$$T_{min} = \frac{\sqrt{3}}{2\pi L} \sqrt{1 - \Phi^2}. \quad (3.11)$$

Hence in the region  $\Phi < 1$ ,  $T < T_{min}$ , the charged black hole cannot exist. Above  $T_{min}$ , the plot shows that there exist exactly two black hole solutions.

Summarizing, for a fixed value of  $\Phi$  and  $T$  we have the following possible phases.

- For  $\Phi < 1$  and  $T < T_{min}(\Phi)$ , the only possible phase is the pure thermal AdS solution.
- For  $\Phi < 1$  and  $T = T_{min}(\Phi)$ , the possible phases are pure thermal AdS and one charged black hole solution.
- For  $\Phi < 1$  and  $T > T_{min}(\Phi)$ , the possible phases are pure thermal AdS and two charged black hole solutions.
- For  $\Phi \geq 1$  and any  $T \geq 0$ , the possible phases are pure thermal AdS and one charged black hole solution.

The next question is which of these phases are actually stable.

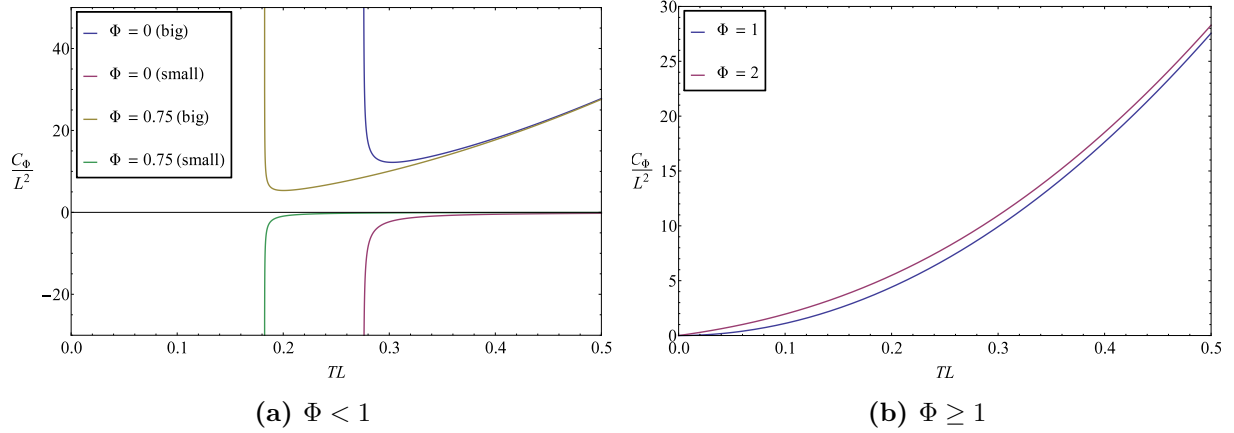


**Figure 3.2:** The heat capacities of the charged black holes as a function of the Hawking temperature. For the case  $\Phi < 1$  there are two branches, labeled by "big" for the larger radius and "small" for the smaller one. For  $\Phi \geq 1$  there is only one branch.

### 3.2.2 Thermal stability of the phases

As stated in the previous chapter, thermal stability of the black hole solutions is equivalent to a nonnegative heat capacity, which is defined by

$$C_{\Phi} = T \left( \frac{\partial S}{\partial T} \right)_{\Phi}. \quad (3.12)$$

Naturally,  $T \geq 0$ . Furthermore, the Hawking entropy  $S = \pi r_+^2$  tells us that  $\left( \frac{\partial S}{\partial r_+} \right)_{\Phi} > 0$ . Therefore, the solution is thermally stable if and only if  $\left( \frac{\partial T}{\partial r_+} \right)_{\Phi} > 0$ . From Fig. 3.1 it immediately follows that the black hole solution for  $\Phi \geq 1$  is thermally stable. For  $\Phi < 1$ , the solution with the largest radius is always thermally stable, while the other solution is always unstable. Note that this is similar to what we found for the Hawking-Page phase transition, which is the  $\Phi = 0$  case.

Using Eq. (3.10), we can plot the heat capacity as a function of  $T$ . This is done in Fig. 3.2. If  $\Phi < 1$ , the heat capacity diverges at  $T_{min}$ . As in the uncharged case, no phase transition occurs at this point, as we shall see in the next subsection. The divergence merely denotes the point at which the black hole can start to exist in a (meta)stable equilibrium.

To summarize, we have the following possible stable phases:

- For  $\Phi < 1$  and  $T < T_{min}(\Phi)$ , the only stable phase is the pure thermal AdS solution.
- For  $\Phi < 1$  and  $T \geq T_{min}(\Phi)$ , the stable phases are pure thermal AdS and one charged black hole solution. There is one unstable black hole solution.
- For  $\Phi \geq 1$  and all  $T \geq 0$ , the stable phases are pure thermal AdS and one charged black hole solution. There are no unstable solutions.

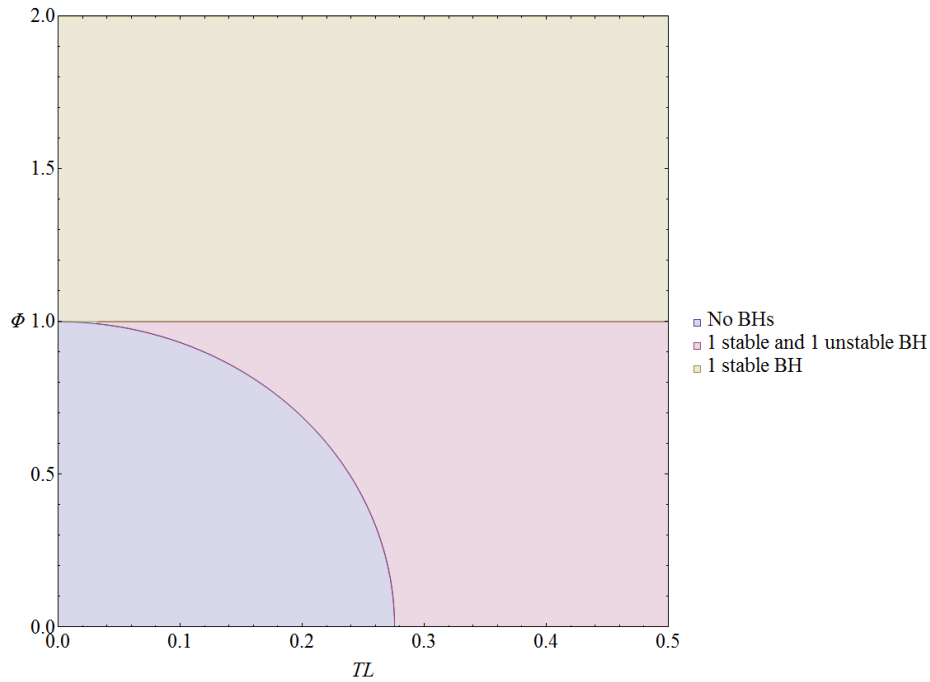


**Figure 3.3:** The stable phases in the  $(T, \Phi)$ -plane. Besides the black hole solutions, thermal AdS is also a solution for any  $T$  and  $\Phi$ .

The stable phases are displayed in the diagram in Fig. 3.3. With this plot we are one step closer to the full phase diagram: all that is left is to calculate which of the phases is thermodynamically favorable. This will be done in the next subsection.

As in the uncharged case, there exists a temperature at which pure thermal AdS becomes unstable against collapse to a black hole. We will not take this into account in this chapter.

### 3.2.3 The phase diagram

To find out whether phase transition between a black hole state and the thermal AdS state can occur, we calculate the grand-potential difference of the black hole solution and thermal AdS. In the zero-loop approximation the grand potential is given by

$$\Omega(T, \Phi) = TI_E \quad (3.13)$$

where  $I_E$  is the on-shell Euclidean action Eq. (3.1)<sup>3</sup>. In this section we will take a shortcut: rather than calculating the difference between the actions, we just use Eq. (3.9).<sup>4</sup> It can be shown that this yields the same result as evaluating the on-shell action.

<sup>3</sup>The Euclidean action has an additional overall minus sign with respect to Eq. (3.1).

<sup>4</sup>Here, we used that parameter  $M$  is really the mass of the black hole. This is non-trivial, see appendix A and [15][16][17] for more details.

Using the Hawking entropy, the grand potential difference is given by

$$\Delta\Omega(T, \Phi) \equiv \Omega_{BH} - \Omega_{AdS} = M - \frac{T_H A}{4} - \Phi Q \quad (3.14)$$

where  $A = 4\pi r_+^2$  is the black hole's area. Using Eq. (3.7), Eq. (3.10) and Eq. (3.3) we can write this as

$$\Delta\Omega(T, \Phi) = \frac{r_+}{4} \left( 1 - \frac{r_+^2}{L^2} - \Phi^2 \right) \quad (3.15)$$

where  $r_+$  should be understood as a function of  $T$  and  $\Phi$ . The grand potential difference is negative if and only if  $r_+ > L\sqrt{1 - \Phi^2} \equiv r_c$ . Since we found that the unstable black hole radius is always smaller than  $r_c$ , it follows that the unstable black hole is *never* thermodynamically preferred over pure thermal AdS. Moreover, it immediately follows that for  $\Phi \geq 1$ , the stable black hole solution is *always* preferred over the pure thermal AdS solution. For  $\Phi < 1$ , the stable black hole is only preferred if  $r_+ > r_c$ . This criterion corresponds to a critical temperature

$$T_c = \frac{1}{\pi L} \sqrt{1 - \Phi^2}. \quad (3.16)$$

At  $T_c$  a phase transition from pure thermal AdS to the stable black hole occurs. This is similar to the Hawking-Page phase transition.

In figure Fig.3.4 the grand potential is plotted as function of the temperature. With these results we can plot the phase diagram. This is displayed in Fig.3.5. Summarizing, we have the following results:

- For  $\Phi \geq 1$ , there is one possible black hole solution which is always stable and preferred over pure thermal AdS. An exception is the point  $(T, \Phi) = (0, 1)$ , at which  $r_+ = 0$ , so there is no black hole solution.
- For  $\Phi < 1$  and  $T < T_{min}$  there are no black hole solutions, making pure thermal AdS the only possibility.
- For  $\Phi < 1$  and  $T_{min} < T < T_c$  we have  $\Delta\Omega(T, \Phi) > 0$  for both branches of the temperature. Hence the pure thermal AdS spacetime is preferred. The largest black hole solution is metastable.
- For  $\Phi < 1$  and  $T > T_c$  we have  $\Delta\Omega(T, \Phi) < 0$  for the thermally stable black hole solution and  $\Delta\Omega(T, \Phi) > 0$  for the unstable solution. Hence the thermally stable solution is preferred over the pure thermal AdS solution. The unstable solution acts as a free energy barrier.
- For  $\Phi < 1$  and  $T = T_c(\Phi)$  we have  $\Omega(T, \Phi) = 0$  for the stable black hole solution and  $\Omega(T, \Phi) > 0$  for the unstable solution. Here a first-order phase transition takes place which is similar to the Hawking-Page phase transition.

The obtained results are very similar to the uncharged case if  $\Phi < 1$ . However, as we increase the value of  $\Phi$ , the critical temperature Eq. (3.16) decreases, until it vanishes for  $\Phi = 1$ . Hence for  $\Phi \geq 1$ , no phase transitions occur.

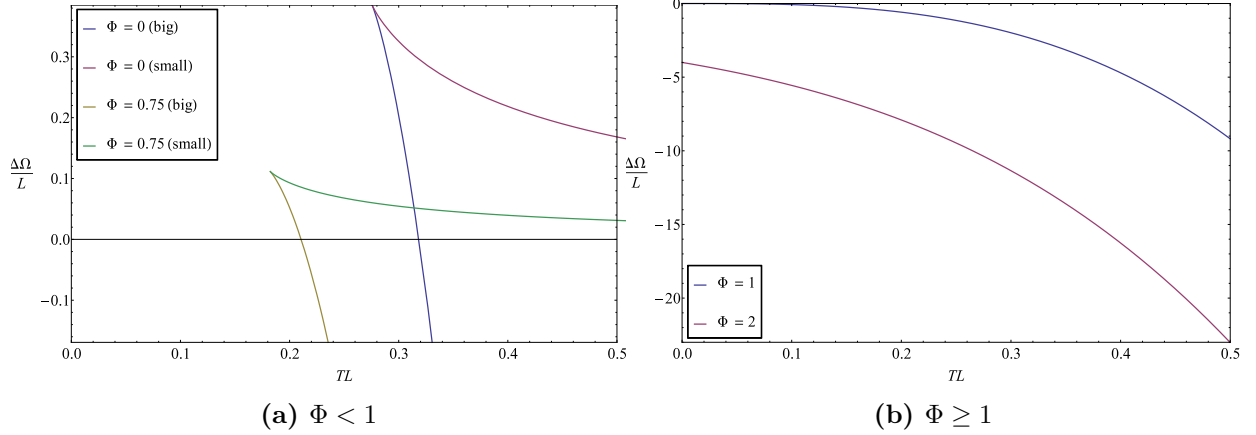


**Figure 3.4:** The grand potentials of the charged black holes as a function of the Hawking temperature. For the case  $\Phi < 1$  there are two branches, labeled by "big" for the larger radius and "small" for the smaller one. For  $\Phi \geq 1$  there is only one branch.

### 3.3 The canonical ensemble

In the canonical ensemble, we fix the temperature  $T$  and the charge  $Q$ . The relevant thermodynamic potential is the Helmholtz free energy, defined by

$$F(T, Q) = M - TS. \quad (3.17)$$

As we shall see, the phase diagram in the canonical ensemble is completely different from the grand canonical one.

#### 3.3.1 The phases

In the canonical ensemble, we do not have a pure thermal AdS solution. The reason is that this solution is a vacuum solution, which implies that  $Q = 0$ . Therefore, it is not a solution for arbitrary values of the charge.<sup>5</sup> From this it also follows that we cannot have a Hawking-Page phase transition when  $Q \neq 0$ .

In the previous cases we considered, thermal AdS served as a reference solution for calculating the free energy difference. The subtraction of this reference solution was necessary, since the on-shell action of the black hole solutions diverged. This time we will need a difference reference solution, namely the extremal black hole. The extremal black hole solution is a solution for any value of  $T$  and  $Q$  [13]. This might sound strange, since from Eq. (3.8) it clearly follows that the limit of an extremal black hole has zero temperature. However, note that when deriving Eq. (3.8) as in section 4, we implicitly assumed in Eq. (2.4) that  $f'(r_+) \neq 0$ . Therefore, the derivation does not hold for the extremal black hole. Indeed, if we assume an extremal black hole solution,

<sup>5</sup>Alternatively, this can be seen from Eq. (3.6): if  $Q \neq 0$ , then  $r_+ \neq 0$ , which means we are dealing with a black hole solution rather than thermal AdS.

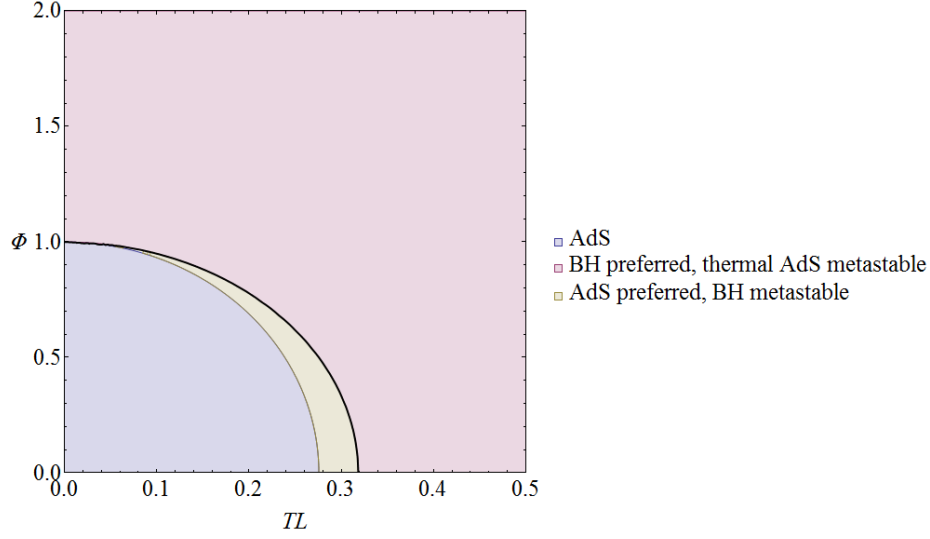


**Figure 3.5:** The phase diagram of the charged black hole in the  $(T, \Phi)$ -plane. The legend only mentions the (meta)stable states. Everywhere but in the region  $\Phi \geq 1$ , there is also an unstable black hole state. In crossing the thick black curve, a first-order phase transition occurs.

i.e.  $f'(r_+) = 0$ , we will not find any conical singularities arising in the metric. Hence we can assign an arbitrary periodicity to the imaginary time coordinate, which implies that the solution can exist at any temperature. However, since an extremal black hole viewed as the limit of a non-extremal black hole does have vanishing temperature, we expect that the extremal black hole at an arbitrary temperature  $T \neq 0$  will not occur. Its only purpose is therefore to serve as a reference solution. We will indeed find that there is always another solution with a lower free energy than the extremal black hole.

The temperature is given by Eq. (3.8). This is plotted in figure Fig. 3.6 for several values of  $Q$ . This figure clearly shows the effect of the additional term in Eq. (3.8), with respect to Eq. (2.6). Since this additional term dominates as  $r_+ \rightarrow 0$ , adding a small charge to the black hole cancels the divergence to  $+\infty$  at  $r_+ = 0$  which was present in the uncharged case.<sup>6</sup> As a result, a black hole solution can exist at any temperature. From the plot we can see that there is some range of temperatures  $(T_1(Q), T_2(Q))$  in which three black hole solutions exist. For temperatures  $T < T_1$  and  $T > T_2$ , there is only one black hole solution.

As we increase the black hole charge, the temperature interval  $(T_1, T_2)$  becomes smaller, until at a charge  $Q_c = L/6$ ,<sup>7</sup>  $T_1$  and  $T_2$  coincide. Consequently, for charges  $Q \geq Q_c$  there is only one black hole solution for each temperature. The value  $Q_c$  at which  $T_1 = T_2 = T_c$  corresponds to a critical point. At the critical point, one branch of the black hole solutions disappears, while the other two merge into one branch. Compare this to the critical point in the phase diagram of

<sup>6</sup>Actually, it replaces the divergence to  $+\infty$  by a divergence to  $-\infty$ , but we do not consider negative temperatures.

<sup>7</sup>This value follows from the point of inflection in the temperature graph, i.e.  $\left(\frac{\partial T}{\partial r_+}\right)_Q = \left(\frac{\partial^2 T}{\partial r_+^2}\right)_Q = 0$  at  $Q = Q_c$ .

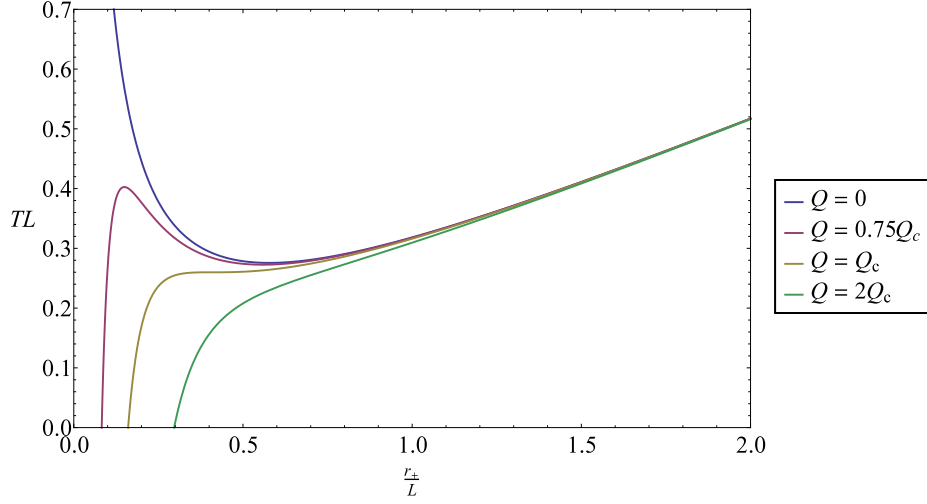


**Figure 3.6:** The temperature of the black hole solution for different values of  $Q$ .

water: above the critical temperature the conversion between the gas and liquid phase becomes continuous. The full set of parameters corresponding to the critical point are given by

$$(r_c, T_c, Q_c) = \left( \frac{L}{\sqrt{6}}, \frac{2}{\pi\sqrt{6}L}, \frac{L}{6} \right). \quad (3.18)$$

Summarizing, for a fixed value of  $Q$  and  $T$  we have the following phases:

- For  $Q < Q_c$  and  $T < T_1(Q)$  or  $T > T_2(Q)$  there is one possible charged black hole phase.
- For  $Q < Q_c$  and  $T \in (T_1(Q), T_2(Q))$  there are three possible charged black hole phases.
- For  $Q < Q_c$  and  $T = T_1(Q)$  or  $T = T_2(Q)$  there are two possible charged black hole phases.
- For  $Q \geq Q_c$  there is one possible charged black hole phase for each temperature.

Furthermore, for any value of  $Q$  and  $T$  there is an extremal black hole phase. However, as stated before, one should consider this phase purely as a reference phase.

### 3.3.2 Thermal stability of the phases

As usual, to investigate the thermal stability of the phases we study the heat capacity, which is given by

$$C_Q = T \left( \frac{\partial S}{\partial T} \right)_Q. \quad (3.19)$$

Using the same argument as in the previous Section, it follows that a solution is thermally stable if and only if  $\left( \frac{\partial T}{\partial r_+} \right)_Q > 0$ . Hence from Fig. 3.6 we learn that the black hole solution for  $Q \geq Q_c$  is thermally stable. If  $Q < Q_c$ , we see that there are two stable solutions: the black hole with the smallest radius and the one with the largest radius. The intermediate black hole is unstable.



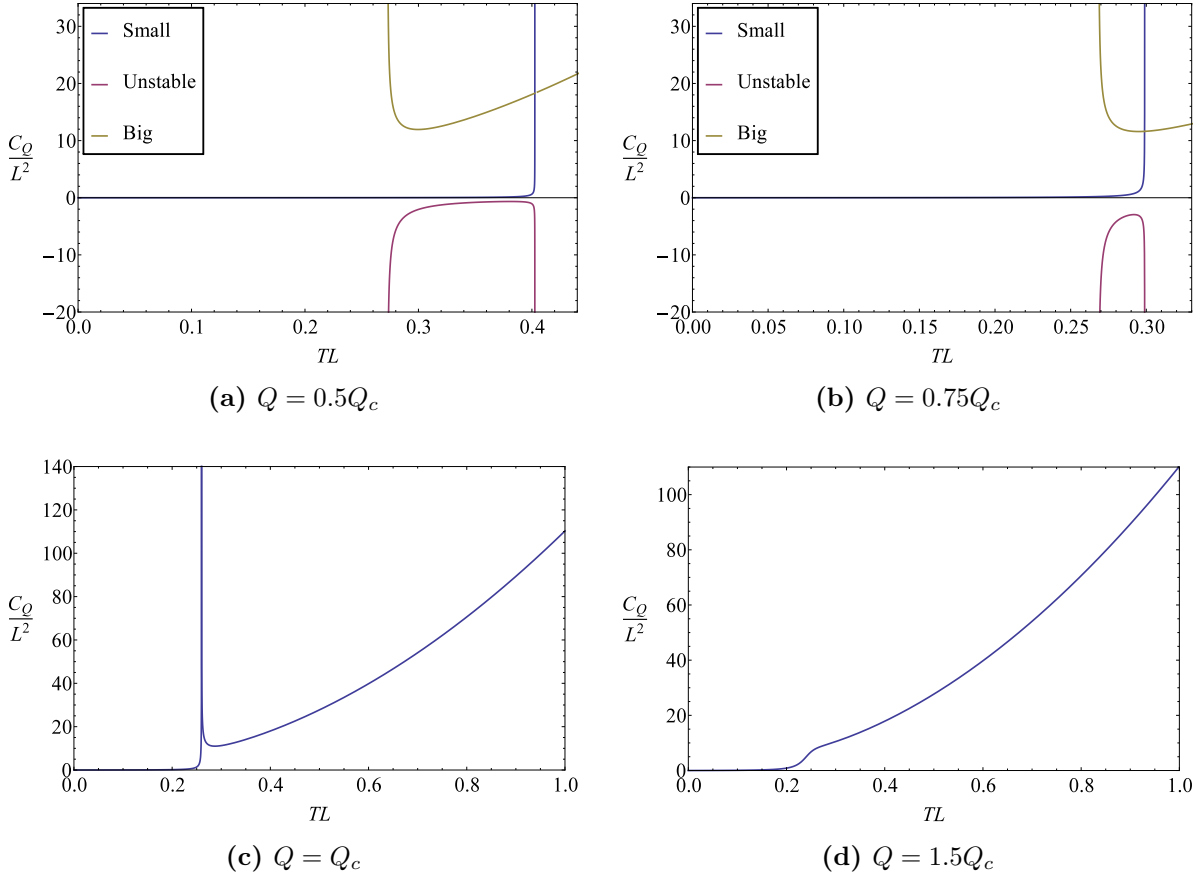


**Figure 3.7:** The heat capacities of the charged black holes as a function of the Hawking temperature. For the case  $Q < Q_c$  there are three branches, labeled by "big" for the largest radius, "small" for the smallest radius and "unstable" for the intermediate one. For  $Q \geq Q_c$  there is only one branch.

Henceforth we will refer to the stable solutions as the "small black hole" and the "big black hole" respectively.

Using Eq. (3.8), we can plot the heat capacity as a function of  $T$ . This is done in Fig. 3.7. Note from Fig. 3.7a and Fig. 3.7b that  $C_Q$  has divergences at  $T_1$  and  $T_2$ . In particular,  $C_Q$  diverges at the critical point  $T_c$ , which is visible in Fig. 3.7c. The distinction between the big and small black hole vanishes at this point. As we shall see, a first-order phase transition does occur if  $Q < Q_c$ , at a temperature between  $T_1$  and  $T_2$ .

To summarize, apart from the extremal black hole solution, we have the following possible stable black hole phases.

- For  $Q < Q_c$  and  $T < T_1(Q)$  the small black hole is the only stable solution.
- For  $Q < Q_c$  and  $T \in [T_1(Q), T_2(Q)]$  the small black hole and the big black hole are the two stable solutions.

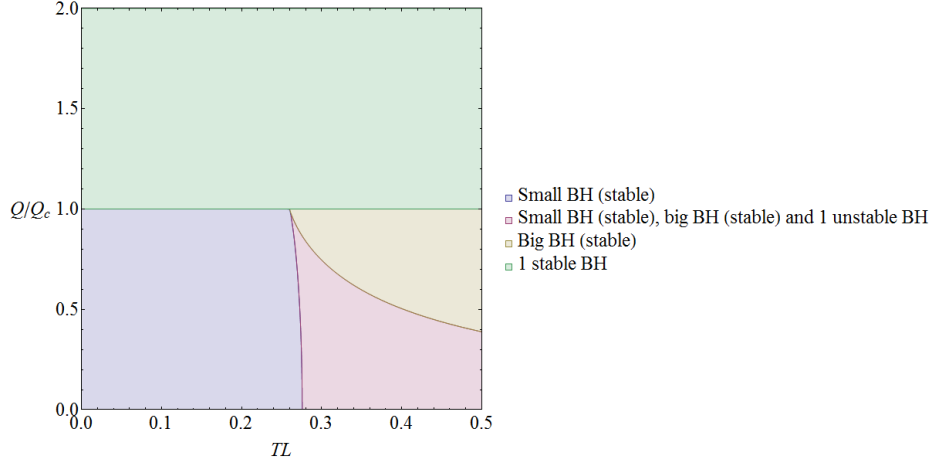


**Figure 3.8:** The stable phases in the  $(T, Q)$ -plane. The extremal black hole is also a solution for any  $T$  and  $\Phi$ .

- For  $Q < Q_c$  and  $T > T_2(Q)$  the big black hole is the only stable solution.
- For  $Q \geq Q_c$  there is one stable charged black hole phase for each temperature.

The stable phases are displayed in the diagram in Fig. 3.8. To promote this diagram to a phase diagram, we only need to find out which of the phases is thermodynamically favorable. This will be done in the next subsection.

In a theory in which electric fluctuations are possible<sup>8</sup>, one must also consider electric stability of the black holes. A black hole is electrically stable if it has a nonnegative isothermal relative permittivity[14], defined by

$$\epsilon_T \equiv \left( \frac{\partial Q}{\partial \Phi} \right)_T. \quad (3.20)$$

Here we do not consider such theories.

### 3.3.3 The phase diagram

Similar to the previous subsection, we calculate the Helmholtz free-energy difference by substituting Eq. (3.7), Eq. (3.8) and the Hawking entropy in Eq. (3.17) and subtract the extremal background<sup>9</sup>. Alternatively, we could use the on-shell action with an extra boundary term to provide the right boundary conditions, see Appendix B for more details. Either method yields a free-energy difference of

$$\Delta F(T, Q) = (M - M_e) - T \frac{A}{4} = \frac{r_+}{4} \left( 1 - \frac{r_+^2}{L^2} + \frac{3Q^2}{L^2} \right) - M_e(Q), \quad (3.21)$$

<sup>8</sup>For example, in a theory which includes charged Kaluza-Klein particles.

<sup>9</sup>One can also use  $F = \Omega + \Phi Q$  and use the result from the grand canonical ensemble.

where  $r_+$  should be considered a function of  $T$  and  $Q$ . Here  $M_e$  is the mass of the extremal black hole, given by Eq. (3.7) with  $r_+ = r_e$  as in Eq. (3.6). The free energy difference is plotted in Fig. 3.9. These free energy plots contain all the information about the phase structure. First of all, notice that for all nonzero temperatures there is always at least one solution with  $\Delta F < 0$ , such that the extremal black hole is never thermodynamically preferred. Secondly, for  $Q < Q_c$ , the unstable black hole is never thermodynamically preferred over any of the (meta)stable states, as follows from Fig. 3.9a and Fig. 3.9b. These figures also show that a phase transition occurs between the small and the big black hole at some temperature  $T_{tr}(Q)$  in the range  $(T_1(Q), T_2(Q))$ . Clearly, as the black hole radius discontinuously changes with at phase transition, the entropy is also discontinuous, making this a first order phase transition. From Fig. 3.9c and Fig. 3.9d it follows that for  $Q > Q_c$ , the unique black hole solution is always thermodynamically favorable. The main difference between these two figures is that the free energy at  $Q = Q_c$  contains a kink at the critical point, whereas the free energy for  $Q > Q_c$  is smooth. One can show that at this kink, the second derivative  $\left(\frac{\partial^2 F}{\partial T^2}\right)_Q$  is discontinuous, so that the Ehrenfest classification suggests a second order phase transition.

With the information above, we are able to plot the phase diagram in Fig. 3.10. Summarizing, the phase diagram looks as follows, ignoring the extremal black hole solution.

- For  $Q < Q_c$  and  $T \leq T_1(Q)$ , the small black hole is thermodynamically preferred and it is the only stable solution.
- For  $Q < Q_c$  and  $T_1(Q) < T < T_{tr}(Q)$ , the small black hole is thermodynamically preferred and the big black hole is metastable.
- For  $Q < Q_c$  and at  $T = T_{tr}(Q)$ , a first-order phase transition between the small black hole and the big black hole occurs.
- For  $Q < Q_c$  and  $T_{tr}(Q) < T < T_2(Q)$ , the big black hole is thermodynamically preferred and the small black hole is metastable.
- For  $Q < Q_c$  and  $T \geq T_2(Q)$ , the big black hole is thermodynamically preferred and it is the only stable solution.
- At  $Q = Q_c$  and  $T = T_c$  there is a critical point. The transition between the small and the big black hole vanishes and the phases become indistinguishable, i.e. they merge into one phase.
- For  $Q \geq Q_c$ , there is only one black hole solution, which is the thermodynamically preferred solution.

Note that in the range  $(T_1(Q), T_2(Q))$ , the unstable black hole solution provides a free energy barrier between the small and the big black hole.

To conclude, we compute the critical exponent corresponding to the heat capacity at the critical point. In order to do so, we expand  $T - T_c$  around the critical event horizon  $r_c$ . Since the critical

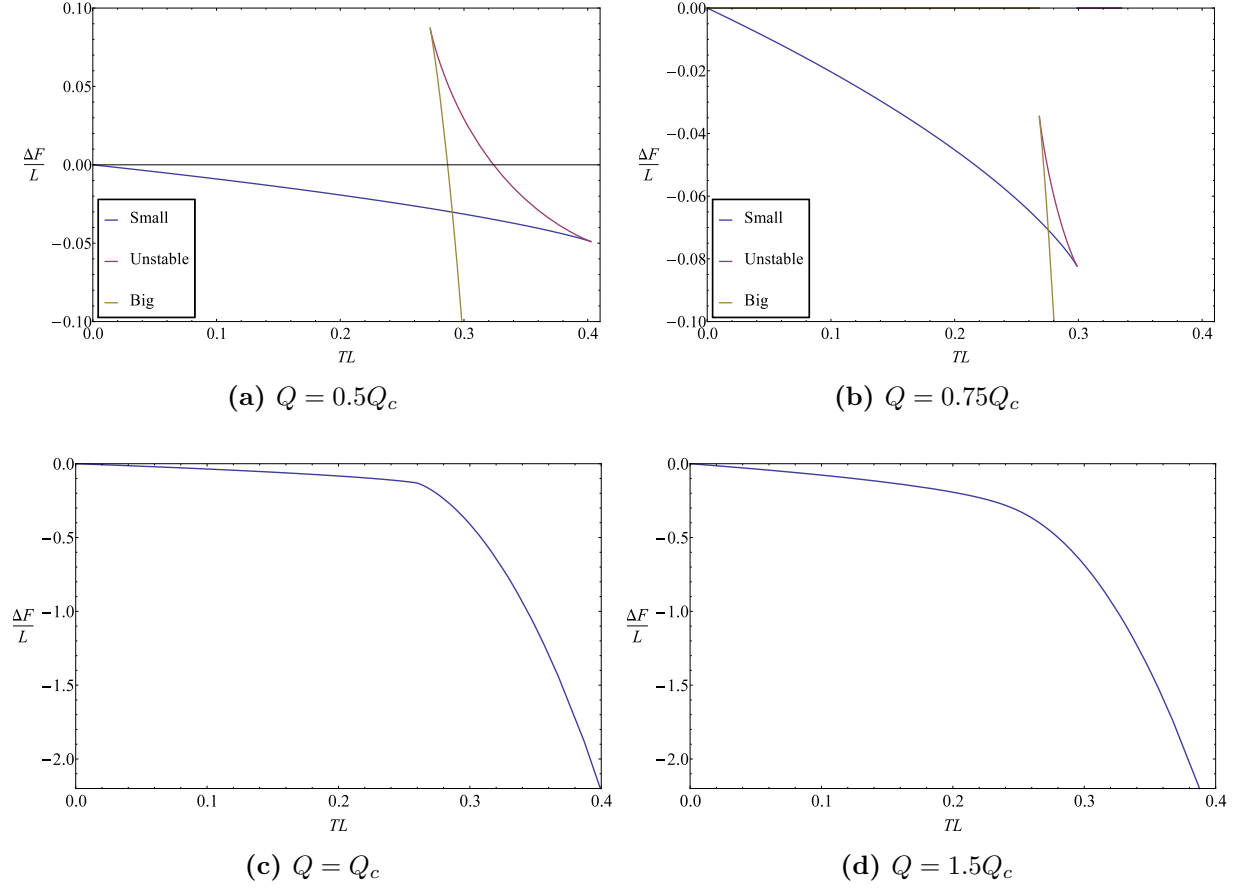


**Figure 3.9:** The Helmholtz free energies of the charged black holes as a function of the Hawking temperature, with respect to the extremal black hole solution. For the case  $Q < Q_c$  a phase transition occurs at the intersection of the free energy of the small and big black hole. For  $Q \geq Q_c$  there is only one branch. Note the kink in the free energy for  $Q = Q_c$ .

point is a point of inflection, this yields that  $T - T_c \propto (r_+ - r_c)^3$ . Therefore

$$\left(\frac{\partial T}{\partial r_+}\right)_Q = \left(\frac{\partial}{\partial r_+}(T - T_c)\right)_Q \propto (r_+ - r_c)^2 \quad (3.22)$$

Furthermore, at the critical point, the temperature is  $T = T_c$  and using the Hawking entropy we find that  $\left(\frac{\partial S}{\partial r_+}\right)_Q = 2\pi r_c$ . Therefore we find for the heat capacity that near the critical point

$$C_Q \approx T_c \frac{2\pi r_c}{\alpha(r_+ - r_c)^2} \propto (r_+ - r_c)^{-2} \propto (T - T_c)^{-2/3} \quad (3.23)$$

with  $\alpha$  a constant. Hence we find a critical exponent  $\frac{2}{3}$  for the heat capacity.

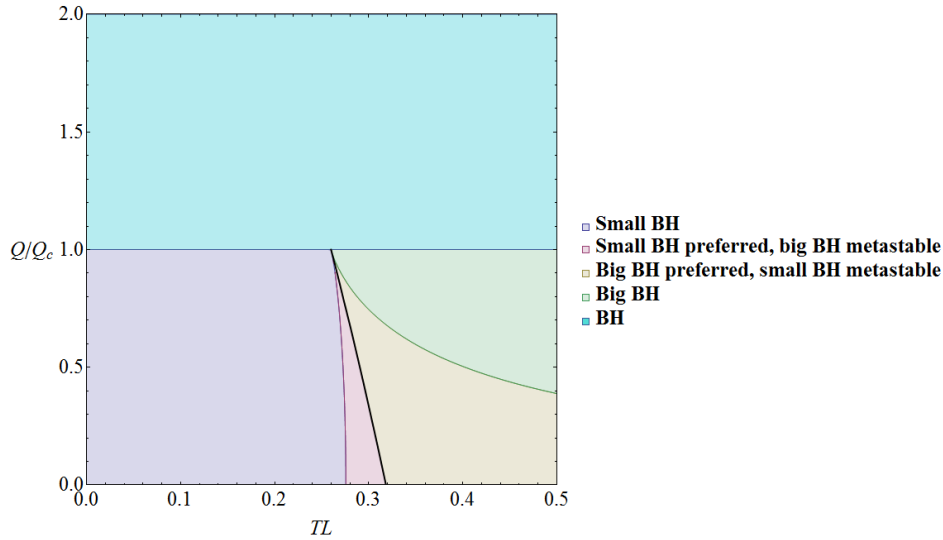


**Figure 3.10:** The phase diagram of the charged black hole in the  $(T, Q)$ -plane. The legend only mentions the (meta)stable states. In the purple and the yellow region, there is also an unstable black hole state. In crossing the thick black curve, a first-order phase transition occurs. This curve of phase transitions ends in a critical point.

### 3.4 Summary

In this chapter we outlined the phase structure of charged black holes in an asymptotically AdS spacetime. These phase structures depend on the choice of our ensemble. If we choose to fix the electric gauge field at infinity  $\Phi$ , the phase diagram shows behavior very similar to the Hawking-Page phase transition, showing a transition from a thermal radiation phase to the black hole phase. However, above some critical value of  $\Phi$ , the black hole phase becomes the globally stable solution at any temperature, so that no phase transitions occur above this value of  $\Phi$ .

In contrast, if we choose to fix the total black hole charge  $Q$ , the phase structure changes completely. For any nonzero charge, the thermal AdS phase is no longer a solution to the Einstein equations, making a phase transition similar to the Hawking-Page phase transition impossible. Rather, the nonzero charge creates another stable branch of black hole solutions, so that a discontinuous phase transition can occur between two differently sized black holes. Above some critical value of  $Q$ , these two black hole solutions coalesce and phase transitions no longer occur. As in the grand canonical ensemble, the unique black hole phase is then the globally stable solution at any temperature. Notice the similarity here with the well-known result from thermodynamics that the differences between thermodynamic ensembles vanish in the thermodynamic limit. Moreover, notice the similarity with the liquid-vapour phase diagram, as it contains a curve of first-order phase transitions with a second-order phase transition as its end point.

A peculiar feature of the phase diagrams in this chapter is that at zero temperature, the dominating phase can still be a black hole. This happens in the canonical ensemble for any nonzero

$Q$ , and in the grand canonical ensemble when  $\Phi > 1$ . Naturally, these extremal black holes have a nonzero area, and therefore a positive Hawking entropy. Thus, if the black hole entropy at zero temperature is indeed given by the Hawking entropy, this could imply that the ground state is unstable as it is highly degenerate. Over the years it has been argued several times that an extremal black hole *does* have a vanishing entropy, thereby violating the Hawking entropy [18]. On the other hand, in certain cases string theory can provide us with a number of extremal black hole microstates which exactly yield the Hawking entropy [19]. To circumvent a highly degenerate ground state, one could argue that there must be more solutions than the ones we have considered this chapter. For example, one could add a charged scalar field to the action and see whether this yields new solutions, which at  $T = 0$  have vanishing entropy and are favorable over the black hole solution. We will not do this here, but in chapter 5 we will see that this is indeed what happens for planar black hole solutions.

## Chapter 4

# Black Hole Phase Transitions in a Minkowski Box

In the previous chapter, we obtained a beautiful phase structure for charged black holes in asymptotically anti-de Sitter spacetimes. What happens if we repeat the same analysis in an asymptotically flat spacetime? Unfortunately, the answer is rather boring, as not much will happen. Let us take the Schwarzschild solution as an example. Computing the temperature using the same method as section yields

$$T_H = \frac{1}{4\pi r_h}. \quad (4.1)$$

One can immediately see from this that the Schwarzschild solution is thermally unstable for any value of its event horizon  $r_h$ , or equivalently its mass  $M$ . Even though the time it would take for the black hole to evaporate is usually several orders larger than the age of the universe<sup>1</sup>[20], in the framework of ensemble theory which we use we consider phase transitions between minima of the free energy.<sup>2</sup>

Then what is so special about asymptotically anti-de Sitter spacetime? The negative cosmological constant basically acts as a confining box. Due to the extra term in the anti-de Sitter metric with respect to the Minkowski metric, massive particles cannot escape to infinity [1]. Indeed, the extra term yields an effective potential which *increases* as  $O(r^2)$  as one approaches spatial infinity [21]. The effect is that there is an infinite potential barrier at spatial infinity, which acts as a confining wall.

As we shall see in this chapter, it is exactly this confinement that yields a phase diagram such as the ones from the previous chapter. In Minkowski spacetime, there is no such confinement present. However, we can artificially create a confining box by considering asymptotically flat spacetime solutions and introducing a cut-off for the radial coordinate  $r$ . This chapter is devoted

---

<sup>1</sup>Unless the black hole is very small, i.e. if its mass is of the order  $10^{12}$  kg or smaller.

<sup>2</sup>Even if we ignored the Schwarzschild black hole being unstable and continued calculating its free energy, it would never be thermodynamically preferred.

to black hole phase transitions in such Minkowski boxes. In particular, we consider four spacetime dimensions and spherically symmetric charged black hole solutions.

We will start by introducing the formalism of thermodynamic ensembles in curved spacetimes with boundary, as proposed in various papers by York et al. This differs from the approach used in the previous chapters in that we use quantities like the physical temperature at the boundary, rather than the Hawking temperature, to define the ensemble. Using this formalism, we will then continue in the same way as the previous chapters. In particular, we will calculate the temperature of charged black hole solutions, investigate their thermal stability and calculate the thermodynamic potential to see which solution is thermodynamically preferred. For this, we were inspired by [23] and [33].

## 4.1 The York formalism

The York formalism is a formalism for thermodynamic ensembles in curved spacetimes with boundary. It was first introduced in [22] and later reintroduced in various other papers by York, Brown, Braden and others [11][23].

In flat spacetime, one can specify a thermodynamic ensemble by keeping a certain set of macroscopic quantities constant throughout the entire system. For example, in the microcanonical ensemble, the number of particles  $N$ , the volume  $V$  and the total energy  $E$  are fixed. The partition function can then be expressed as a function of these parameters, from which all thermodynamic properties of the system can be derived.

In curved spacetime, this definition cannot be used. For example, we cannot fix the total energy throughout the system. Taking the Schwarzschild solution as an example, we have that the energy-momentum tensor vanishes everywhere. There is no well-defined notion of a local gravitational energy-momentum tensor [24]. Even for quantities for which a local notion does exist, we run into trouble if we try to fix them throughout the system. For example, equation Eq.(2.10) tells us that the temperature is redshifted in curved spacetime, such that we cannot keep it constant throughout the system.

Then how do we define, for example, the energy of the system? There exist many different notions of mass or energy in general relativity [15][16][17][24][25][26][27][28], which are not all equivalent [29]. For more information on this, see appendix A. However, the notions have in common that the mass or energy is defined as a surface integral over the boundary of the spacetime. Similarly, all variables which are derived from the energy-momentum tensor (e.g. energy and angular momentum), as well as other extensive variables like electric charge, can be expressed in terms of such surface integrals [26]. Hence these variables are *globally defined quantities, completely determined by the boundary data*.

Similarly, when dealing with variables such as temperature and electrostatic potential, *we consider their fixed value at the boundary of the spacetime*. It can be checked that this is consistent with



the definition of the extensive quantities above, if we use the definitions as in [26]. For example, fixing the temperature  $T = \beta^{-1}$  at the boundary  $r = r_B$  of the spacetime, we can check that the (quasilocal) energy as defined by the surface integral indeed coincides with [11]

$$E = - \left( \frac{\partial \log Z}{\partial \beta(r_B)} \right)_X \quad (4.2)$$

where  $Z$  is the partition function and  $X$  is short for the other fixed quantities in the ensemble.

Thus, in the York formalism, the quantities which are fixed in the definition of the thermodynamic ensemble are all boundary data. Indeed, the partition function in the path integral formulation depends on the boundary values which need to be chosen in order to make the variational problem well defined. These are exactly the boundary data which define the ensemble. In order to change to a different ensemble, one adds boundary terms to the action. This is similar to a Legendre transformation. Intuitively, we can for example think of the spacetime being immersed in a heat bath, such that its boundary should attain the temperature of the heat bath in case of thermal equilibrium.

Note that this formalism differs from the method we applied in the previous two chapters. In particular, in those chapters we defined the ensembles using the Hawking temperature and the temporal gauge field  $A_t$  at infinity. In contrast, the York formalism uses the physical temperature and electrostatic potential at the boundary of the spacetime. In an asymptotically AdS spacetime this is troublesome. To see why, try to calculate the physical temperature at the boundary of an asymptotically AdS spacetime. Using that for such spacetimes  $g_{\tau\tau} \rightarrow \infty$ , Eq. (2.10) immediately yields that the physical temperature vanishes at the boundary. Similarly, the electrostatic potential vanishes on the boundary. Nevertheless, it is possible to apply the York formalism by introducing a cut-off at some finite radius  $r_B$  and taking the limit  $r_B \rightarrow \infty$  at a suitable moment in the calculation. We will not discuss this method here. However, in [31] it is shown that this yields the phase structure from the previous chapter for the grand canonical ensemble. Notice that we indeed matched the *asymptotics* of the temperatures of two solutions at some cut-off when we calculated the on-shell action.

Let us think for a moment about the question *why* the temperature vanishes at the boundary of an asymptotically AdS spacetime. At first sight this might be counterintuitive. In such spacetimes, massless particles can reach the boundary in a finite time. Then why would Hawking radiation consisting of such particles<sup>3</sup> not yield a finite temperature? Although the massless particles will indeed reach the boundary, when they do so, their energy will be completely redshifted to zero. Therefore the spectrum at infinity has no energy and hence does not give a finite temperature.

---

<sup>3</sup>For black holes with large mass ( $\gtrsim 10^{14}$  kg) Hawking radiation indeed consists of massless particles [30]. Although for smaller black holes massive particles do appear in the spectrum, they cannot reach the boundary of an asymptotically AdS spacetime.

## 4.2 The black hole solutions

The Euclidean action we consider in this chapter is the Einstein-Hilbert-Maxwell action given by [23]

$$I = -\frac{1}{16\pi} \int_M d^4x \sqrt{g} (R - F_{\mu\nu} F^{\mu\nu}) - \frac{1}{8\pi} \int_{\partial M} d^3x \sqrt{h} (K - K^0). \quad (4.3)$$

Here  $K$  is the extrinsic curvature, as defined in appendix A, and  $\gamma$  is the determinant of the induced metric on the boundary. The boundary action is added to make the variational method well defined and such that the free energy of flat spacetime equals zero. The black hole solution to the corresponding Einstein Equations is the well-known Reissner-Nordström solution with mass  $M$  and charge  $Q$ . The Euclidean metric tensor is given by[1]

$$ds^2 = f(r)d\tau^2 + \frac{1}{f(r)}dr^2 + r^2d\Omega_2^2 \quad (4.4)$$

with

$$f(r) = 1 - \frac{2M}{r} + \frac{Q^2}{r^2} = \left(1 - \frac{r_+}{r}\right) \left(1 - \frac{Q^2}{r_+r}\right). \quad (4.5)$$

Here,  $r_+$  is the largest event horizon, i.e. the largest real solution of  $f(r) = 0$ . We eliminated  $M$  using  $f(r_+) = 0$ , i.e.

$$M = \frac{r_+}{2} \left(1 + \frac{Q^2}{r_+^2}\right). \quad (4.6)$$

In order to prevent a naked singularity, we require that

$$r_+ \geq Q. \quad (4.7)$$

When the equality holds, the black hole is extremal. Preventing conical singularities using the same method as in section 4 yields the Hawking temperature

$$T_H = \frac{1}{4\pi r_+} \left(1 - \frac{Q^2}{r_+^2}\right). \quad (4.8)$$

The physical temperature is then given by

$$T(r) = \frac{T_H}{\sqrt{f(r)}}. \quad (4.9)$$

In the coordinates we have chosen, the imaginary time is periodic in the inverse Hawking temperature rather than the physical temperature.

As explained in the introduction, we consider a spacetime with a cut-off  $r_B$  for the radial coordinate  $r$ . The thermodynamic ensemble is then defined by the physical temperature at  $r_B$ . Using Eq. (4.9) this is equal to

$$T \equiv T(r_B) = \frac{1}{4\pi r_+} \left(1 - \frac{Q^2}{r_+^2}\right) \left( \left(1 - \frac{r_+}{r_B}\right) \left(1 - \frac{Q^2}{r_+ r_B}\right) \right)^{-1/2}. \quad (4.10)$$

Notice the difference with the temperature in the asymptotically AdS spacetime, Eq. (3.8). In contrast to the black hole in AdS spacetime, the second factor misses a term  $\frac{3r_+^2}{L^2}$ . This term is a consequence of the confining potential of AdS spacetime and it is exactly this term that results in the stable big black hole solution. Indeed, it results in a positive heat capacity for large  $r_+$ . Here, instead of this confining potential, we have an extra factor  $1/\sqrt{f(r_B)}$ , corresponding to the redshifted temperature. Although this term is very different from the confining potential term in AdS, we see they have one effect in common: they both result in an additional stable big black hole solution. One can see this immediately from elementary analysis. First notice that  $1/\sqrt{f(r_B)} \geq 1$ . Moreover, as  $r_+ \rightarrow r_B$  the factor and hence the temperature diverges to  $\infty^4$ . By continuity this must imply that there exists an open interval with limit point  $r_B$  where the temperature increases as a function of  $r_+$ , which means that the heat capacity is positive there.

As in the previous chapter, the gauge field is given by

$$A = \left( -\frac{Q}{r} + \phi \right) dt \quad (4.11)$$

and for black hole solutions, the gauge is fixed using

$$\phi = \frac{Q}{r_+} \quad (4.12)$$

such that the norm of  $A$  does not diverge on the event horizon. Thus, on the boundary we have

$$A_t(r_B) = \frac{Q}{r_+} - \frac{Q}{r_B} \quad (4.13)$$

such that the redshifted physical electrostatic potential on the boundary is given by

$$\Phi \equiv \frac{1}{\sqrt{f(r_B)}} \left( \frac{Q}{r_+} - \frac{Q}{r_B} \right). \quad (4.14)$$

As usual, the phase structure depends on the thermodynamic ensemble. In the remaining of this chapter, we will first treat the uncharged case and then proceed with the grand canonical and the canonical ensemble. In each case we will compare the obtained results with the ones from the previous chapter.

Since the action does not depend on the sign of  $Q$ , we will assume without loss of generality that  $Q \geq 0$  and  $\Phi \geq 0$ .

### 4.3 The Schwarzschild black hole

For the uncharged black hole, the boundary temperature is given by

$$T = \frac{1}{4\pi r_+} \left( 1 - \frac{r_+}{r_B} \right)^{-1/2}. \quad (4.15)$$

---

<sup>4</sup>Indeed, the physical temperature measured at the event horizon is infinite. Note that  $r_+ = r_B$  is meaningless, since then the range of the radial coordinate is empty, so that we are not describing a spacetime at all.

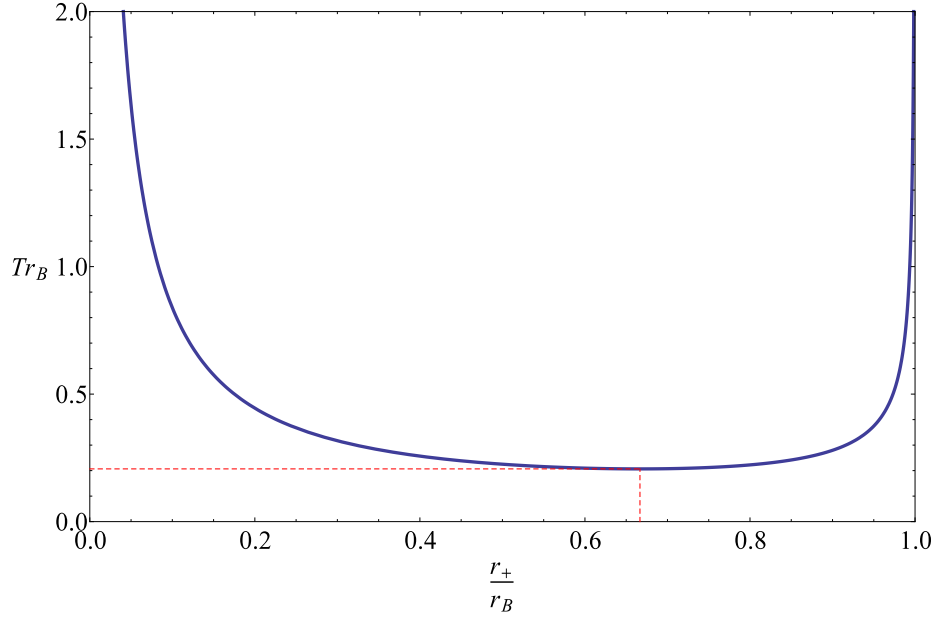


**Figure 4.1:** The temperature of the Schwarzschild black hole solution as a function of its radius. The red dashed line pieces mark the positions of  $r_{min}$  and  $T_{min}$ .

Notice that in this case, we cannot use the First Law in the form  $dM = TdS$ , as this form is based on the Hawking temperature of the black hole. The First Law is now given by

$$dE(r_B) = T(r_B)dS \quad (4.16)$$

where  $E(r_B)$  is the so-called quasilocal energy as defined in [26]. The relation between the mass  $M$  and the quasilocal energy is given by [23]

$$M = E(r_B) - \frac{E(r_B)^2}{2r_B} \quad (4.17)$$

such that they coincide when  $r_B \rightarrow \infty$ . Notice that the second term can be interpreted as the gravitational binding energy needed to bring the mass from infinity to the inside of the cavity.

The temperature Eq. (4.15) has a minimum at  $r_{min} = \frac{2}{3}r_B$ , given by

$$T_{min} = \frac{3\sqrt{3}}{8\pi r_B}. \quad (4.18)$$

This is visible in Fig. 4.1. Hence the Schwarzschild black hole cannot exist for temperatures  $T < T_{min}$ . For temperatures  $T > T_{min}$  we see that there are two black hole solutions. Furthermore, for each temperature the thermal Minkowski solution, given by Eq. (4.4) with  $f \equiv 1$ , is a solution. Let us immediately discuss the thermal stability of the phases. As always, the heat capacity is positive if and only if  $\frac{\partial T}{\partial r_+} > 0$ . Hence, only the larger of the two black hole solutions is thermally stable. The smaller black hole solution provides an energy barrier between the large black hole

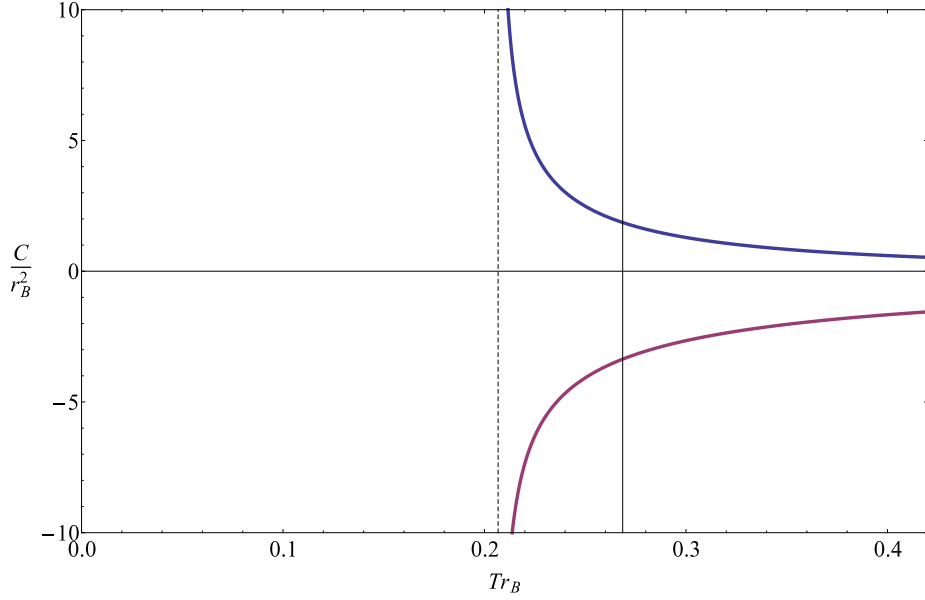


**Figure 4.2:** The heat capacities of the Schwarzschild black holes as a function of the temperature. The blue curve corresponds to the big black hole solution, which is stable. The purple curve corresponds to the small black hole solution, which is unstable. The vertical gray line denotes the temperature of the Hawking-Page phase transition, while the dashed line marks  $T_{min}$ .

solution and thermal Minkowski. To summarize, for a fixed temperature  $T$  we have the following stable possible phases<sup>5</sup>:

- For  $T < T_{min}$ , the only possible phase is the thermal Minkowski solution.
- For  $T \geq T_{min}$ , the stable phases are thermal Minkowski and the big Schwarzschild black hole.

In Fig. 4.2 the heat capacities of the two black hole solutions are plotted as a function of the temperature  $T$ . The heat capacity diverges at the point  $r_{min}$ , where one black hole branch ends and the other begins. As before, this is not the point where a phase transition occurs, but rather the point at which a black hole solution can start to exist in (meta)stable equilibrium. To see where the phase transition does occur, we investigate the free energy difference between the black hole solutions and thermal Minkowski. Evaluating the on-shell action Eq. (4.3), this yields

$$\Delta F = r_B \left( 1 - \sqrt{1 - \frac{r_+}{r_B}} \right) - \frac{r_+}{4\sqrt{1 - \frac{r_+}{r_B}}} \quad (4.19)$$

This can also be obtained by simply substituting the quasilocal energy, the Hawking entropy and Eq. (4.15) in  $F(r_B) = E(r_B) - T(r_B)S$ . The free energy is plotted as a function of the temperature in Fig. 4.3. We see that the unstable black hole is never thermodynamically preferred over a stable

<sup>5</sup>Here we ignore the possible existence of a temperature above which any thermal radiation would collapse to a black hole.

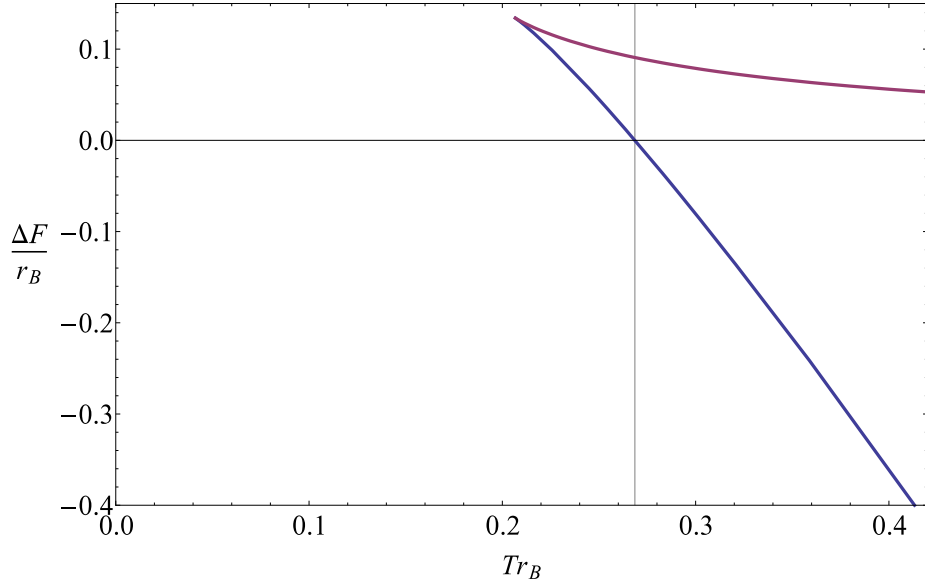


**Figure 4.3:** The Helmholtz free energies of the Schwarzschild black holes as a function of the temperature. The blue curve corresponds to the big black hole solution, whereas the purple curve corresponds to the small black hole solution. The vertical line denotes the phase transition temperature.

solution. Moreover, a first-order phase transition occurs at the temperature

$$T_c = \frac{27}{32\pi r_B}. \quad (4.20)$$

Using the free energy, we can plot the diagram in figure 4.4. Here, the blue curve denotes the energetically favorable state while the red dashed curves denote metastable states. The mass of the black hole is an order parameter. At the critical temperature  $T_c$ , the energetically favorable mass jumps to a nonzero value  $M_c$ . According to the Ehrenfest classification, this implies that the phase transition is a first-order phase transition.

To summarize, we have found the following results for the phase diagram:

- For all temperatures at which the unstable black hole exists, it is thermodynamically unfavorable.
- For temperatures  $T < T_{min}$ , the Schwarzschild black hole cannot exist, so Minkowski space-time filled with thermal radiation is the only possible solution.
- For temperatures  $T \in [T_{min}, T_c)$  with  $T_c$ , thermal Minkowski is the energetically favorable solution and the Schwarzschild black hole is a metastable state.
- At the temperature  $T = T_c$  a first-order phase transition takes place.
- For temperatures  $T > T_c$ , the stable Schwarzschild black hole is the energetically favorable solution and thermal radiation is a metastable state.

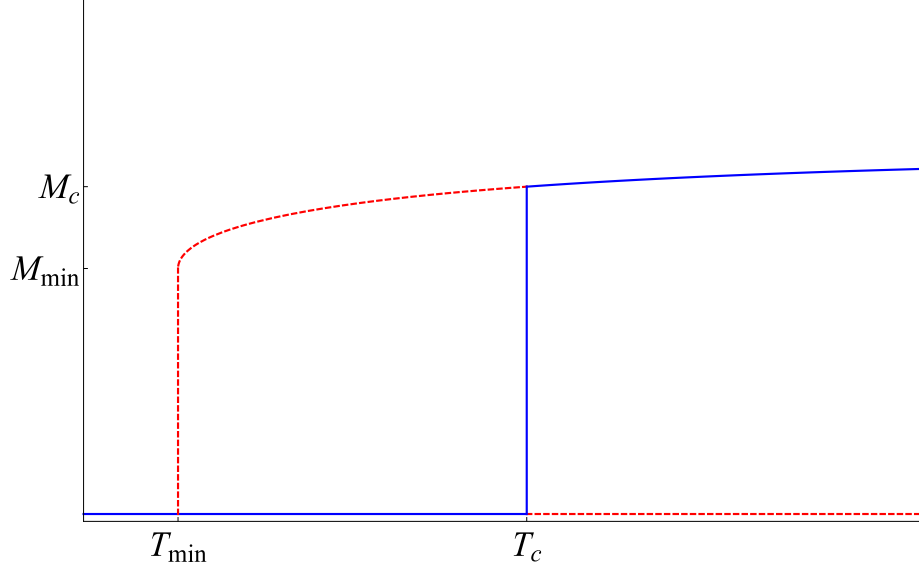


**Figure 4.4:** The order parameter for the Schwarzschild black hole. The blue curve represents the energetically favorable solution, whereas the dashed curves denote a metastable solution.

Notice that these results are very similar to the Hawking-Page phase transition. Comparing the graphs Fig. 4.1, Fig. 4.2 and Fig. 4.3 to their AdS counterparts Fig. 2.1, Fig. 2.2 and Fig. 2.3, we see that they are not completely identical. There is no reason that we would expect them to be. However, the thermodynamics are very similar. Hence we see that redshift factor in the temperature due to the confinement within the box  $r < r_B$  has an effect similar to the confining potential in asymptotically AdS spacetimes. Both result in an additional larger black hole which is stable and in the occurrence of a first-order phase transition.

## 4.4 The Reissner-Nordström black hole in the grand canonical ensemble

In the grand canonical ensemble we fix the temperature  $T$  and the electrostatic potential  $\Phi$  at the boundary. As before, we start with investigating which phases exist for given values of  $T$  and  $\Phi$ .

### 4.4.1 The stable phases

One phase that exists for any value of  $T$  and  $\Phi$  is the thermal Minkowski solution together with the constant gauge field  $A_t = \Phi$ . To investigate the black hole solutions, we write the temperature in terms of the electrostatic potential  $\phi$  using Eq. (4.14). After a bit of algebra this yields [23]

$$T = \frac{1}{4\pi r_+} (1 - \Phi^2) \left( 1 - (1 - \Phi^2) \frac{r_+}{r_B} \right)^{-1/2}. \quad (4.21)$$

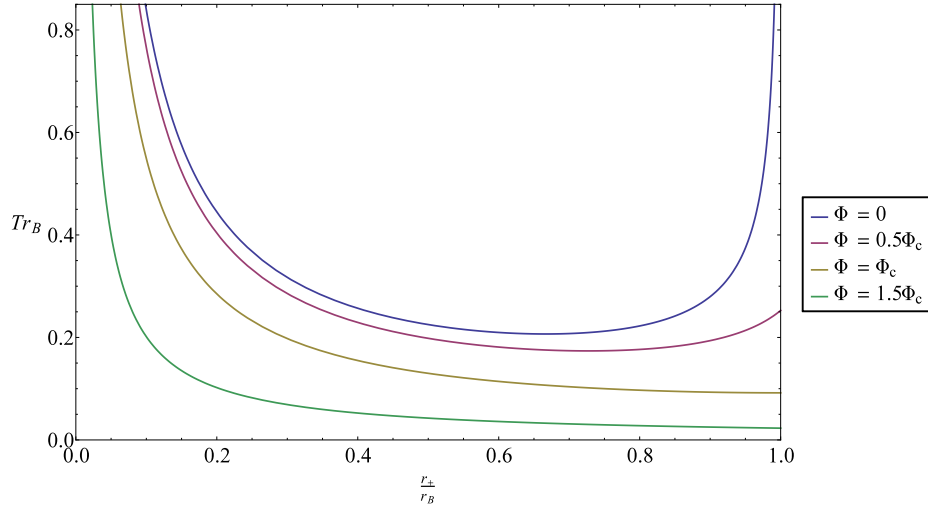


**Figure 4.5:** The temperature of the black hole solution for different values of  $\Phi$ .

It immediately follows from this equation that there are no black hole solutions for  $\Phi > 1$ . The value  $\Phi = 1$  corresponds to an extremal black hole. The temperature is plotted in Fig. 4.5 for several values of  $\Phi$ . We see that when  $\Phi$  is small enough, i.e.  $\Phi < \Phi_c = \frac{1}{\sqrt{3}}$ , there are two black hole solutions. As we increase  $\Phi$ , the bigger black hole solution's radius increases, until for  $\Phi \geq \Phi_c$  it falls outside the range  $r_+ < r_B$ , so that there is only one black hole solution if  $\Phi_c \leq \Phi \leq 1$ . Moreover, we see that for any  $\Phi < 1$  there is a minimal temperature required for a black hole to exist. It is given by

$$T_{min}(\Phi) = \frac{3\sqrt{3}}{8\pi} (1 - \Phi^2)^2 \quad (4.22)$$

if  $\Phi \leq \Phi_c$ , or by

$$T_{min}(\Phi) = \frac{1}{4\pi\Phi} (1 - \Phi^2) \quad (4.23)$$

if  $\Phi \geq \Phi_c$ .<sup>6</sup> What is new here, is that for  $\Phi < \Phi_c$  there must also be a supremum temperature for the big black hole solution, in order to make sure that  $r_+ < r_B$ . This we denote by  $T_{max}(\Phi)$  and it is given by the same equation as Eq. (4.23), but here for  $\Phi < \Phi_c$ .

We can infer the thermal stability of the solutions from the plot. As usual, the solution is stable if  $\left(\frac{\partial T}{\partial r_+}\right)_\Phi > 0$ . From this it follows that for a given  $T$  and  $\Phi$ , we have the following stable phases:

- For any  $\Phi$  and for  $T < T_{min}(\Phi)$ , the only possible phase is the thermal Minkowski phase.
- For  $\Phi < \Phi_c$  and  $T_{min}(\Phi) \leq T < T_{max}(\Phi)$  the stable phases are the thermal Minkowski phase and the big black hole solution. The small black hole is unstable.
- For  $\Phi < \Phi_c$  and  $T \geq T_{max}(\Phi)$  the only stable phase is the thermal Minkowski phase. The small black hole is unstable.

<sup>6</sup>Actually, for  $\Phi \geq \Phi_c$   $T_{min}$  is not a minimum but only an infimum, since  $r_+ < r_B$ .



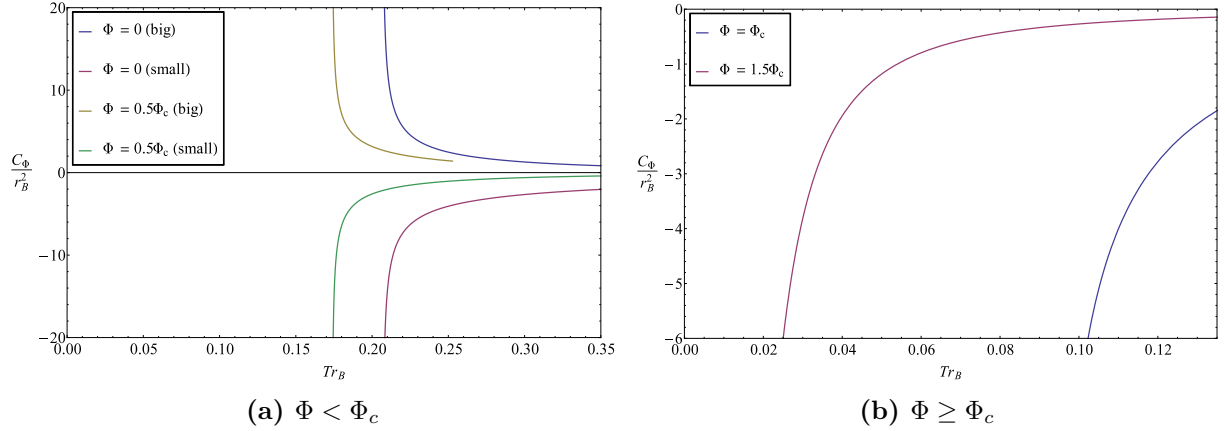


**Figure 4.6:** The heat capacities of the charged black holes as a function of the temperature. For the case  $\Phi < \Phi_c$  there are two branches, labeled by "big" for the larger radius and "small" for the smaller one. For  $\Phi \geq \Phi_c$  there is only one branch.

- For  $\Phi_c \leq \Phi \leq 1$  and  $T \geq T_{min}(\Phi)$ , the only stable phase is the thermal Minkowski phase. The small black hole is unstable.
- For  $\Phi > 1$  the only possible phase is the thermal Minkowski phase.

We have plotted the heat capacity, from which the thermal stability follows, in Fig.4.6 as a function of the temperature. The heat capacity diverges at  $T_{min}$  for  $\Phi \leq \Phi_c$ . As usual, this does not denote a phase transition, but the point where a black hole solution can start to exist in a (meta)stable equilibrium. For  $\Phi \geq \Phi_c$ , the heat capacity is negative, indicating the instability of the black hole solution. Notice that the black hole solutions can only exist for  $r_+ < r_B$ , since we are describing a black hole *inside* the box  $r < r_B$ . This is why the heat capacity of the big black hole at  $\Phi = 0.5\Phi_c$  in Fig. 4.6a is cut off at  $T_{max}$ .

#### 4.4.2 The phase diagram

Next, we will study the grand potential difference with respect to thermal Minkowski in order to find out if and when phase transitions occur. Evaluating the action Eq. (4.3) on shell, or using the definition  $\Omega = E(r_B) - TS - \Phi Q$  yields the grand potential difference

$$\Delta\Omega(T, \Phi) = r_B (1 - f(r_B)) - T\pi r_+^2 - \Phi Q \quad (4.24)$$

where  $f(r_B)$ ,  $r_+$  and  $Q$  are understood as functions of  $T$ ,  $\Phi$  and  $r_B$  through Eq. (4.5), Eq. (4.10) and Eq. (4.14). Numerically, we can plot this as a function of  $T$  for a given  $\Phi$ . This is done in Fig. 4.7. First of all, we see that the unstable solutions are never thermodynamically preferred over a stable solution or thermal Minkowski spacetime. Secondly, from Fig. 4.7a it follows that a first-order phase transition can occur for certain values of  $\Phi < \Phi_c$ . The temperature corresponding to this transition is [23]

$$T_c(\Phi) = \frac{27}{32\pi r_B} (1 - \Phi^2)^2. \quad (4.25)$$



**Figure 4.7:** The grand potential differences of the charged black holes as a function of the temperature. For the case  $\Phi < \Phi_c$  there are two branches, labeled by "big" for the larger radius and "small" for the smaller one. For  $\Phi \geq \Phi_c$  there is only one branch.

Comparing this to the maximum temperature of the big black hole solution, it is easy to show that  $T_c < T_{max}$  iff  $\Phi < \frac{1}{3}$ . Thus a phase transition between thermal Minkowski spacetime and the big black hole can only occur if  $\Phi < \frac{1}{3}$ . Above  $T_c$ , the big black hole solution is thermodynamically unfavorable. Hence we find the following results for the phase diagram:

- For any  $\Phi$  and for  $T < T_{min}(\Phi)$ , the only possible phase is the thermal Minkowski phase.
- For  $\Phi < \frac{1}{3}$  and  $T_{min}(\Phi) \leq T < T_c(\Phi)$  the thermal Minkowski phase is thermodynamically preferred and the big black hole solution is metastable.
- For  $\Phi < \frac{1}{3}$  and  $T_c(\Phi) \leq T < T_{max}(\Phi)$  the big black hole is thermodynamically preferred and the thermal Minkowski solution is metastable.
- For  $\frac{1}{3} \leq \Phi < \Phi_c$  and  $T_{min}(\Phi) \leq T < T_{max}(\Phi)$  the thermal Minkowski phase is thermodynamically preferred and the big black hole solution is metastable.
- For  $\Phi < \Phi_c$  and  $T \geq T_{max}(\Phi)$  the only stable phase is the thermal Minkowski phase.
- For  $\Phi_c \leq \Phi \leq 1$  and  $T \geq T_{min}(\Phi)$ , the only stable phase is the thermal Minkowski phase.
- For  $\Phi > 1$  the only possible phase is the thermal Minkowski phase.

With this we can plot the phase diagram in Fig.4.8. In this diagram we did not include the unstable black hole solution.

Let us compare the results from this section to the results from the asymptotically AdS spacetimes. For small values of  $\Phi$ , meaning  $\Phi < 1$  for the AdS case and  $\Phi < \sqrt{1}\sqrt{3}$  for the Minkowski case, Fig.4.5 and Fig.3.1 show quite similar behavior. In both cases, there are two black hole solutions, of which only the bigger one is thermally stable. Moreover, a first-order phase transition can occur in both cases, if  $\Phi < \frac{1}{3}$  in the Minkowski case. However, there are differences between the confining potential in AdS and the introduction of a cut-off in Minkowski. This is best seen when looking at large values of  $\Phi$ . In the AdS case, when  $\Phi > 1$ , the unstable black hole solution disappears. While this is also true in the Minkowski case, there the stable solution disappears before the unstable one does! This is an artifact of the cut-off: for  $\Phi \geq \frac{1}{\sqrt{3}}$  all stable black hole solutions acquire a radius  $r_+ \geq r_B$  and therefore do not describe a black hole inside the cavity. Moreover, for  $\Phi < \frac{1}{3}$ , all stable black hole solutions which would be thermodynamically preferred over thermal Minkowski spacetime acquire a radius  $r_+ \geq r_B$ , so that a phase transition no longer

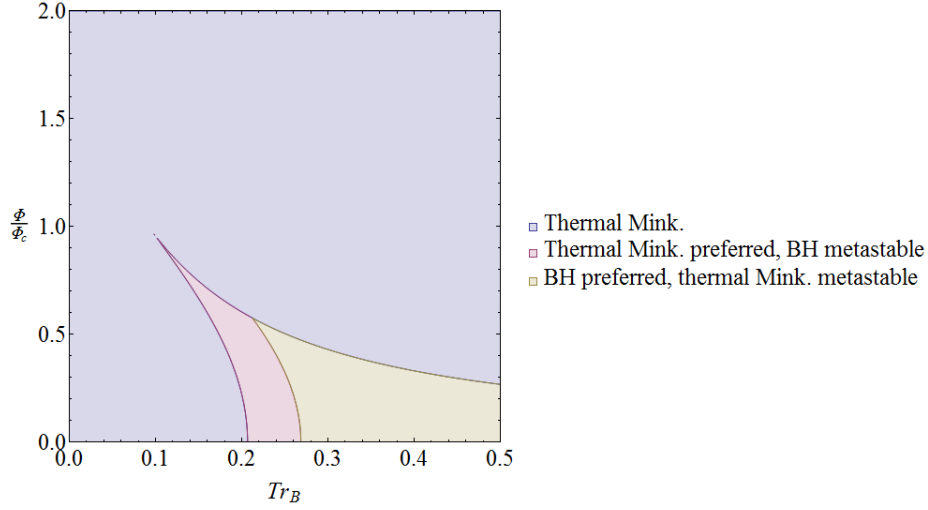


**Figure 4.8:** The phase diagram of the charged black hole in the  $(T, \Phi)$ -plane. The legend only mentions the (meta)stable states. As  $\Phi$  approaches zero, the maximum temperature at which the black hole is preferred goes to infinity.

occurs. In AdS we do not use a cut-off, so that we always have a stable black hole solution which is thermodynamically preferred above some temperature.

## 4.5 The Reissner-Nordström black hole in the canonical ensemble

In the canonical ensemble we fix the temperature  $T$  at the boundary and the charge  $Q$ . As before, we start with investigating which phases exist for given values of  $T$  and  $Q$ .

### 4.5.1 The stable phases

By the same argument as in subsection 3.3.1, we cannot use the thermal Minkowski as a background solution. Instead, we must use an extremal black hole. As we shall see, there is always a stable black hole solution which is preferred over the extremal black hole.

To see which other solutions exist at a given  $T$  and  $Q$ , we look at the plot of the temperature Eq. (4.10) in Fig. 4.9. We see that adding a small charge to the black hole cancels the divergence of the temperature to  $\infty$  at  $r_+ = 0$ . Moreover, a new branch of solutions arises, such that an uncharged black hole can exist at any temperature. We also see that there is a range of temperatures  $(T_1(Q), T_2(Q))$  in which three black hole solutions exist, while for  $T < T_1$  and  $T > T_2$  there is only one black hole solution.

As we increase the charge of the black hole, the range  $(T_1, T_2)$  shrinks until at the charge

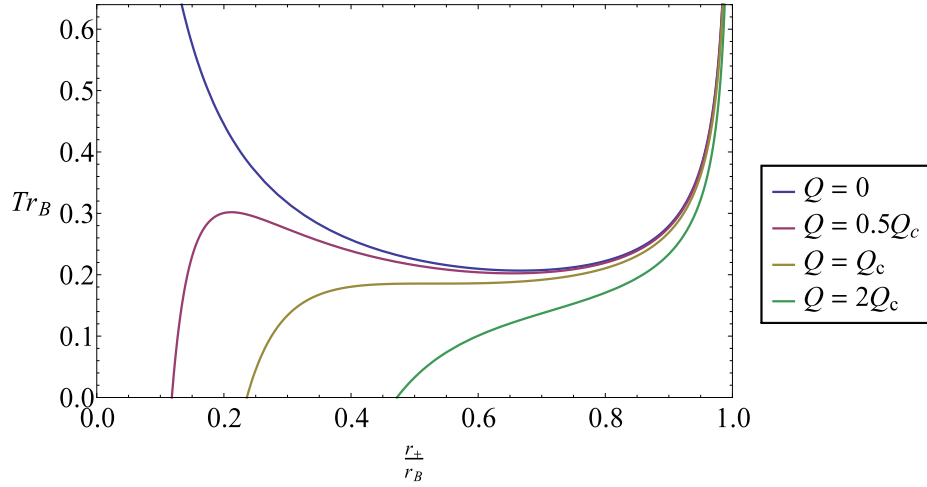


**Figure 4.9:** The temperature of the black hole solution for different values of  $Q$ .

$Q_c = (\sqrt{5} - 2)r_B$ , we have that  $T_1 = T_2 \equiv T_c$ . The point  $(Q_c, T_c)$  corresponds to a critical point, at which the intermediate black hole solution disappears and the distinction between the small and the big black hole vanishes. For charges above  $Q_c$ , there is only one black hole solution.

As usual, we use the criterion  $\left(\frac{\partial T}{\partial r_+}\right)_Q > 0$  to see whether a is stable. Applying this to Fig. 4.9 it follows that for a given  $T$  and  $Q$ , we have the following stable phases:

- For  $Q < Q_c$  and  $T < T_1(Q)$  the small black hole is the only stable solution.
- For  $Q < Q_c$  and  $T \in [T_1(Q), T_2(Q)]$  the small black hole and the big black hole are the two stable solutions. The intermediate black hole solution is unstable.
- For  $Q < Q_c$  and  $T > T_2(Q)$  the big black hole is the only stable solution.
- For  $Q \geq Q_c$  there is one stable charged black hole phase for each temperature.

Fig. 4.10 displays the heat capacities of the black hole solutions as a function of the temperature. The first two figures, Fig. 4.10a and Fig. 4.10b, show that  $C_Q$  has divergences at  $T_1$  and  $T_2$ . In particular this implies  $C_Q$  diverges at the critical point  $(Q_c, T_c)$ , which is visible in Fig. 4.10c. One can show by calculation of the second derivative of  $F$  with respect to the temperature that a second-order phase transition occurs here. First-order phase transitions do occur if  $Q < Q_c$ , at a temperature between  $T_1$  and  $T_2$ . This will be shown in the next subsection.

## 4.5.2 The phase diagram

All that is left is the calculation of the Helmholtz free-energy difference  $\Delta F$ , which will provide us with all the information on the phase structure of the system. The easiest way to calculate the Helmholtz free energy is by using  $F = \Omega + \Phi Q$  and using the grand potential Eq. (4.24).

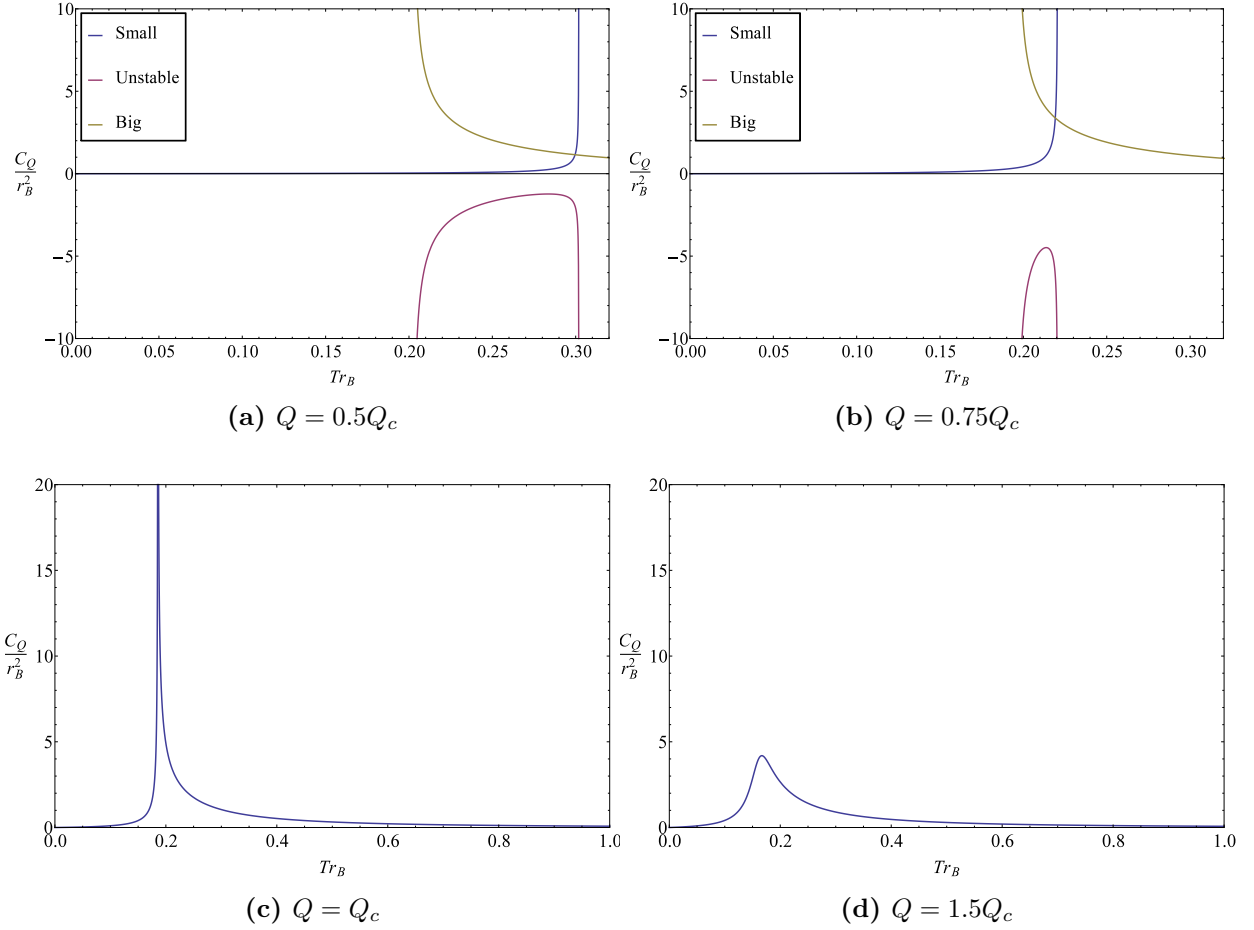


**Figure 4.10:** The heat capacities of the charged black holes as a function of the temperature. For the case  $Q < Q_c$  there are three branches, labeled by "big" for the largest radius, "small" for the smallest radius and "unstable" for the intermediate one. For  $Q \geq Q_c$  there is only one branch.

Subtracting the extremal background, this yields

$$\Delta F(T, Q) = r_B \left( 1 - \sqrt{f(r_B)} \right) - T\pi r_+^2 - M_e Q, \quad (4.26)$$

where  $M_e(Q) = Q$  is the extremal black hole mass. The free-energy difference is shown in Fig. 4.11. The first thing to notice is that for any charge and at any nonzero temperature, there is always at least one non-extremal black hole solution which is thermodynamically favorable. Furthermore, from Fig. 4.11a and Fig. 4.11b we deduce that the unstable black hole is never thermodynamically preferred over a (meta)stable solution. In addition, these figures show that a first-order phase transition occurs between the small and the big black hole at some temperature  $T_{tr}(Q)$  between  $T_1(Q)$  and  $T_2(Q)$ . In Fig. 4.11c we see a kink in the free energy, which marks the critical point. Finally, Fig. 4.11c and Fig. 4.11d show that the unique black hole solution for  $Q \geq Q_c$  is always thermodynamically preferred.

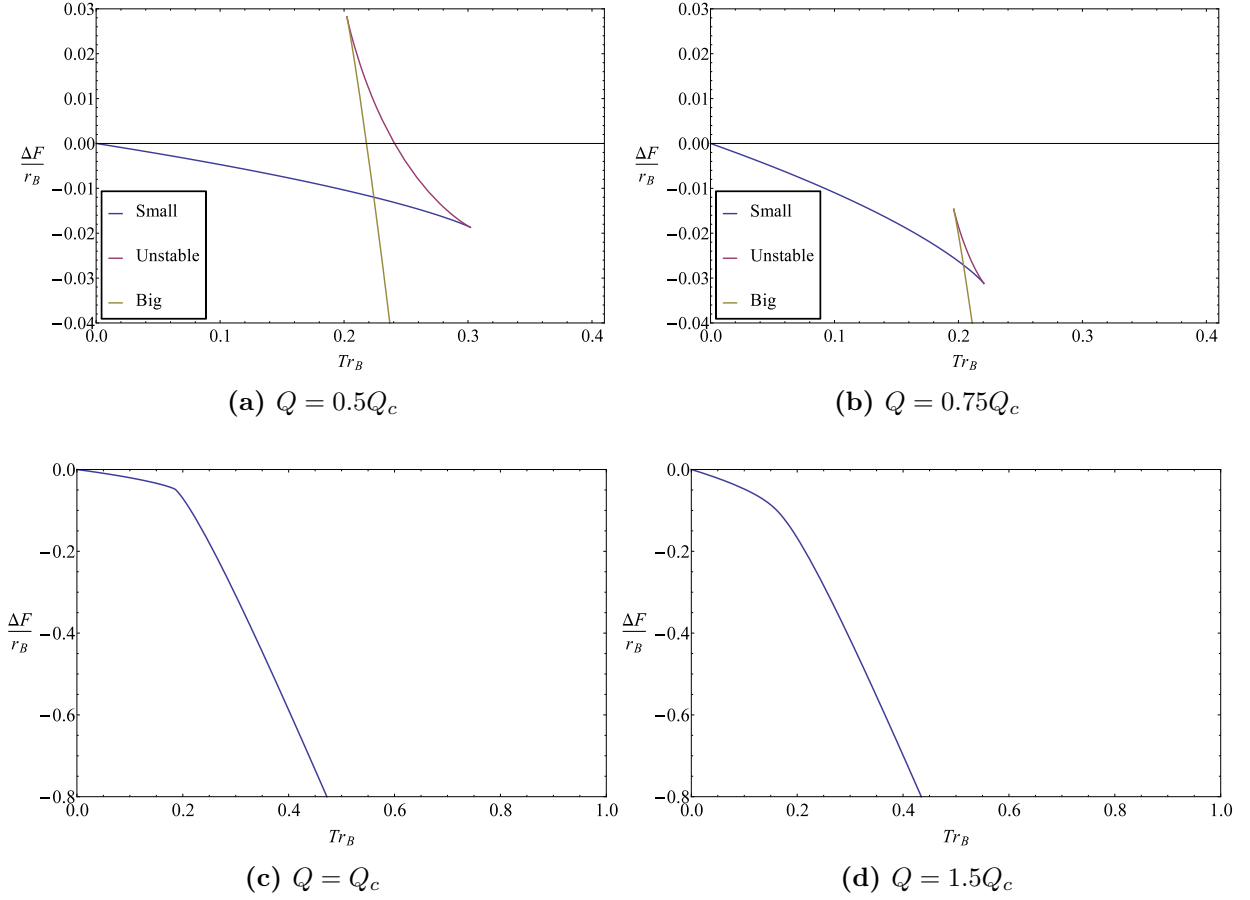


**Figure 4.11:** The Helmholtz free energies of the charged black holes as a function of the temperature, with respect to the extremal black hole solution. For the case  $Q < Q_c$  a phase transition occurs at the intersection of the free energy of the small and big black hole. For  $Q \geq Q_c$  there is only one branch. Note the kink in the free energy for  $Q = Q_c$ .

Having extracted the above information on the phase structure from the free energy, we can draw the phase diagram in Fig. 4.12. The results are summarized below.

- For  $Q < Q_c$  and  $T \leq T_1(Q)$ , the small black hole is thermodynamically preferred. It is the only thermally stable solution.
- For  $Q < Q_c$  and  $T_1(Q) < T < T_{tr}(Q)$ , the small black hole is thermodynamically preferred, while the big black hole is metastable.
- For  $Q < Q_c$  and at  $T = T_{tr}(Q)$ , a first-order phase transition between the small and the big black hole occurs.
- For  $Q < Q_c$  and  $T_{tr}(Q) < T < T_2(Q)$ , the big black hole is thermodynamically preferred, while the small black hole is metastable.
- For  $Q < Q_c$  and  $T \geq T_2(Q)$ , the big black hole is thermodynamically preferred. It is the

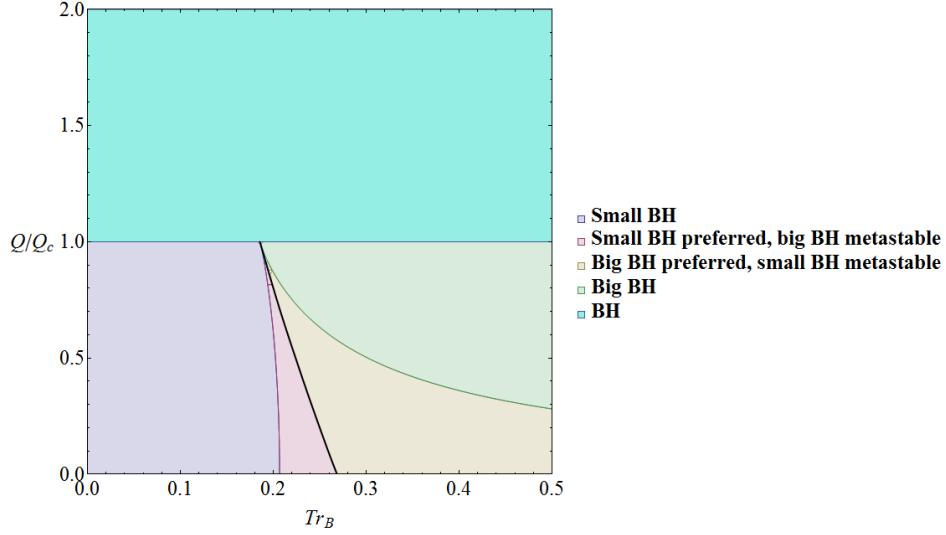


**Figure 4.12:** The phase diagram of the charged black hole in the  $(T, Q)$ -plane. The legend only mentions the (meta)stable states. In the purple and the yellow region, there is also an unstable black hole state. In crossing the thick black curve, a first-order phase transition occurs. This curve of phase transitions ends in a critical point.

only thermally stable solution.

- At  $Q = Q_c$  and  $T = T_c$  there is a critical point. The transition between the small and the big black hole vanishes and the phases become indistinguishable, i.e. they merge into one phase.
- For  $Q \geq Q_c$ , there is only one black hole solution, which is the thermodynamically preferred solution.

The unstable black hole appearing when  $Q < Q_c$  provides a free-energy barrier between the small and the big black hole solution.

At the critical point, the heat capacity diverges. Using the same argument as in subsection 2.3.3, we find a critical exponent of  $\frac{2}{3}$  for the heat capacity.

Readers of this section might strongly feel like having experienced a *déjà vu*. Indeed, the results in this section are completely analogous to the ones in the asymptotically AdS case. As mentioned before, the redshift factor in the temperature Eq. (4.10) introduces a big stable black hole solution. In the AdS case, this is done by the additional term  $\frac{r_+^2}{L^2}$  in second factor of the temperature Eq. (3.8). Moreover, the appearance of the small black hole solution is due to the term  $-\frac{Q^2}{r_+^2}$  in the second factor of the temperature Eq. (4.10). This term is also present in the AdS temperature Eq. (3.8). Furthermore, the free energies in Fig. 4.11 and Fig. 3.9 show very similar behavior, so that the resulting phase diagrams in Fig. 4.12 and Fig. 3.10 are qualitatively the same.

## 4.6 Summary

In this chapter we have basically performed the same analysis as in the previous two chapters. However, we replaced negative cosmological constant by a cutoff in the radial coordinate, turning our spacetime into a finite cavity. Both the negative cosmological constant and the radial cutoff yield a confined spacetime. We have seen that in both cases, this confinement enables the existence of thermally stable black holes. Moreover, the phase structure of the two cases showed huge similarities. Some small differences arised in the grand canonical ensemble due to the Minkowski cavity having finite volume, in contrast to the AdS spacetime. The canonical ensemble results were qualitatively identical.

The above similiarities between the thermodynamic properties could suggest that one does not necessarily need an asymptotically AdS spacetime to perform holography [32]. Indeed, it could be that it is specifically the confinement which results in the rich thermodynamic phase structures as the ones from the last few chapters. More evidence for this can be found in [33], where an analysis similar to the one performed in this chapter has been performed in an asymptotically de Sitter spacetime with a cutoff for the radial coordinate in the canonical ensemble. The obtained phase diagram is again qualitatively the same. It would therefore be interesting to find out whether we can apply holographic methods to such spacetimes. A difference here is that the dual theory lives on the boundary which has a finite volume. Moreover, massive particles cannot reach the boundary of an asymptotically AdS spacetime, but this is not the case in the spacetimes with a cutoff. Therefore, if this<sup>7</sup> is of importance for the correspondence, applying holography to spacetimes with a cutoff could still be troublesome.

There is however a more important reason why one does not generally apply holographic methods to asymptotically flat spacetimes with a cutoff. In the AdS/CFT correspondence, one often works with *planar* rather than spherical black holes. As a consequence, the dual field theory is also defined on a plane, which is usually desired when describing condensed matter systems for example. In the next chapter we shall investigate the thermodynamics of such planar black holes in asymptotically AdS spacetimes. The negative cosmological constant is crucial in this case. Indeed, as we shall see, a planar Schwarzschild black hole cannot even exist in an asymptotically flat spacetime, because this solution contains a naked singularity. Since this cannot be remedied by introducing a cutoff, the holographic approach in asymptotically AdS spacetimes is usually the way to go.

---

<sup>7</sup>Or another specific property of AdS spacetime which is not present when simply introducing a radial cutoff.



## Chapter 5

# Black Brane Phase Transitions and Holographic Superconductivity

Until now we have only considered spherically symmetric black hole solutions. However, spherical symmetry is by no means a prerequisite for a solution to the Einstein equations. In this chapter we will therefore study the thermodynamics of different solutions to the Einstein equations, in particular, spacetimes with planar symmetry.

Planar black holes are sometimes also called black branes. These black brane solutions are omnipresent in the AdS/CFT correspondence. The reason is that we often wish to describe a conformal field theory on  $\mathbb{R}^n$  rather than  $S^n$ . One can achieve this by using an asymptotically  $\text{AdS}_{n+1}$  solution with planar symmetry, such that the boundary is indeed  $\mathbb{R}^n$ . As an example, this is done in the holographic description of superconductivity [34], which we will treat in this chapter as well.

We will start with describing four-dimensional charged black hole solutions enjoying planar symmetry. It turns out that an asymptotically AdS spacetime is required for this. Subsequently, we will describe how to assign a temperature to the black brane solutions, similar to what we did for the spherical black holes. We will then proceed by describing the thermodynamics of the charged black branes. For this we will use the same approach as in Chapter 3. Finally, we will look at the effect of adding a complex scalar field to the theory and discuss how this leads to a dual field theory resembling a superconductor.

### 5.1 Black brane solutions

The action we consider in this chapter is again the Einstein-Hilbert-Maxwell action with a negative cosmological constant

$$I = \frac{1}{16\pi} \int_M d^4x \sqrt{g} \left( R - F_{\mu\nu} F^{\mu\nu} + \frac{6}{L^2} \right), \quad (5.1)$$

which should be complemented with suitable boundary actions depending on what boundary conditions are required. Due to planar symmetry, we can write a general solution to the Einstein equations as

$$ds^2 = -f(r)dt^2 + \frac{1}{f(r)}dr^2 + \frac{r^2}{L^2}d\mathbf{x}_2^2, \quad (5.2)$$

where  $\mathbf{x}_2 = (x, y) \in \mathbb{R}^2$ . Notice that  $r$  is not a radial coordinate as in the spherical coordinate system. Indeed, for the above metric a static slice of constant  $r$  describes an infinite plane rather than a sphere.

Note that the cosmological constant is crucial in this case. Indeed, Hawking and Ellis showed that a four-dimensional stationary asymptotically flat black hole solution which obeys the dominant energy condition<sup>1</sup> can only have a spherical event horizon [35]. Let us see what happens if we ignore this theorem and try to find a solution to Einstein's equations anyway. As an example, we concentrate on the uncharged case, i.e.  $F = 0$ . In this case one can find that a solution is given by [36]

$$ds^2 = -\frac{2m}{r}dt^2 + \frac{r}{2m}dr^2 + r^2d\mathbf{x}_2^2. \quad (5.3)$$

This solution does not admit an event horizon and has a naked singularity. Thus, the Schwarzschild black brane does not exist in asymptotically flat spacetimes.

Now let us return to the asymptotically AdS case. One solution is given by  $F = 0$  and

$$ds^2 = -\frac{r^2}{L^2}dt^2 + \frac{L^2}{r^2}dr^2 + \frac{r^2}{L^2}d\mathbf{x}_2^2. \quad (5.4)$$

This is just the anti-de Sitter solution in Poincaré coordinates as discussed in section 1.1. Substituting the Ansatz Eq. (5.2) into the Einstein equations and the covariant Maxwell equations, one can show that other solutions can be written as

$$f(r) = -\frac{2m}{r} + \frac{q^2}{r^2} + \frac{r^2}{L^2} \quad (5.5)$$

together with

$$A = \left(-\frac{q}{r} + \Phi\right) dt \quad (5.6)$$

with  $\Phi$  constant [37]. This solution needs an event horizon to conceal the singularity at  $r = 0$ . In general there are two event horizons  $r_+$  and  $r_- \leq r_+$ , provided

$$r_+ \geq \sqrt[4]{\frac{q^2 L^2}{3}} \equiv r_e, \quad (5.7)$$

where we eliminated  $m$  using  $f(r_+) = 0$ , i.e.

$$m = \frac{r_+}{2} \left( \frac{q^2}{r_+^2} + \frac{r_+^2}{L^2} \right). \quad (5.8)$$

---

<sup>1</sup>Intuitively, this condition states that one can only observe non negative energy densities and that one can never observe mass or energy to go faster than light.

Eq. (5.7) must hold in order to prevent a naked singularity. If the equality  $r_+ = r_e$  holds, the event horizons coincide so that the black hole is extremal.

If we are considering black brane solutions, we fix the constant  $\Phi$  appearing in the gauge field by setting

$$\Phi = \frac{Q}{r_+} \quad (5.9)$$

so that the norm of  $A$  does not diverge on the event horizon.

We will not derive the solution Eq. (5.5) from the Einstein equations and Maxwell's equations. However, we can also find this solution by "blowing up" the spherically symmetric solutions. To this end, one defines new coordinates  $\tilde{r} = \alpha^{1/3}r$ ,  $\tilde{t} = \alpha^{-1/3}t$  and new parameters  $m = \alpha M$ ,  $q = \alpha^{2/3}Q$ . Simultaneously, one blows up the two-sphere by taking  $d\mathbf{x}_2^2 = L^2\alpha^{2/3}d\Omega_2^2$  [13]. Substituting this in the metric given by Eq. (3.5) and taking the limit  $\alpha \rightarrow \infty$  yields the black brane metric Eq. (5.5).

The parameters  $m$  and  $q$  are chosen such that the metric resembles the familiar spherical black hole solution. However, these parameters do *not* coincide with the mass and the charge of the black brane. Indeed, since the black brane's topology is that of an infinite plane, its mass and charge are also infinite, being extensive quantities. The actual mass and charge density, which are not infinite, can be calculated from the free-energy density, which follows from the on-shell action. This will be done in the next sections. Moreover, in appendix A it is shown that the mass obtained in this way coincides with the mass obtained using the AMD formalism.

Finally, in the literature one often encounters a different coordinate  $z$  instead of  $r$ , such that the boundary is located at  $z = 0$ . To this effect, define  $z = \frac{L^2}{r}$ , such that the new metric becomes

$$ds^2 = \frac{L^2}{z^2} \left( -g(z)dt^2 + \frac{1}{g(z)}dr^2 + dx^2 + dy^2 \right) \quad (5.10)$$

with<sup>2</sup>

$$g(z) = 1 - \frac{z^3}{z_+^3} \left( 1 + \frac{q^2 z_+^4}{L^6} \right) + \frac{z^4}{z_+^4} \frac{q^2 z_+^4}{L^6}. \quad (5.11)$$

This form is particularly convenient when applying holography. Using the conformal invariance of the dual field theory living on the boundary  $z = 0$  to omit the conformal factor in Eq. (5.10), we can immediately see that the field theory's metric is just the three-dimensional Minkowski metric

$$ds^2 = -dt^2 + dx^2 + dy^2. \quad (5.12)$$

For this we also used that  $g = 1$  on the boundary.

---

<sup>2</sup>Note that  $z_+$  still corresponds to the largest event horizon, i.e. the *smallest* solution to  $g(z) = 0$ .

### 5.1.1 The black brane temperature

Next, we will give an expression for the Hawking temperature associated to the general black brane solution Eq. (5.5). To do so, we follow the same procedure as in Section 4. Upon performing a Wick rotation to the solution, the inverse Hawking temperature is given by the period of the imaginary-time coordinate  $\tau = it$ .

The derivation of this period is identical to the derivation in Section 4, with  $d\Omega_2^2$  replaced by  $\frac{1}{L^2}d\mathbf{x}_2^2$ . In particular, this means that in order for the spacetime to be free of conical singularities, the temperature must be given by

$$T = \frac{f'(r_+)}{4\pi} = \frac{1}{4\pi r_+} \left( \frac{3r_+^2}{L^2} - \frac{q^2}{r_+^2} \right). \quad (5.13)$$

Note that in the extremal limit  $r_+ \rightarrow r_e$ , the temperature vanishes as expected. Upon comparing this temperature to its spherically symmetric counterpart Eq. (3.8), it follows that the black brane temperature is the same except for the absence of the term  $\frac{1}{4\pi r_+}$ . In the spherically symmetric case, any instability in a black hole solution was caused exactly by this term. Therefore, one can anticipate that the absence of this term will greatly simplify the thermodynamic properties. We will see in the next sections that this is indeed true. We will start by treating the uncharged case and subsequently we will study the thermodynamics in both the grand canonical and the canonical ensemble. Since we are not considering spacetimes with a cutoff, we will apply the same formalism as in Chapter 3.

## 5.2 The Schwarzschild black brane

The Hawking temperature of the Schwarzschild black brane is found by putting  $q = 0$  in Eq. (5.13), which yields

$$T = \frac{3r_h}{4\pi L^2}. \quad (5.14)$$

Hence the temperature, which is plotted in Fig. 5.1, is linear in  $r_h$ . Comparing this to the spherically symmetric counterpart Fig. 2.1, we see that the temperatures coincide for large values of  $r_h$ . For smaller values of  $r_h$ , the branch of unstable black hole solutions has disappeared. Consequently, for each temperature  $T > 0$  there is exactly one black brane solution. This solution is thermally stable, as the heat capacity density<sup>3</sup> is clearly positive for any nonzero  $r_h$ . The heat capacity density is plotted in Fig. 5.2a, where we defined  $V_2 = \int d\mathbf{x}_2$ .

In addition to the above black brane, another solution which exists at any temperature  $T$  is the thermal AdS solution. This is given by the Euclidean version of Eq. (5.4). However, by calculating the on-shell Euclidean Einstein-Hilbert action and subtracting the thermal AdS background, one

---

<sup>3</sup>Here we define the heat capacity density as the heat capacity per unit area of  $\mathbb{R}^2$ . The heat capacity itself is extensive and therefore infinite.

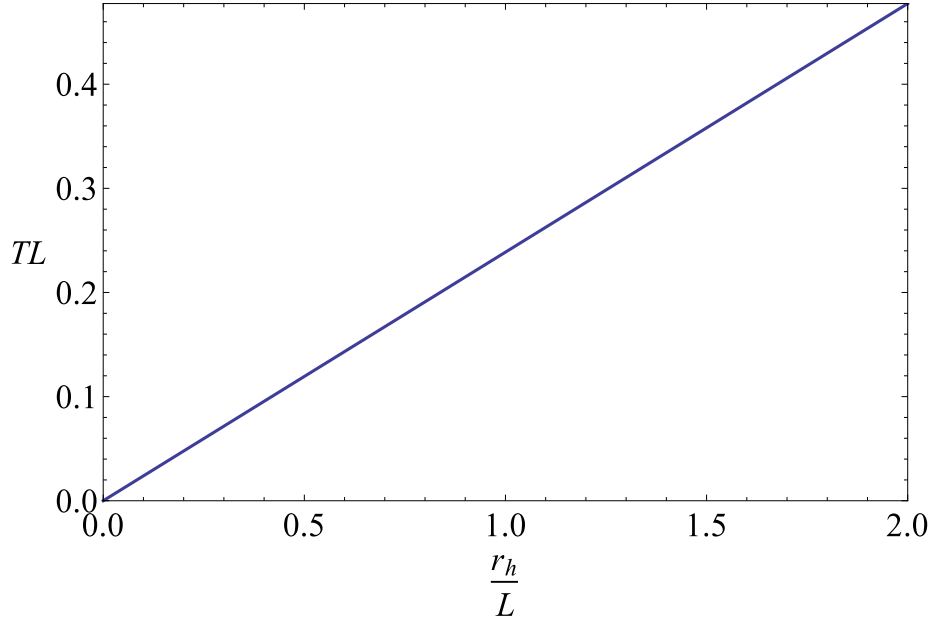


**Figure 5.1:** The temperature of the Schwarzschild black brane as a function of its event horizon. For each temperature, there is exactly one black brane solution.

finds a free-energy density difference of

$$\Delta f \equiv \frac{\Delta F}{V_2} = -\frac{4}{27}\pi^2 L^2 T^3. \quad (5.15)$$

Therefore the black brane solution has the lowest free energy at any nonzero temperature, making it the thermodynamically preferred phase. The free-energy density is shown in Fig. 5.2b. We find that in the uncharged case, *phase transitions do not occur*.

Notice that the free energy is not equal to  $m - TS$ . The reason for this is that  $m$  is not equal to the mass of the black brane. Indeed, by subsequent use of Eq. (5.15), Eq. (5.14) and Eq. (5.8) it follows that the actual black brane mass is equal to<sup>4</sup>

$$M = \frac{\partial(\beta F)}{\partial\beta} = \frac{mV_2}{4\pi L^2}, \quad (5.16)$$

hence the parameter  $m$  is proportional to the mass per unit volume  $V_2$ . As a check, from Eq. (5.15) and Eq. (5.14) we also find the entropy

$$S = -\frac{\partial F}{\partial T} = \frac{V_2 r_h^2}{4L^2} \quad (5.17)$$

which is indeed one quarter of the black brane area. One could still use the definition  $F = M - TS$  to obtain the free energy, but for this one first has to obtain Eq. (5.16) by different means, for example by using the AMD formalism (see appendix A).

<sup>4</sup>In a quantum theory of gravity which includes fluctuations in  $M$ , the quantity calculated here would correspond to the macroscopic value  $\langle M \rangle$ .

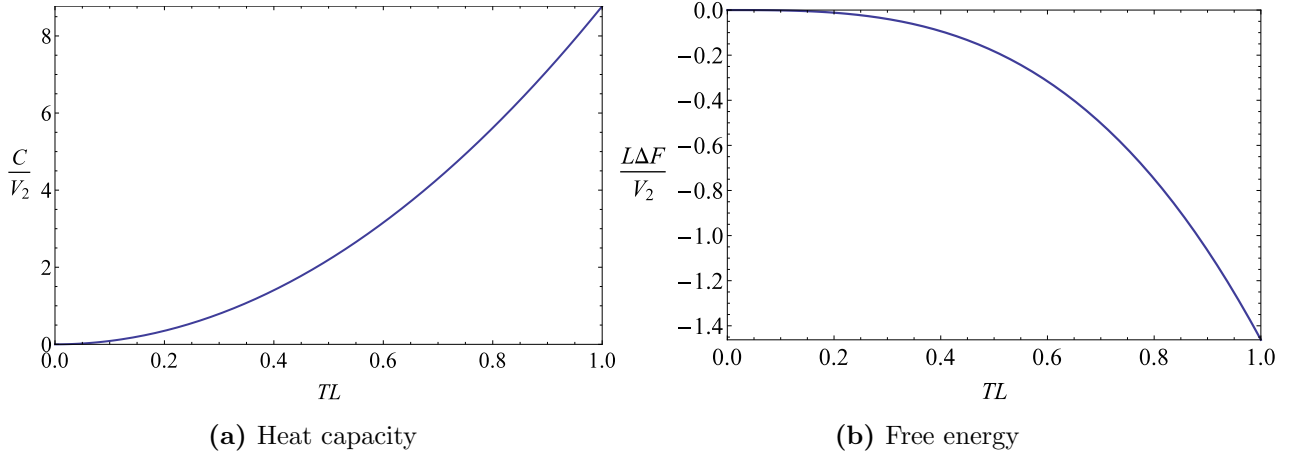


**Figure 5.2:** The heat capacity (a) and the free energy (b) of the Schwarzschild black brane as a function of the Hawking temperature. It follows immediately that the unique black hole solution is always stable and thermodynamically preferable.

### 5.3 The grand canonical ensemble

Next, we consider the charged black brane in the grand canonical ensemble. This means we fix the electrostatic potential  $\Phi$  and the temperature  $T$  and study the grand potential  $\Omega = M - TS - \Phi Q$ . As stated before, the mass is not equal to the parameter  $m$ . Similarly, the charge  $Q$  of the black brane is not equal to  $q$ .

#### 5.3.1 The phases

One phase that always exists is the thermal AdS phase, given by the Euclidean version of Eq. (5.4) together with the constant gauge field  $A = \Phi dt$ . For the black brane solutions, we rewrite the temperature Eq. (5.13) in terms of  $\Phi$  using Eq. (5.9), yielding

$$T = \frac{1}{4\pi r_+} \left( \frac{3r_+^2}{L^2} - \Phi^2 \right). \quad (5.18)$$

This is plotted in figure Fig. 5.3 for several values of  $\Phi$ . Comparing this plot to its spherically symmetric counterpart in Fig. 3.1, we see that the branch of unstable solutions has disappeared, as was the case for the uncharged black brane. Hence we see that for each value of  $\Phi$  and  $T$  there is exactly one black brane solution<sup>5</sup>. Clearly this solution is thermally stable, which can also be seen from the heat capacity density in figure Fig. 5.4a.

<sup>5</sup>Except at  $(T, \Phi) = (0, 0)$ .

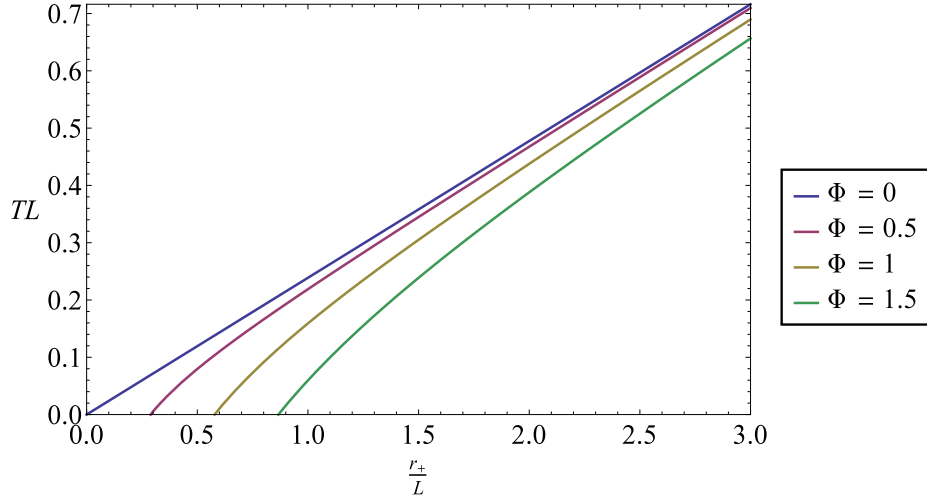


**Figure 5.3:** The temperature of the charged black brane as a function of its event horizon. For each value of the electrostatic potential, there is exactly one black brane solution for a given temperature.

### 5.3.2 The phase diagram

By calculating the on-shell Euclidean Einstein-Hilbert action and subtracting the thermal AdS background, one finds a grand-potential density difference of

$$\Delta\omega(T, \Phi) \equiv \frac{\Delta\Omega(T, \Phi)}{V_2} = -\frac{r_+}{16\pi L^2} \left( \frac{r_+^2}{L^2} + \Phi^2 \right). \quad (5.19)$$

We immediately see that this is always negative, so that the black brane solution is always preferred over the thermal AdS phase. Therefore, as in the uncharged case, *phase transitions do not occur* and the phase diagram is trivial. Using Eq. (5.18) we can plot the grand-potential difference as a function of the temperature. This is done in Fig. 5.4b for several values of  $\Phi$ .

From the grand potential Eq. (5.19) one can verify that the mass and the entropy are still given by Eq. (5.16) and Eq. (5.17). Furthermore, the charge of the black brane is given by

$$Q = -\left( \frac{\partial\Omega}{\partial\Phi} \right)_T = \frac{qV_2}{4\pi L^2}. \quad (5.20)$$

Thus the parameter  $q$  is proportional to the charge per unit volume  $V_2$ , with the same proportionality factor as the one between  $m$  and  $M$ .

## 5.4 The canonical ensemble

In the canonical ensemble, we fix the electric charge  $Q$  and the temperature  $T$ . Notice that since the charge is proportional to the parameter  $q$ , we can equivalently work in ensemble with fixed  $q$ .

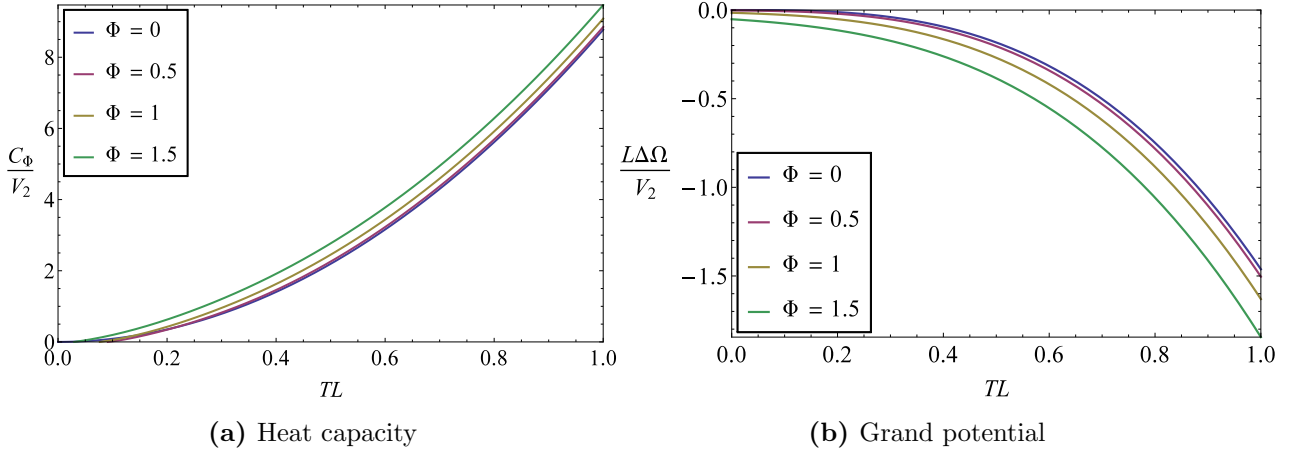


**Figure 5.4:** The heat capacity (a) and the free energy (b) of the charged black brane as a function of the Hawking temperature, for several values of the electrostatic potential  $\Phi$ . It follows immediately that the unique black hole solution is always stable and thermodynamically preferable.

### 5.4.1 The phases

As explained in the previous chapters, we cannot use the thermal AdS phase as a reference state in the canonical ensemble. Therefore we will again make use of an extremal black brane background.

The additional black brane solutions can be found from the temperature Eq.(5.13), which is shown in Fig.5.5. Comparing this plot to its spherically symmetric counterpart in Fig.3.6, we see that the branch of unstable solutions has disappeared again. For each value of  $q$  and  $T$  there is exactly one black brane solution<sup>6</sup>. Clearly this solution is thermally stable, which can also be seen from the heat capacity density in figure Fig. 5.6a.

### 5.4.2 The phase diagram

Either by means of the on shell Einstein-Hilbert action or by the results of the grand canonical ensemble, one can show that the Helmholtz free-energy density difference is given by

$$\Delta f(T, q) \equiv \frac{\Delta F(T, q)}{V_2} = -\frac{r_+}{16\pi L^2} \left( \frac{r_+^2}{L^2} - \frac{3q^2}{r_+^2} \right) - \frac{M_e(q)}{V_2} \quad (5.21)$$

where as usual we subtracted the contribution from the extremal black brane mass  $M_e$ , which is found using Eq.(5.8) with  $r_+ = r_e$  as in Eq.(5.7) and subsequently using Eq.(5.16) to convert to the real mass. The obtained free energy is a decreasing function of  $r_+$  for all  $r_+ > r_e$ . Moreover, for any  $q$ , the temperature is a strictly increasing function of  $r_+$ . Since in the extremal limit we have  $\Delta f = 0$ , it follows that the black brane solution has a lower free-energy density than the extremal black brane background for any nonzero temperature. This can also be seen in

<sup>6</sup>Except at  $(T, q) = (0, 0)$ .



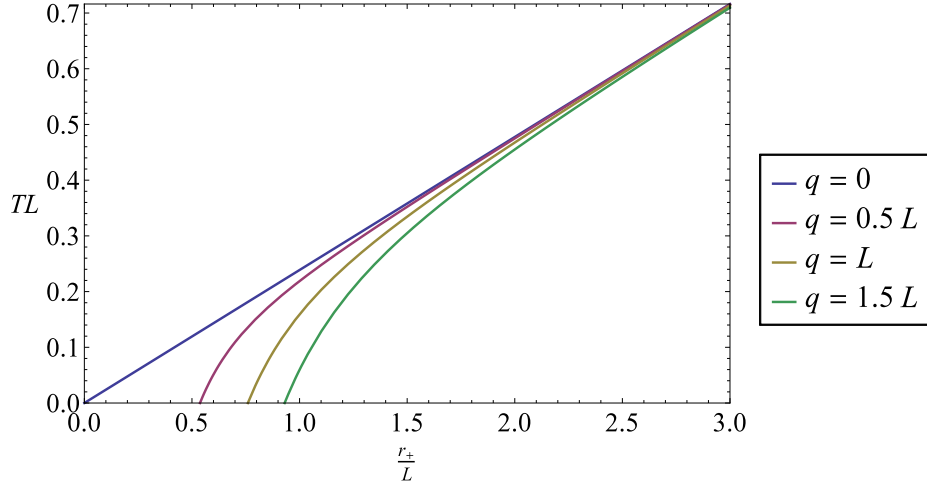


**Figure 5.5:** The temperature of the charged black brane as a function of its event horizon. For each value of  $q$ , there is exactly one black brane solution for a given temperature.

Fig. 5.6b. Therefore, we are once again forced to conclude that *phase transitions do not occur*. Consequently, the phase diagram is trivial.

## 5.5 Summary

In contrast to the rich phase structure found before for the charged spherical black hole, we have seen in this chapter that no phase transitions occur for the charged planar black holes. In particular, for the uncharged black brane there is no Hawking-Page phase transition and the black brane is thermodynamically favorable at any temperature. Actually, we could have predicted this by a simple argument. Let us take a look at the Schwarzschild black brane metric, given by Eq. (5.2) and

$$f(r) = \frac{r_h^2}{L^2} \left( 1 - \frac{r_h^3}{r^3} \right). \quad (5.22)$$

Performing a coordinate change

$$(t, r, \mathbf{x}_2) \rightarrow \left( \frac{r_h}{L^2} t, \frac{r}{r_h}, \frac{r_h}{L^2} \mathbf{x}_2 \right) \quad (5.23)$$

eliminates  $r_h$  and  $L$  from the metric. In doing so, we have eliminated all scales from the theory. Hence there are no scales with which we can compare the temperature<sup>7</sup>. This implies that all nonzero temperatures in the theory are equivalent[36], so that there can be no critical temperature at which a phase transition occurs.

Adding a charge to the black brane does not change a lot. Although the parameters  $\Phi$  or  $q$

<sup>7</sup>Indeed, the Hawking temperature becomes a constant in these coordinates, see Eq. (5.14).

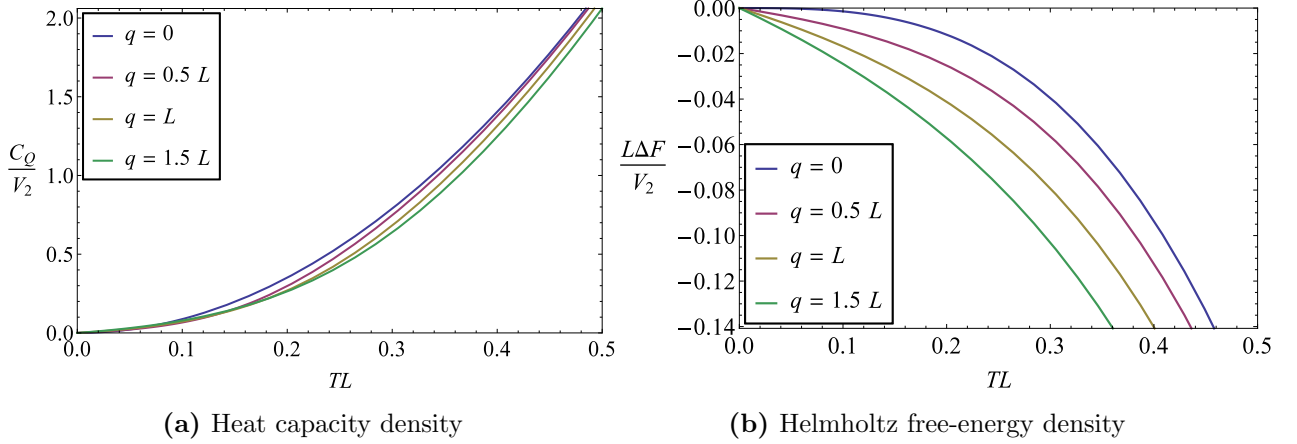


**Figure 5.6:** The heat capacity (a) and the free-energy (b) density of the charged black brane as a function of the Hawking temperature, for several values of the electric charge  $Q$ . It follows immediately that the unique black hole solution is always stable and thermodynamically preferable.

provide us with a new scale, making a nonzero critical temperature possible<sup>8</sup>, we find that the thermodynamics is still dominated by a black brane at any temperature.

It would appear from this that black branes are much less interesting than spherical black holes. Still, black branes are widely used in the AdS/CFT correspondence, for reasons mentioned earlier. Being dominant at any temperature and charge, black branes provide a convenient way of introducing a temperature and a chemical potential to the dual field theory. The thermodynamics can be made nontrivial by adding more ingredients to our theory. As an example, we will now proceed by considering a theory containing a charged black brane together with a complex scalar field. This is one of the classic theories used in AdS/CMT, i.e. in AdS/CFT with a condensed matter system as the holographic dual, which in this case gives a superconducting phase.

The addition of the complex scalar field to our theory has another advantage. Notice that as in the spherically symmetric case, we again find that a black brane can be the globally stable phase at  $T = 0$ , yielding a highly degenerate ground state. This suggests that there are more solutions than the ones we have considered until now, which should dominate and have vanishing entropy at  $T = 0$ . Adding the scalar field will provide us with such a solution, as we shall see next.

## 5.6 Black brane solutions with a complex scalar field

The addition of a complex scalar field  $\phi$  to the theory gives rise to the following action:

$$I = \frac{1}{16\pi} \int_M d^4x \sqrt{g} \left( R - F_{\mu\nu} F^{\mu\nu} + \frac{6}{L^2} - |\partial\phi - iqA\phi|^2 - m^2 |\phi|^2 \right). \quad (5.24)$$

<sup>8</sup>In case the critical temperature exists, it should be proportional to  $\Phi$  or  $\sqrt{q}$  [38].

Here the scalar field is charged under the  $U(1)$  gauge field and has charge  $q$ . As before, we consider a temporal gauge field  $A = A_t(r)dt$  and assume solutions enjoying planar symmetry. Moreover, we choose the mass of the scalar field to be equal to  $m^2 = -2/L^2$ . This implies that our scalar field is a tachyon, but one can show that this value of  $m^2$  does not lead to instabilities [39]. Moreover, this tachyonic mass does not imply that the corresponding particles move faster than the speed of light. Consequently, we need not be afraid that the particles can escape to infinity.

There are several reasons why it is interesting to study this action. First of all, as we shall see, this action will yield the nontrivial phase structure that was absent for the pure black brane solutions. Secondly, this system has an interesting holographic dual consisting of a superconducting phase, which we shall briefly describe in the next section. Here, we shall only consider the so-called probe limit, a simplified version of the above theory which is already enough to show a nontrivial phase structure as well as the holographic superconductor.

In the past decade, a vast amount of publications on the topic of holographic superconductivity has appeared. Most of the following discussion can be found in these papers. The following sections closely follow [39], [34] and [38], though with slightly different conventions. Moreover, we will work in the grand canonical ensemble, in contrast to [34].

### 5.6.1 The phases

We will start by outlining the possible phases. To this end, we must solve the equations of motion following from Eq. (5.24). These are the Einstein equations for the metric, the covariant Maxwell equations for the gauge field and the covariant Klein Gordon equation for the scalar field. In general, these equations are all coupled, as both the gauge field and the scalar field backreact on the metric tensor. However, this greatly simplifies in the probe limit. This amounts to rescaling the fields  $\phi \rightarrow q\phi$  and  $A_t \rightarrow qA_t$  and taking the limit  $q \rightarrow \infty$  afterwards. One can show that as a result, both the scalar field and the gauge field decouple from the Ricci scalar [38]. An immediate consequence is that the solution to the Einstein equations is given by the Schwarzschild black brane solution, i.e. Eq. (5.2) with

$$f(r) = -\frac{2m}{r} + \frac{r^2}{L^2} = \frac{r^2}{L^2} \left( 1 - \frac{r_h^3}{r^3} \right). \quad (5.25)$$

This also fixes the Hawking temperature to Eq. (5.14). Moreover, the heat capacity is the one shown in Fig. 5.2, so that all solutions are automatically thermally stable, regardless of the solution for  $\phi$  and  $A_t$ .

To find the full solution, we must solve the Maxwell and the Klein Gordon equations. Upon varying the action in  $A_r$ , one finds the Maxwell equation

$$\phi^*(r)\phi'(r) - \phi(r)\phi^{*'}(r) = 0 \quad (5.26)$$

which implies that the phase of  $\phi$  is constant, so we can assume  $\phi$  is real. The other nontrivial Maxwell equation then becomes [34]

$$A_t'' + \frac{2}{r}A_t' - \frac{2\phi^2}{f}A_t = 0 \quad (5.27)$$

while the Klein Gordon equation becomes [34]<sup>9</sup>

$$\phi'' + \left(\frac{f'}{f} + \frac{2}{r}\right)\phi' + \frac{4A_t^2}{f^2}\phi + \frac{2}{L^2 f}\phi = 0. \quad (5.28)$$

One obvious solution is given by  $\phi = 0$  and<sup>10</sup>

$$A_t = \mu \left(1 - \frac{r_h}{r}\right), \quad (5.29)$$

which describes a charged black brane, with a gauge field which is too weak to influence the metric. This solution is nothing new.

Next, we wish to find another solution for which the scalar field does not vanish. Such a solution is said to contain scalar hair. To find such a hairy black brane, we must find nontrivial solutions to the system of coupled second-order nonlinear ordinary differential equations given by Eq. (5.27) and Eq. (5.28). This system can easily be solved numerically. We will give a brief description of the numerical method used for this, since we wish to apply a similar method again when we are looking for new black hole solutions in chapter 7.

To be able to solve the system given by Eq. (5.27) and Eq. (5.28), we will need four initial conditions, e.g.  $\phi(r_h)$ ,  $\phi'(r_h)$ ,  $A_t(r_h)$  and  $A_t'(r_h)$ . As usual, we must choose  $A_t(r_h) = 0$ . Furthermore, evaluation of Eq. (5.28) at  $r_h$  yields that  $\phi'(r_h) = \frac{8}{5r_h}\phi(r_h)$ . Thus, we are left with two free initial conditions, making our solution a two-parameter family of solutions.

Furthermore, we also have asymptotic boundary conditions. First of all, the scalar field must vanish as  $r \rightarrow \infty$  for it to be normalizable. Secondly, the gauge field need not vanish at the boundary, but it must approach a constant. In the grand canonical ensemble, we denote this constant by  $\mu$ . In this way the gauge field corresponding to the hairless and the one corresponding to the hairy solution both approach  $\mu$ , so that we can compare them and see which solution is thermodynamically favorable. We can say more by investigating the asymptotics of the equations of motion near the AdS boundary, from which the following asymptotic power law behavior follows<sup>11</sup>:

$$\phi = \frac{\alpha}{r} + \frac{\beta}{r^2} + \dots \quad (5.30)$$

$$A_t = \mu - \frac{Q}{r} + \dots \quad (5.31)$$

---

<sup>9</sup>Note that we use a different normalization of the gauge field than in [34], to be consistent with the normalization used in the previous sections.

<sup>10</sup>Here we use  $\mu$  for the gauge field at infinity rather than  $\Phi$  to avoid confusion with the field  $\phi$  and because of the dual interpretation of  $\mu$  as a chemical potential (see the next section).

<sup>11</sup>The simple power law behavior (i.e. with integer powers) for  $\phi$  is an artifact of our choice of the mass  $m$ .

This means that given the two initial conditions, the corresponding solutions will behave as Eq. (5.30) and Eq. (5.31), so that we obtain a mapping

$$(\phi(r_h), A'_t(r_h)) \mapsto (\mu, Q, \alpha, \beta). \quad (5.32)$$

The usefulness of this mapping resides in the fact that the parameters on the right hand side of the mapping correspond to physical properties of the holographic dual of this theory.

We now proceed by looking for solutions where  $\alpha = 0$ <sup>12</sup>. For this one can use the shooting method: given an initial condition  $\phi(r_h)$ , we look for a second initial condition  $A'_t(r_h)$  such that the resulting solution obeys  $\alpha = 0$ . Due to this constraint, we are then left with a one-parameter family of solutions. Notice that if given a value of  $\phi(r_h)$ , we acquire a solution and hence a corresponding value of  $\mu$ . Consequently, by computing the solution for arbitrary values of  $\phi(r_h)$ , we can use the resulting data to plot quantities corresponding to this solution (e.g.  $\beta$ , or the free energy) as a function of  $\mu$ . The strategy for solutions with  $\beta = 0$  is completely analogous.

With the procedure described above, we have found additional phases which can compete with the hairless black brane solution. Notice that the solution also depends on the value of  $r_h$ , since this is where we take our initial conditions. However, this is not relevant for the thermodynamic quantities we wish to compute. Indeed, one can show that the equations of motion are invariant under certain coordinate transformations which enable us to put both  $L$  and  $r_h$  to 1. By dimensional analysis we can then conclude that dimensionless thermodynamic quantities in the grand canonical ensemble can only depend on the dimensionless combination  $T/\mu$ .<sup>13</sup> Therefore, we can safely put the event horizon to  $r_h = 1$  in our numerics, thereby fixing the temperature, and plot temperature-dependent quantities by varying  $1/\mu$ .

### 5.6.2 The phase diagram

In the previous sections of this chapter we have seen that the black brane solutions are always preferred over the thermal AdS solution. The most commonly used method find phase transitions corresponding to holographic superconductivity theories is by using an order parameter. In this case, the order parameter used is either the  $\alpha$  or the  $\beta$  in Eq. (5.30), while the other is set to zero. These parameters correspond to the expectation value of some conformal operator in the dual field theory, such that a phase transition occurs when they become nonzero. Nevertheless, here we will pursue the route we have always followed when searching for phase transitions: we will calculate the grand-potential difference between the two solutions. We will see that the two methods are equivalent, i.e. the grand-potential difference will become negative exactly when  $\alpha$  or  $\beta$  are nonzero.

We will find the grand-potential difference  $\Delta\Omega = \Omega_{\text{hairly}} - \Omega_{\text{hairless}}$  by calculating the on-shell Euclidean action Eq. (5.24). First of all, notice that in the probe limit we are considering, the

<sup>12</sup>The physical meaning of this will be given in the next section.

<sup>13</sup>In the canonical ensemble, the relevant dimensionless combination is  $T/\sqrt{Q}$ . Note that with dimensionless we mean that the *scaling* dimension is zero.

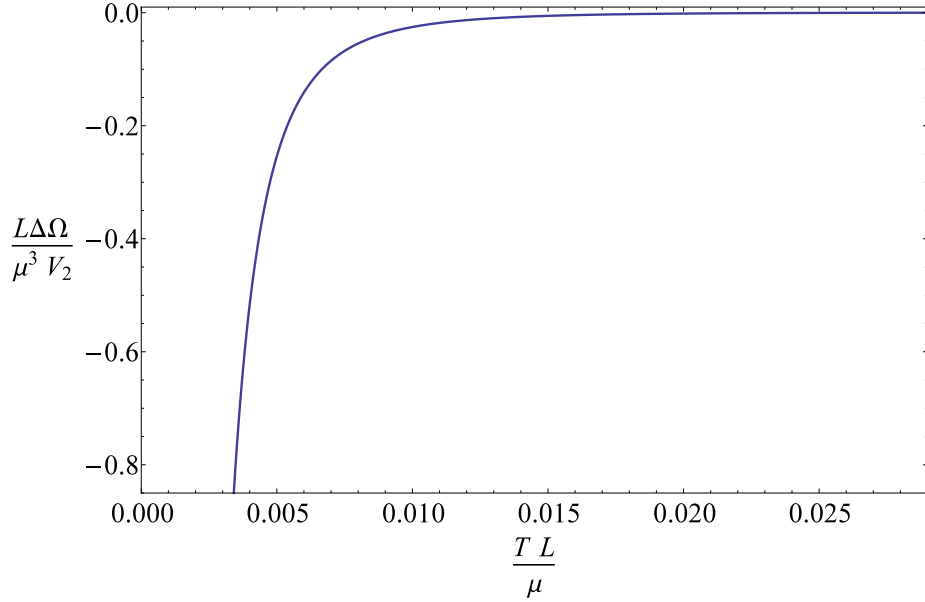


**Figure 5.7:** The grand-potential difference between the hairy black brane and the hairless black brane solution. The grand-potential difference is always negative in the domain shown, whereas it is zero for larger values of  $T/\mu$ .

metric is given by Schwarzschild black brane metric for both phases. Therefore, any terms not containing the fields  $\phi$  or  $A$  in the action (i.e. the Ricci scalar and the cosmological constant term) will cancel when calculating the difference. For the same reason, one can ignore the Gibbons-Hawking boundary term. We should however add a boundary term to fix either  $\alpha$  or  $\beta$  on the boundary. Referring to appendix B for details, the grand-potential difference is given by<sup>14</sup>

$$\Delta\omega = \frac{\Delta\Omega}{V_2} = \frac{1}{8\pi L^2} \left( \mu r_h \left( \mu - \frac{Q}{r_h} \right) + 2 \int_{r_h}^{\infty} dr \frac{r^3 A_t^2 \phi^2}{r^3 - r_h^3} \right). \quad (5.33)$$

Here,  $Q$  is the parameter appearing in the expansion Eq. (5.31) of the hairy black brane solution, and *not* the charge of the hairless solution. Hence  $Q \neq \mu r_h$  when scalar hair is present. The last term clearly shows the coupling between the scalar hair and the gauge field. As a check, notice that for the hairless solution with  $Q = \mu r_h$  and  $\phi = 0$ , the grand-potential difference vanishes as expected. Upon evaluating Eq. (5.33) numerically, we obtain the plot in Fig. 5.7. The numerical result also shows that for higher values of  $T/\mu$  than the ones shown in the plot, there is no scalar hair solution. Clearly, from this it follows that the hairy black brane is always preferred over the hairless black brane, whenever it exists.

From Fig. 5.7 it follows that there is a critical temperature at which a phase transition occurs. We will see in the next section that this is a second-order phase transition. Naturally, the critical temperature is proportional to  $\mu$ , which results in the phase diagram in Fig. 5.8.

<sup>14</sup>We ignore the overall factor containing  $q^{-2}$  which appeared when rescaling the fields for the probe limit.

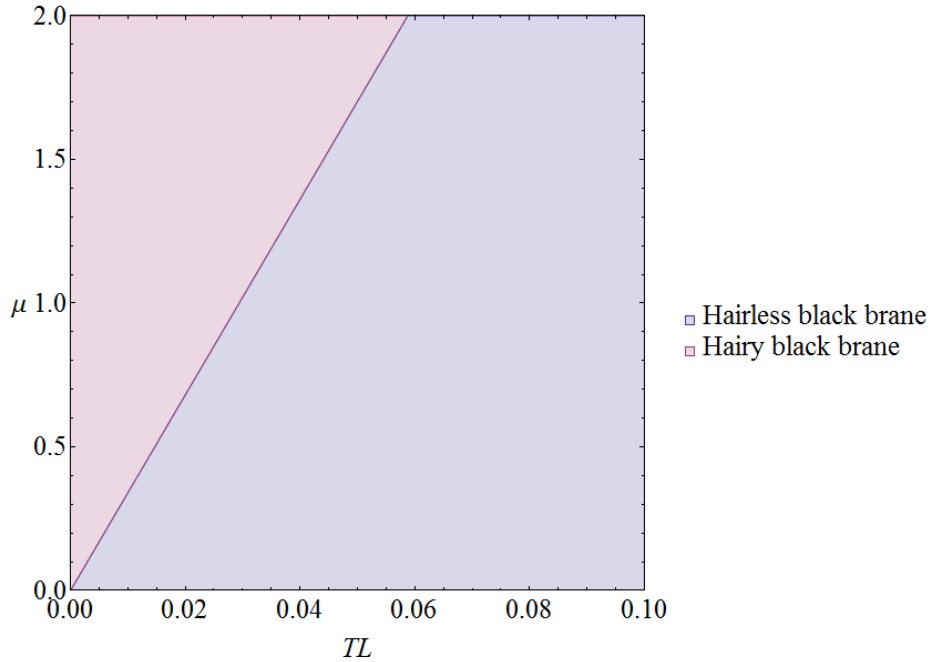


**Figure 5.8:** The phase diagram of the black brane with scalar hair. As expected, the phase is only dependent on the ratio  $T/\mu$ .

Introducing a scalar field in our theory indeed resulted in a nontrivial phase diagram. One can furthermore show that the solution with scalar hair has an event horizon which shrinks to zero as the temperature approaches zero [40]. Therefore, the entropy indeed vanishes as in the zero-temperature limit.

## 5.7 Holographic superconductivity

As mentioned before, the hairy black brane solution from the previous section has a holographic dual description exhibiting properties of superconductivity. Let us first clarify why one can expect this bulk solution to be a good candidate for the description of a holographic superconductor.

- First of all, to describe the phase transition to a superconducting phase, one needs a critical temperature at which a transition can occur. Thus, we need a black hole in our bulk spacetime, which introduces a temperature scale in our dual field theory. As many superconductors are effectively realized in two spatial dimensions, i.e. on  $\mathbb{R}^2$ , we need a  $3 + 1$ -dimensional black hole with planar symmetry.

- Secondly, above the critical temperature, there is a global  $U(1)$  symmetry<sup>15</sup>. A global symmetry in the dual field theory corresponds to a local symmetry in the bulk. Hence we add the gauge field  $A$  to the bulk, corresponding to the gauged  $U(1)$  symmetry.
- Furthermore, the transition to the superconducting phase occurs by breaking the  $U(1)$  symmetry, which is described by an order parameter in the form of a charged operator  $\hat{O}$ . This is where the charged scalar field  $\phi$  in the bulk comes in. By choosing the field to be a scalar, we will describe  $s$ -wave superconductors<sup>16</sup>. The choice of a scalar field is however by no means unique; different choices can lead to the description of unconventional superconductors [41].
- Lastly, above the critical temperature the order parameter has a vacuum expectation value of 0, which becomes nonzero below the critical temperature. Hence, we need to add the complex scalar field to the theory in a way such that at high temperatures, the thermodynamics are dominated by a black hole without scalar hair, whereas at low temperatures the hairy solution dominates. As we have seen, this is precisely what happens in the theory described in the previous section. Notice that the fact that we are working in an asymptotically AdS spacetime also ensures that the scalar hair cannot escape to infinity.

The parameters  $\mu$  and  $Q$  of our bulk theory correspond to the chemical potential and the charge density of the dual field theory. Moreover, the parameters  $\alpha$  and  $\beta$  appearing in the asymptotic expansion Eq. (5.30) of  $\phi$  correspond to vacuum expectation values of a bosonic operator in the dual field theory. Putting  $\alpha$  to zero implies that we are studying the vacuum expectation value of an operator with conformal dimension 2. Using the numerical results from the previous section allows us to plot this vacuum expectation value. This is done in Fig. 5.9. As expected, the order parameter  $\langle O_2 \rangle$  acquires a nonzero value below  $T_c$ . We also see that the phase transition is second order: the order parameter becomes nonzero continuously.

The behavior in Fig. 5.9 is exactly what we need for the transition to the superconducting phase. However, is this enough to conclude that the new phase is actually a superconductor? The answer is no; however, one can perform further analysis to the new phase and see that it shares many interesting features characteristic of superconductors. We will not treat this further analysis here and for more details the reader is referred to [34]. Here we will only list some important characteristics which follow from this analysis.

- By including fluctuations of the vector potential  $A_x$ , one can calculate the conductivity of the new phase by using Ohm's law. The result is that the DC conductivity becomes infinite.
- It also follows that an energy gap forms below the critical temperature.
- Moreover, when adding a magnetic field to the theory one can show that a transition from the superconducting phase back to the nonsuperconducting phase occurs. This characteristic is due to the fact that superconductors expel magnetic fields, which is known as the Meissner effect. The holographic superconductor is of type II, meaning that magnetic fields can

---

<sup>15</sup>Actually, as we are breaking a *global*  $U(1)$  symmetry, the dual theory should be a superfluid rather than a superconductor.

<sup>16</sup>Here the  $s$  denotes the state with azimuthal quantum number  $l = 0$ .



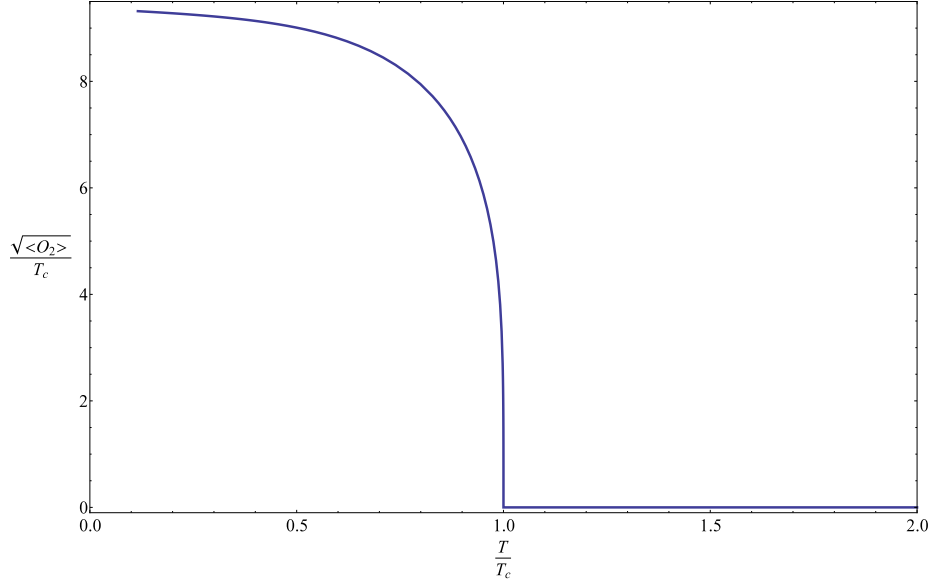


**Figure 5.9:** The vacuum expectation value of the operator  $O_2$  dual to  $\beta$ . The figure is a reproduced version of Fig. 1 in [34], using the same convention  $\langle O_2 \rangle = \sqrt{2}\beta$ . This figure was produced in the grand canonical ensemble, whereas [34] uses the canonical ensemble. However, by scaling with  $T_c$  rather than  $\mu$ , the figures are identical. Clearly  $\langle O_2 \rangle = 0$  for  $T > T_c$ .

penetrate the superconductor when the magnetic field strength is above some critical value  $B_{c1}$ , before the transition to the normal phase occurs above  $B_{c2} > B_{c1}$ .

## 5.8 Summary

In this chapter we have seen that although black brane theories without any hair lead to a trivial phase structure, adding more ingredients to the theory can yield more interesting phase diagrams. Such theories are omnipresent in the AdS/CFT correspondence as they often yield interesting holographic duals. The holographic superconductor is one of the most well-known examples.

Upon comparing with previous chapters, we can also conclude that the topology of the black hole greatly affects the phase structure. Indeed, the rich phase diagram we obtained for spherically symmetric charged black holes completely disappeared when switching to planar symmetry. In the next chapter we will examine more precisely how the relevant thermodynamic quantities depend on the topology of the black hole. In particular, we will study the thermodynamics of hyperbolic black holes.

## Chapter 6

# Topological Black Hole Phase Transitions

In all previous chapters, we have described the most commonly seen black hole solutions. The spherical black hole solutions are the most well-known solutions. A reason for this is that the first black hole solution ever found was the Schwarzschild solution, which is spherically symmetric<sup>1</sup>. Moreover, in asymptotically flat spacetimes, all black holes are spherical. The black brane solutions are well known for their applications in the AdS/CFT correspondence.

However, there are many more solutions to the Einstein equations, including black hole solutions with different topologies than the one we have covered until now. Moreover, the Einstein equations do not exist only in four dimensions. Thus, in this chapter we will study more general black hole solutions, again focusing on charged black holes in asymptotically AdS spacetimes. We will start by being quite general: in the first section we shall give a solution to the Einstein equations, in an arbitrary spacetime dimension  $d = n + 1$  and with a parameter defining the topology. This solution incorporates the solutions from the previous chapters in asymptotically AdS spacetimes. After extracting as much information on the thermodynamics as possible from this general solution in the second section, we will continue by concentrating on the specific case of a four-dimensional hyperbolic black hole in the final section. Therefore, the first two sections will consist of a rather formal analysis with many tedious equations, but the last section will be more down to earth as we provide plots corresponding to one particular case which we did not study in previous chapters.

---

<sup>1</sup>Although nowadays we usually use the term Schwarzschild for any vacuum black hole solution, for example the Schwarzschild black brane.

## 6.1 The topological black hole solution

In this chapter we again look at the classical solutions corresponding to the Einstein-Hilbert-Maxwell action

$$I = \frac{1}{16\pi} \int_M d^{n+1}x \sqrt{g} (R - 2\Lambda - F_{\mu\nu}F^{\mu\nu}), \quad (6.1)$$

where we leave the spacetime dimension  $n + 1$  arbitrary, but  $n > 2$ . We will concentrate on the solutions which satisfy the Ansatz

$$ds^2 = -f(r)dt^2 + \frac{1}{f(r)}dr^2 + \frac{r^2}{L^2}d\Sigma_{k,n-1}^2. \quad (6.2)$$

Here the coordinates  $(t, r) \in \mathbb{R}_+^2$  as usual and the AdS radius is defined by  $L^2 = \frac{n(n-1)}{-2\Lambda}$ . Furthermore, the parameter  $k$  determines the topology of static constant  $r$  slices. For the three interesting cases  $k \in \{-1, 0, 1\}$  the volume element of such a slice is given by [42]

$$\frac{1}{L^{n-1}}d\Sigma_{k,n-1}^2 = \begin{cases} d\Omega_{n-1}^2 = d\theta_1^2 + \sum_{i=2}^{n-1} \left( \left( \prod_{j=1}^{i-1} \sin^2 \theta_j \right) d\theta_i^2 \right) & \text{if } k = 1 \\ \frac{1}{L^{n-1}}d\mathbf{x}_{n-1}^2 = \frac{1}{L^{n-1}}(d\theta_1^2 + \dots + d\theta_{n-1}^2) & \text{if } k = 0 \\ dH_{n-1}^2 = d\theta_1^2 + \sinh^2 \theta_1 \left( d\theta_2^2 + \sum_{i=3}^{n-1} \left( \left( \prod_{j=2}^{i-1} \sin^2 \theta_j \right) d\theta_i^2 \right) \right) & \text{if } k = -1. \end{cases} \quad (6.3)$$

Hence, for  $k = 1$ , static constant  $r$  slices have spherical topology, which is the case treated in chapter 3. The coordinates have range  $\theta_1 \in [0, 2\pi)$ ,  $\theta_{i \neq 1} \in [0, \pi)$ . For  $k = 0$ , the slices have planar topology, as in chapter 5. The coordinates have range  $(\theta_1, \dots, \theta_{n-1}) \in \mathbb{R}^{n-1}$ . For  $k = -1$ , the slices have hyperbolic topology. The coordinates have range  $\theta_1 \in \mathbb{R}_{\geq 0}$ ,  $\theta_{i \neq 1} \in [0, \pi)$ .<sup>2</sup>

Because of the symmetry of our Ansatz Eq. (6.2), thermodynamic quantities will not depend on the above coordinates in Eq. (6.3), but rather contain a constant volume term corresponding to these volume elements. We will denote this volume term by

$$V_{k,n-1} = \int d\Sigma_{k,n-1} = \int \sqrt{h}d\theta_1 \dots d\theta_{n-1} \quad (6.4)$$

with  $h$  the determinant of the induced metric. Clearly,  $V_{k,n-1}$  is infinite for the cases  $k = 0$  and  $k = -1$ .

By solving the Einstein equations and the covariant Maxwell equations, one can find the solution [43]

$$f(r) = k - \frac{2m}{r^{n-2}} + \frac{q^2}{r^{2n-4}} + \frac{r^2}{L^2} \quad (6.5)$$

together with the temporal gauge field [13]

$$A = \left( -\frac{q}{\alpha r^{n-2}} + \Phi \right) dt, \quad (6.6)$$

---

<sup>2</sup>Notice that  $k$  is a parameter for the curvature of the slices. A spherical topology means a positive curvature, a planar topology means zero curvature and a hyperbolic topology means a negative curvature.

where  $\alpha = \sqrt{\frac{2(n-2)}{n-1}}$ . We fix the gauge for black hole solutions as

$$\Phi = \frac{q}{\alpha r_+^{n-2}} \quad (6.7)$$

where  $r_+$  is the outer event horizon. In this way the norm of  $A$  does not diverge at the event horizon.

If  $m \neq 0$  or  $q \neq 0$ , the solution Eq. (6.5) contains a singularity at  $r = 0$ . Hence it must also admit an event horizon behind which the singularity can hide. By graphically investigating the function  $f(r)$  while varying the parameters  $m$  and  $q$ , it follows that there are at most two event horizons. Eliminating the  $m$  using  $f(r_+) = 0$ , i.e.

$$m = \frac{r_+^{n-2}}{2} \left( k - \frac{q^2}{r_+^{2n-4}} + \frac{n}{n-2} \frac{r_+^2}{L^2} \right), \quad (6.8)$$

one can show that the outer event horizon must satisfy

$$k \left( \frac{r_+}{L} \right)^{2n-4} + \frac{n}{n-2} \left( \frac{r_+}{L} \right)^{2n-2} \geq \frac{q^2}{L^{2n-4}} \quad (6.9)$$

in order to prevent a naked singularity. When the equality in Eq. (6.9) holds, the two black hole horizons coincide so that we have an extremal black hole. We denote the corresponding horizon by  $r_e$ <sup>3</sup>.

Taking  $k \in \{0, 1\}$  and  $n = 3$ , we retrieve the results from chapters 3 and 5. The hyperbolic case  $k = -1$  has some new features. First of all, consider the solution given by  $m = q = 0$ . The resulting spacetime is isometric to AdS spacetime [44], as is the case for the spherical and the planar black holes. However, the solution describes only the portion of AdS with  $r > L$ . Indeed, we see that there is a horizon at  $r_0 = L$ . It is not a black hole horizon, since there is no singularity behind it. Rather, it behaves like a Rindler horizon. As such there is also has an associated temperature

$$T_0 = \frac{1}{2\pi L}. \quad (6.10)$$

needed to prevent a conical singularity at  $r_0$ . This has important consequences for the thermodynamics, as we shall discuss shortly.

Furthermore, consider the extremal solution given by the equality in Eq. (6.9). For  $k = -1$ , we see that this equality has a solution  $r_e > 0$  even when  $q = 0$ . To make things even more peculiar, for some  $q$  there are even solutions for which the mass parameter  $m$  is zero or negative. Although  $m$  is not the actual black hole mass, one can show using the ADM formalism that the mass is given by<sup>4</sup>

$$M = \frac{(n-1)V_{k,n-1}}{8\pi} m \quad (6.11)$$

<sup>3</sup>Eq. (6.9) then simply follows from  $f'(r_e) = f''(r_e) = 0$ .

<sup>4</sup>This is shown in Appendix A for the case  $n = 3$ .

which implies that also the real mass can be negative. These negative-mass solutions do neither violate the cosmic censorship, nor do they describe strange or acausal physics. For example, the Penrose diagram of a solution given by  $q = 0, m < 0$  is like that of the spherical charged black hole in AdS [44]. For applications in AdS/CFT, introducing a black hole with negative mass in the bulk corresponds to a positive temperature for the dual field theory, so that a negative mass has no peculiar consequences for the conformal field theory. As the extremal solutions are important for calculating thermodynamic quantities, we will not discard negative-mass solutions.

## 6.2 Topological black hole thermodynamics

In this next section we will calculate thermodynamic quantities corresponding to the solutions from the previous section. As usual, we will focus on the temperature, the heat capacity and the relevant thermodynamic potential of the thermodynamic ensemble. We will try to acquire as much information as possible from the general solution just by analyzing the equations, before we consider a more specific case of the four-dimensional hyperbolic black hole in the next section which we will supplement with plots.

Let us first derive the temperature, for which we switch to the Euclidean section as usual. The derivation of the temperature is identical to the derivation given in Section 4, with  $d\Omega_2^2$  replaced by  $\frac{1}{L^2}d\Sigma_{k,n-1}^2$ . In particular, we find that requiring the absence of conical singularities yields a temperature

$$T = \frac{f'(r_+)}{4\pi} = \frac{n-2}{4\pi r_+} \left( k + \frac{n}{n-2} \frac{r_+^2}{L^2} - \frac{q^2}{r_+^{2n-4}} \right). \quad (6.12)$$

One can show that this indeed goes to zero in the extremal limit  $r_+ \rightarrow r_e$ . Before discussing this result, we will specify the thermodynamic ensemble.

### 6.2.1 The grand canonical ensemble

#### Temperature and heat capacity

Since one fixes the temperature and electrostatic potential in the grand canonical ensemble, we rewrite the temperature in terms of  $\Phi$ , yielding

$$T = \frac{f'(r_+)}{4\pi} = \frac{n-2}{4\pi r_+} \left( k + \frac{n}{n-2} \frac{r_+^2}{L^2} - \Phi^2 \alpha^2 \right). \quad (6.13)$$

Now let us take a look at the first term, which up to a positive constant is  $\frac{k}{r_+}$ . If  $k > 0$ , this term diverges to  $\infty$  as  $r_+ \rightarrow 0$ . This divergence is the origin of the branch of unstable black hole solutions found in chapter 3, where we treated the spherical case  $k = 1$ . For the other cases  $k \in \{0, -1\}$ , this divergence is absent<sup>5</sup> and hence the unstable black hole is not present. This is

<sup>5</sup>As temperatures are positive, the divergence to  $-\infty$  is not physically relevant. Indeed, to reach this divergence one has to violate the extremality condition Eq. (6.9).

indeed what we found in chapter 5 for  $k = 0$ , where for any  $\Phi$  there was one black hole solution for any nonzero temperature. We expect similar behavior for the hyperbolic black holes.

To confirm this expectation, we first notice that if  $k \neq 1$ , then for any value of  $\Phi$  there is a black hole solution with zero temperature. If  $k = 1$  this is only true if  $\Phi^2\alpha^2 > 1$ , in accordance with what we found in chapter 3<sup>6</sup>. Hence, similar to the black brane solutions, there is no minimum temperature for the hyperbolic black hole solutions. Neither do we have a maximum temperature, because the temperature diverges for large  $r_+$ . To check that there is exactly one solution for each temperature, we calculate

$$\left(\frac{\partial T}{\partial r_+}\right)_\Phi = \frac{n-2}{4\pi r_+^2} \left(-k + \Phi^2\alpha^2 + \frac{n}{n-2} \frac{r_+}{L^2}\right). \quad (6.14)$$

If  $k \in \{0, -1\}$ , this is clearly positive for all  $r_+ > 0$ , so that  $T$  is always increasing. Therefore, there can indeed only be one hyperbolic black solution at a given value of  $T$  and  $\Phi$ . This does not hold for  $k = 1$  unless  $\Phi\alpha > 1$ , in accordance with the results from Chapter 3. Furthermore, it follows that the heat capacity

$$C_\Phi = T \left(\frac{\partial S}{\partial T}\right)_\Phi = T \frac{\left(\frac{\partial S}{\partial r_+}\right)_\Phi}{\left(\frac{\partial T}{\partial r_+}\right)_\Phi}, \quad (6.15)$$

is always positive for  $k \in \{0, -1\}$ <sup>7</sup>. Therefore, similar to the black branes but in contrast to the spherical black holes, *the hyperbolic black hole solutions are always thermally stable.*

### The grand potential

To see whether phase transitions occur in the grand canonical ensemble, we should study the grand-potential density difference between phases. Using the Euclideanized on-shell action Eq. (6.1) to calculate the grand potential, one must be careful to subtract the right reference solution. In chapters 3 and 5 we took this to be the thermal AdS solution for  $k \in \{0, 1\}$ . However, as we have seen, in the hyperbolic case the solution with  $m = q = 0$  does not have an arbitrary temperature. Rather, its temperature is set by Eq. (6.10). As a result, we cannot match the asymptotics of this reference solution to the black hole solution. In contrast, given a value of  $\Phi$ , it follows from Eq. (6.9) that the solution with

$$r_e = L \frac{n-2}{n} \sqrt{\Phi^2\alpha^2 + 1} \quad (6.16)$$

is extremal. As extremal solutions can be assigned an arbitrary period of the imaginary time, we can match the extremal background to any black hole solution. Therefore we should use the extremal black hole as the reference solution for  $k = -1$  [46].

---

<sup>6</sup>Note that  $\alpha = 1$  for  $n = 3$ .

<sup>7</sup>Here we use that in higher dimensions, the Hawking entropy is still  $S = A/4$ , where  $A$  is now a codimension 2 volume rather than an area. See for example [45].

Knowing the reference solution to be extremal, we can actually immediately say that hyperbolic black holes are always thermodynamically preferred, even without calculating the grand-potential difference explicitly. Indeed, for the cases  $k \in \{0, -1\}$  we found that for any fixed  $\Phi$ , there is exactly one black hole solution for all temperatures. Since at  $T = 0$  this solution coincides with the reference solution, the grand-potential difference is zero there. Therefore, using the thermodynamic relation

$$\left(\frac{\partial\Omega}{\partial T}\right)_{\Phi} = -S, \quad (6.17)$$

and the positivity of the Hawking entropy, it follows that the grand-potential difference must be negative for any nonzero temperature.<sup>8</sup> Therefore the hyperbolic black holes are always thermodynamically preferred.

For completeness, we show the explicit expression for the grand-potential density difference. By a calculation similar to a more involved version of the one in section 2.4, we obtain that

$$\frac{\Delta\Omega}{V_{k,n-1}} = -\frac{r_+^{n-2}}{16\pi L^{n-1}} \left( \frac{r_+^2}{L^2} + \Phi^2\alpha^2 - k + \frac{2(kr_0^{n-2} - m_0)}{r_+^{n-2}} \right) \quad (6.18)$$

where the parameters  $r_0$  and  $m_0$  correspond to the subtracted reference solution. That is,  $r_0$  and  $m_0$  are zero for  $k \in \{0, 1\}$ , whereas for  $k = -1$  we have that  $r_0 = r_e$  and  $m_0 = m(r_+ = r_e)$ . From the expression it immediately follows that for  $k = 0$ , the black branes are always thermodynamically preferred. For  $k = 1$  this is not always true. These results are in agreement with our findings in chapters 3 and 5. Finally, for  $k = -1$  it is not immediate that  $\Delta\Omega$  is always negative, but this readily follows from the fact that  $\Delta\Omega$  is a decreasing function of  $r_+ > r_e$  and 0 for  $r_+ = r_e$ .

To summarize, for  $k \in \{0, 1\}$  we obtain the same results as in the previous chapters, now generalized to higher dimensions. For  $k = -1$  we find that *no phase transitions occur*. Note that in [43], the solution with  $m = \Phi = 0$  is used as a reference solution. In this case, a phase transition is found. The phase structure is however largely dependent on the choice of background solution. One must therefore carefully decide whether a certain reference solution can be used. Having done so here, we arrive at a different conclusion than [43].

### Other macroscopic quantities

Knowledge of the grand potential enables us to derive all thermodynamic properties of the system. For example, from Eq. (6.18) we can verify that the mass is indeed given by Eq. (6.11). Moreover, we find that the charge is given by<sup>9</sup>

$$Q = -\left(\frac{\partial\Omega}{\partial\Phi}\right)_T = \frac{(n-1)V_{k,n-1}}{8\pi}q \quad (6.19)$$

<sup>8</sup>A similar argument can be used for black branes, if one also uses that  $\frac{\partial\Omega}{\partial\Phi} = -Q < 0$ .

<sup>9</sup>Note that for these calculations one must take into account the dependence of  $r_+$  on  $\Phi$  and  $T$ .

and the entropy by

$$S = - \left( \frac{\partial \Omega}{\partial T} \right)_{\Phi} = \frac{V_{k,n-1} r_+^{n-1}}{4} = \frac{A}{4} \quad (6.20)$$

as expected. By acquiring these quantities in a different way, one could also have calculated the grand potential difference by using the definition  $\Delta \Omega = M - M_0 - TS - \Phi(Q - Q_0)$ .

## 6.2.2 The canonical ensemble

### Temperature and heat capacity

In the canonical ensemble, the temperature is given by Eq.(6.12). As in the grand canonical ensemble, only for  $k = 1$  there is a term which diverges to  $\infty$  as  $r_+ \rightarrow 0$ . Therefore the unstable black hole solution caused by this term is not present for  $k \in \{0, -1\}$ . Similar to the black brane, we expect there to be one branch of black hole solutions for any value of  $q$ .

Given  $k \in \{0, -1\}$  and any  $q$ , we have a zero-temperature solution for  $r_+ = r_e$ , whereas the temperature diverges as  $r_+ \rightarrow \infty$ . The existence for a solution at any temperature then follows from the continuity of the temperature in  $r_+$ . To check for uniqueness, we calculate that

$$\left( \frac{\partial T}{\partial r_+} \right)_Q = \frac{n-2}{4\pi r_+^2} \left( -k + (2n-3) \frac{q^2}{r_+^{2n-4}} + \frac{n}{n-2} \frac{r_+^2}{L^2} \right). \quad (6.21)$$

From this it follows that the temperature is an increasing function of  $r_+$ , such that there is only one branch of black hole solutions. Moreover, this also shows that the heat capacity

$$C_q = T \left( \frac{\partial S}{\partial T} \right)_q = T \frac{\left( \frac{\partial S}{\partial r_+} \right)_q}{\left( \frac{\partial T}{\partial r_+} \right)_q} \quad (6.22)$$

is always positive, such that also *the unique hyperbolic black hole solution is always thermally stable*. The previous results do not hold for  $k = 1$ , as was found in chapter 3.

### The free energy

For all  $k \in \{-1, 0, 1\}$ , the thermal AdS solution is not a solution for arbitrary  $q$ . Therefore, as has been mentioned many times now, one uses the extremal black hole as a reference solution in the canonical ensemble. This implies that the free energy difference at  $T = 0$  vanishes. Moreover, using the thermodynamic relation

$$\left( \frac{\partial F}{\partial T} \right)_q = -S \quad (6.23)$$

and the positivity of the Hawking entropy, we see that for a given  $q$  the free energy of a branch of black hole solution decreases with the temperature. Since there is only one branch in the cases



$k \in \{0, -1\}$ , it follows that the black brane and hyperbolic black hole solutions are always thermodynamically preferred. Hence *no phase transitions can occur*. For the spherical black holes, this does not hold, because there is more than one branch of black hole solutions.

For completeness, we note that the free-energy density difference is given by

$$\frac{\Delta F}{V_{k,n-1}} = -\frac{r_+^{n-2}}{16\pi L^{n-1}} \left( \frac{r_+^2}{L^2} - (2n-3) \frac{q^2}{r_+^{2(n-2)}} - k \right) - M_e. \quad (6.24)$$

Here,  $M_e$  is the mass of the extremal black hole, related to the parameter  $m_e$  by Eq. (6.11). Although the sign of  $\Delta F$  is not immediately evident from this form<sup>10</sup>, one can easily show that  $\Delta F$  decreases as a function of  $r_+$  and is zero for  $r_+ = r_e$ . From this it follows that  $\Delta F < 0$  for all black hole solutions if  $k \in \{0, -1\}$ . For  $k = 1$ , more research is needed, because there are also branches which do not contain the extremal solution.

The above results for  $k \in \{0, 1\}$  are in agreement with the results from chapters 3 and 5. Hence, we see that these results also generalize to higher dimensions. Moreover, we have found that hyperbolic black holes behave somewhat like black branes, as they are always thermally stable and thermodynamically preferred. That is, no phase transitions occur. Next, we will proceed by concentrating on the hyperbolic black hole solution and showing plots similar to the ones in chapters 3 and 5.

## 6.3 The hyperbolic black hole

In this section we will pick  $k = -1$  and  $n = 3$ , i.e. the hyperbolic black hole solution in four spacetime dimensions. The results are actually already in the previous section, but will be made more down to earth here by presenting some plots similar to the ones in the previous chapters. As we have seen, hyperbolic black holes behave very much like black branes in the sense that there is a unique solution for each temperature, which is stable and always thermodynamically favorable over the reference solution.

### 6.3.1 The temperature

The temperature of the hyperbolic black hole in the both the grand canonical and the canonical ensemble is shown in Fig. 6.1. We indeed see that for any  $\Phi$ , there is one solution for each temperature. This is similar to the black brane temperature in Fig. 5.3 and Fig. 5.5. There is one big difference with the case of planar symmetry, namely, even when  $\Phi = 0$  there exists an extremal black hole with a nonzero event horizon. This solution has a negative mass, which we discussed earlier. Notice that this also implies that we cannot choose an arbitrary event horizon for the hyperbolic black hole. Demanding a nonnegative temperature yields that there is a minimal event

<sup>10</sup>For example, the sign of  $M_e$  depends on  $q$ .

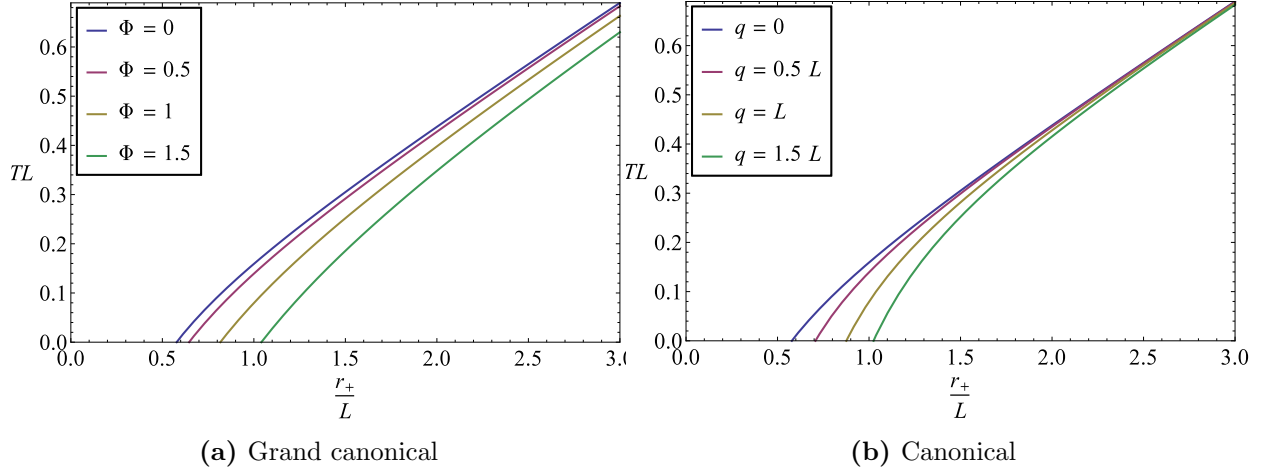


**Figure 6.1:** The temperature of the charged hyperbolic black hole as a function of its event horizon in the grand canonical (a) and the canonical ensemble (b). For each value of the electrostatic potential or the charge, there is exactly one solution for a given temperature. Note that even when  $\Phi = 0$  or  $q = 0$ , there is an extremal solution.

horizon given by

$$r_{+,min} = \frac{L}{\sqrt{3}}, \quad (6.25)$$

which follows from Eq. (6.12).

### 6.3.2 The heat capacity

In Fig. 6.2 we plotted the heat capacity of the hyperbolic black hole. These plots are very similar to the planar counterparts in Fig. 5.4a and Fig. 5.6a. Clearly, it follows from this that the hyperbolic black hole is always thermally stable.

### 6.3.3 The thermodynamic potentials

Fig. 6.3 shows the grand potential of the hyperbolic black hole in the grand canonical ensemble and the Helmholtz free energy energy in the canonical ensemble. Again, the results are very similar to the results for the black branes, i.e. Fig. 5.4b and Fig. 5.6b. It follows from this that the hyperbolic black hole is always the preferred solution. Therefore the phase diagram is trivial, i.e. no phase transitions will occur.

## 6.4 Summary

In this chapter we have shown how the thermodynamics of black holes depends on the topology, thereby focussing on spherical, planar or hyperbolic symmetry. We have shown that for arbitrary

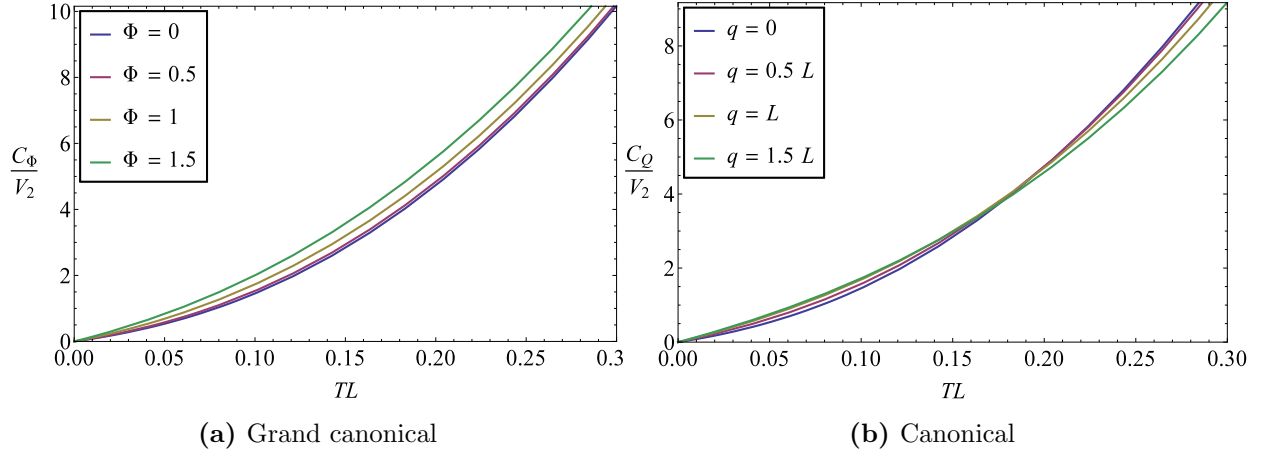


**Figure 6.2:** The heat capacity of the charged hyperbolic black hole as a function of the temperature in the grand canonical (a) and the canonical ensemble (b). For each value of  $\Phi$  or  $q$ , the hyperbolic black hole is thermally stable.

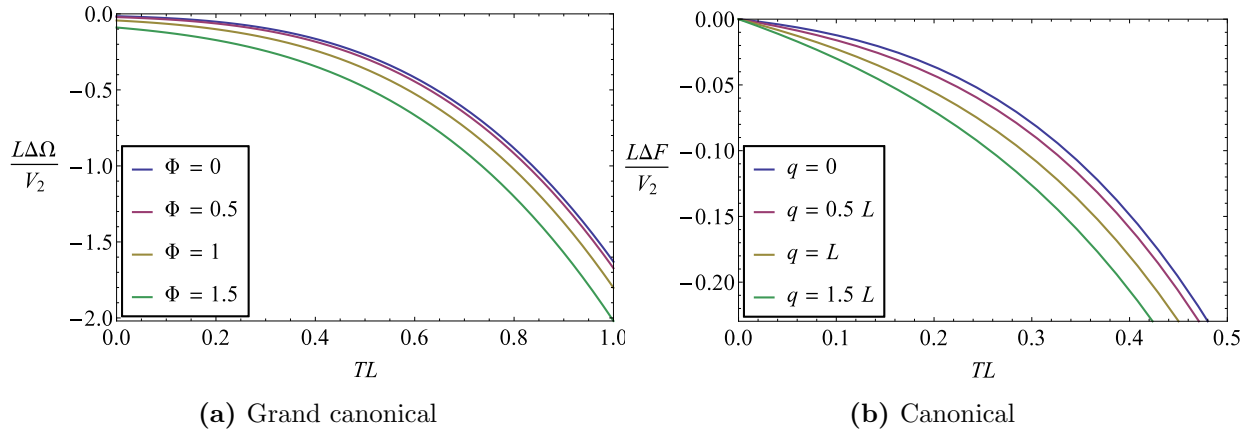


**Figure 6.3:** The grand potential (a) and the Helmholtz free energy (b) of the charged hyperbolic black hole as a function of the temperature in the grand canonical and the canonical ensemble respectively. For each value of  $\Phi$  or  $q$ , the hyperbolic black hole is favored over the background solution.

spacetime dimension  $d \geq 3 + 1$ , only the spherically symmetric black holes allow for multiple solutions for a given temperature and charge or electrostatic potential. Moreover, only the spherically symmetric black holes allowed for unstable black holes. Consequently, the phase diagram for planar and hyperbolic black holes is trivial, whilst phase transition do occur between spherical black holes.

We proceeded by concentrating on the hyperbolic black holes. Although these have some peculiar features, such as allowing for negative masses and uncharged extremal black holes, the thermodynamic characteristics differ very little from the black branes.

In the AdS/CMT correspondence, hyperbolic black holes are probably of little use, since one

does not usually consider a condensed matter system in a hyperbolic spacetime. One application for hyperbolic black holes is the ability to describe field theories for uniformly accelerating observers, i.e. an observer in Rindler spacetime. Although this is probably of little practical use for mankind, studying these theories could give a more complete framework for the AdS/CFT correspondence.

Until now, we have applied the same scheme several times in this thesis: we studied the thermodynamics of particular black hole solutions by looking at their temperature, heat capacity and the relevant thermodynamic potential. In the next chapter, we aim to apply the same scheme to black holes in a supergravity theory. Our ultimate goal is to find a new black hole solution within this theory and subsequently determining its thermodynamics.

# Intermission

Let us take a brief moment to look back on what we have done and see where we are standing now. We started this thesis with the Hawking-Page phase transition. By considering this phase transition in great detail, we acquired a framework of treating black hole thermodynamics that is widely applicable. In the chapters that followed, we started introducing new elements to our theory. Each time, we applied the same framework that we became familiar with when studying the Hawking-Page phase transition.

With the exception of chapter 4, the new elements we added to our theory in each chapter were either adding a new field to the action, or changing the topology of the solution. In chapter 3 we added a gauge field to the theory, while in chapter 5 we added a scalar field to obtain the holographic superconductor. Moreover, in chapter 5 and 6 we discussed what happens when changing the topology of the black hole, in particular considering planar and hyperbolic symmetry. Moreover, in the example of the holographic superconductor we saw an example of how to numerically solve a complex system of differential equations, which arose from the new equations of motion upon adding a scalar field.

Now, the relevance of the previous chapters becomes clear from the second part of the title of this thesis. All the elements described above brought us one step closer to the black hole solution which we aim to describe in the final chapter: namely the magnetic  $\text{AdS}_4$  black brane in  $N = 2$  supergravity. In particular, the previous chapters made us familiar with theories containing gauge fields and scalar fields, solutions enjoying planar symmetry and solving a new system of equations of motion. In the next and final chapter we will apply this knowledge to try and find a *new* black hole solution with these features. If we find such a solution, then we can apply our usual framework of black hole thermodynamics to find out the phase diagram of the solution.

## Chapter 7

# Magnetic Black Holes in $N = 2$ $D = 4$ Supergravity

The framework of studying black hole thermodynamics that we applied in all previous chapter basically consisted of investigating three quantities, namely the temperature, the heat capacity and the relevant thermodynamic potential. Especially since the rise of the AdS/CFT correspondence, this framework has been applied a diverging amount of times to lots of exotic black hole solutions. In this chapter, our goal is to find another such black hole solution. In particular, we will concentrate on AdS<sub>4</sub> black holes solutions  $N = 2$  supergravity.

Naturally, the reason to study supergravity solutions is not because they are more exotic; we are not just randomly trying to increase the complexity of our black holes. In fact, the AdS/CFT correspondence is strictly a correspondence between a conformal field theory in the large- $N$  limit and a supergravity theory that is obtained as the low-energy limit of a full string theory. Hence, when applying holography, we require that our bulk theory has an embedding in string theory. In particular, it must be compatible with a supergravity theory that approximates string theory at low energies. The model describe in this chapter can be embedded directly into an eleven-dimensional supergravity on  $AdS_4 \times S^7$ , thereby describing a string theory compactification on this spacetime[49]. Moreover, also outside the scope of AdS/CFT it is interesting to describe supergravity theories, since they arise from string theories which could lead to an underlying microscopic description of the quantum states of black hole.

Many of the exotic black hole solutions described above become so utterly complicated that one must abandon the search for analytical solutions and use numerical solutions instead. In this chapter we will try and postpone this to the very end. What this means is that we first analyze the most well-known analytical solution within the theory, namely the BPS solution. Afterwards, we study an analytical solution which has been found recently and is a deformation of the BPS solution. We will then try and find a new analytic solution by deforming the known solution even further. In the end we will resort to numerical methods and hope to find a numerical solution to which we can apply our framework of studying thermodynamics.

## 7.1 The supergravity theory

We will consider an  $N = 2$  supergravity theory given by the action Eq. (1.21). Moreover, the cases we consider will have a prepotential given by  $F = -2i\sqrt{X^0(X^1)^2}$ . This implies that  $n_V = 1$ , i.e. there is only one vector supermultiplet and one scalar field  $z$ . Hence, the gauge group is  $U(1)^2$  and there are two FI parameters  $\xi^1$  and  $\xi^0$ . Using the Kähler quantities corresponding to these assumptions [47], the action Eq. (1.21) reduces to

$$S = \int d^4x e \left( \frac{R}{2} - \frac{3}{16z^2} \partial_\mu z \partial^\mu z - \sqrt{z^3} (F^0)^2 - \frac{3}{\sqrt{z}} (F^1)^2 + g^2 \left( \frac{\xi_0 \xi_1}{\sqrt{z}} + \frac{\xi_1^2}{3} \sqrt{z} \right) \right) \quad (7.1)$$

where we defined  $F^2 \equiv F_{\mu\nu} F^{\mu\nu}$ .

### 7.1.1 The equations of motion

From now on we choose to concentrate on magnetic black brane solutions with planar symmetry. This means that for the metric, we take the Ansatz

$$ds^2 = -U^2(r) dt^2 + \frac{dr^2}{U^2(r)} + h^2(r) d\mathbf{x}_2^2, \quad (7.2)$$

following the same notation as [47]<sup>1</sup>. Due to the planar symmetry and the purely magnetic black brane, the field strengths are fixed by

$$F_{xy}^\Lambda = \frac{p^\Lambda}{2} \quad (7.3)$$

while all the other field strength components vanish. Here, the  $p^\Lambda$  are the magnetic charges of the black brane. As the field strengths are fixed, the only equations of motion we have to consider are the Einstein equations and the Klein Gordon equation. One can show that the Einstein equations can be reduced to three independent equations, which can be written as

$$\frac{h''}{h} + \frac{3z'^2}{16z^2} = 0, \quad (7.4)$$

$$-\frac{(U^2 h^2)''}{2h^2} + 2g^2 \left( \frac{\xi_0 \xi_1}{\sqrt{z}} + \frac{1}{3} \xi_1^2 \sqrt{z} \right) = 0, \quad (7.5)$$

$$U^2 h'^2 + h h'' U^2 - h^2 U'^2 - h^2 U U'' + \frac{1}{h^2} \left( (p^0)^2 \sqrt{z^3} + \frac{3(p^1)^2}{\sqrt{z}} \right) = 0. \quad (7.6)$$

Furthermore, the Klein Gordon equation is given by

$$\frac{3}{z^2} \left( 2U U' z' + U^2 \left( \frac{2h'}{h} z' + z'' \right) - U^2 z z'^2 \right) = 4g^2 \left( \frac{\xi_0 \xi_1}{\sqrt{z^3}} - \frac{\xi_1^2}{3\sqrt{z}} \right) + \frac{6}{h^4} \left( (p^0)^2 \sqrt{z} - \frac{(p^1)^2}{\sqrt{z^3}} \right). \quad (7.7)$$

One can however show that if a solution  $(U(r), h(r), z(r))$  satisfies the Einstein equations, then the Klein Gordon equation is satisfied automatically [47]<sup>2</sup>. This does not mean that the Klein Gor-

<sup>1</sup>Except for the fact that we use a  $(-, +, +, +)$  signature.

<sup>2</sup>An exception is the case where  $z$  is constant.

don equation is of no use. For example, we will use it later to find out the asymptotic behavior of  $z$ .

Our goal is now clear: we must solve the system of equations given by Eq. (7.4), Eq. (7.5) and Eq. (7.6). This is a system of coupled non-linear ordinary differential equations which are second order in  $U$  and  $h$  and first order in  $z$ . Naturally, this is no trivial exercise. If we were to solve the system by integrating from the horizon, we would have an at most 8-parameter family of solutions. These parameters the horizon  $r_+$ , the charges  $p^1$  and  $p^0$  and the initial conditions  $f(r_+)$ ,  $f'(r_+)$ ,  $h(r_+)$ ,  $h'(r_+)$ ,  $z(r_+)^3$ , where we defined  $f = U^2$ . Of course, we can reduce this number of parameters. First of all we know that  $f(r_+) = 0$ . We can abuse this fact by dividing Eq. (7.6) by  $h^2$  and subtracting the result from Eq. (7.5). Subsequent evaluation at  $r_+$ , being mindful of the fact that  $U'(r_+)$  diverges, yields the relation

$$\frac{h'(r_+)}{h(r_+)} f'(r_+) = g^2 \left( \frac{\xi_0 \xi_1}{\sqrt{z(r_+)}} + \frac{\xi_1^2}{3} \sqrt{z(r_+)} \right) + \frac{1}{2h(r_+)^4} \left( (p^0)^2 \sqrt{z(r_+)^3} + \frac{3(p^1)^2}{\sqrt{z(r_+)}} \right). \quad (7.8)$$

This gives another constraint on the initial condition, such that in total we are left with six parameters.

We can eliminate two more parameters by using scaling symmetries<sup>4</sup>. In particular, note that the equations of motion, and the metric and the gauge field are invariant under the coordinate transformations

$$r \rightarrow ar, \quad (t, \mathbf{x}) \rightarrow a^{-1}(t, \mathbf{x}), \quad (f, h^2) \rightarrow a^2(f, h^2), \quad p^\Lambda \rightarrow a^2 p^\Lambda \quad (7.9)$$

which can be used to set  $r_+ = 1$  and

$$\mathbf{x} \rightarrow a\mathbf{x}, \quad h \rightarrow a^{-1}h, \quad p^\Lambda \rightarrow a^{-2}p^\Lambda \quad (7.10)$$

which can be used to fix the normalization of  $h$ , i.e.  $h(r_+)$ . In the end, we are left with two initial conditions and two magnetic charges  $p^\Lambda$ . Note that we can put  $g = 1$  by absorbing it in the FI parameters. We usually take  $\xi_\Lambda$  fixed, choosing values which allow for an embedding in a string theory.

## 7.2 The 1/4 BPS solution

Let us first investigate the solutions that are already known. First of all, the magnetic 1/4 BPS black brane was studied in [48]. The term 1/4 BPS denotes that this solution preserves a quarter of the full supersymmetry. The solution is given by

$$U^2(r) = e^{\mathcal{K}(z)} \left( gr + \frac{c}{2gr} \right)^2, \quad (7.11)$$

$$h(r) = e^{-\mathcal{K}(z)/2} r, \quad (7.12)$$

$$z(r) = \frac{X^1(r)}{X^0(r)} \quad (7.13)$$

<sup>3</sup>Notice that we want to use the condition  $f'(r_+)$  rather than  $U'(r_+)$ . The reason is that if  $f'(r_+)$  is nonzero while  $U(r_+) = 0$  then this  $U'(r_+)$  necessarily diverges.

<sup>4</sup>We have also done this in section 5.6 to put the horizon and the AdS radius to 1.



where the  $X^\Lambda = a_\Lambda + \frac{b_\Lambda}{r}$ ,  $\mathcal{K}$  is the Kähler potential given by Eq. (1.14) and the parameters are given by

$$c = -\frac{32}{3}(g\xi_1 b_1)^2, \quad a_0 = -\frac{1}{4\xi_0}, \quad b_0 = -\frac{-\xi_1 b_1}{\xi_0}, \quad a_1 = -\frac{3}{4\xi_1}. \quad (7.14)$$

Additionally, the magnetic charges are fixed to

$$p^0 = \frac{16(g\xi_1 b_1)^2}{3g\xi_0}, \quad p^1 = -\frac{16(g\xi_1 b_1)^2}{3g\xi_1}. \quad (7.15)$$

Notice that the charges satisfy

$$\xi_\Lambda p^\Lambda = 0. \quad (7.16)$$

This quantization condition is similar to a Dirac quantization condition, which states that electric charge  $q$  should be quantized in units inversely proportional to the magnetic charge  $p$ :  $qp \in \mathbb{Z}$ . The condition Eq. (7.16) must hold to make sure that black branes preserve supersymmetry at infinity [49]<sup>5</sup>.

The parameter  $b_1$  is the only parameter which is free. There is however a constraint on  $b_1$ . Notice that the the Kähler potential can be written as

$$e^{\mathcal{K}} = \frac{1}{8\sqrt{(X^1)^3 X^0}} \quad (7.17)$$

so that the metric yields a singularity at a zero of  $X_1$  or  $X_0$ . These values are given by  $r_{s,1} = \frac{4}{3}\xi_1 b_1$  and  $r_{s,0} = -4\xi_1 b_1$  respectively. Since the event horizon is located at  $r_+ = \sqrt{-c/2g^2} = 4\xi_1 |b_1|/\sqrt{3}$ , the requirement  $r_+ > r_s$  enforces  $b_1 > 0$ .

Notice that this solution is extremal<sup>6</sup>: evaluating  $(U^2)'$  at  $r_+ = \sqrt{-c/2g^2}$  clearly yields zero. To describe the thermodynamics, we wish to find a solution which allows a nonzero temperature first. We now proceed by checking if it is possible to find such solutions when the scalar field is constant.

### 7.3 Constant scalars

In [47] a spherically symmetric solution with constant scalars is found. Let us see what happens if we look for such solutions for magnetic black branes. For this we must take into account that the Klein Gordon equation is not automatically met when the Einstein equations are satisfied, in the case of constant scalars.

In fact, let us see what happens with the Klein Gordon equation when  $z$  is constant. One immediately sees that the left-hand side of Eq. (7.7) vanishes in this case. Furthermore, the first term on the right hand side becomes a constant, whereas the second term depends on  $h$ , which

<sup>5</sup>For spherical black holes, this condition becomes  $g\xi_\Lambda p^\Lambda = 1$ .

<sup>6</sup>Actually, BPS solutions imply extremality.

is not constant. Indeed, an asymptotically AdS solution requires that  $h \rightarrow r$  at infinity. As the equation must hold for any  $r$  above the singularity, both terms must vanish independently. The first term then yields

$$z = \frac{3\xi_0}{\xi_1} \quad (7.18)$$

whilst the second term gives

$$z = \frac{p^1}{p^0}. \quad (7.19)$$

Combining these, it would follow that

$$p^1 \xi_1 = 3p^0 \xi_0. \quad (7.20)$$

This would mean that the quantization condition Eq. (7.16) does not hold here. Although we do not require a supersymmetric solution, we do expect that supersymmetry is preserved at infinity [49], so that do we expect Eq. (7.16) to hold. Therefore we reach a contradiction and find no constant scalar solutions.

One can actually show that asymptotically, the condition Eq. (7.18) must always hold. It states that at infinity, the scalar field  $z$  minimizes the potential  $V(z)$  given in Eq. (1.22). This ensures that the theory is asymptotically AdS, with cosmological constant

$$\Lambda = -2g^2 \sqrt{3\xi_0 \xi_1^3}. \quad (7.21)$$

## 7.4 The deformed BPS solution

The next solution we will discuss was found in [47] and is a minimal modification of the BPS solution. It is given by a slightly different form for the function  $U$ , namely

$$U^2(r) = e^{\mathcal{K}(z)} \left( g^2 r^2 + c - \frac{\mu}{r} + \frac{Q^2}{r^2} \right), \quad (7.22)$$

whilst  $z$  and  $h$  are still given by Eq. (7.13) and Eq. (7.12) respectively. The parameter  $c$  also remains as given in Eq. (7.14). The magnetic charges are no longer given by Eq. (7.15), but the condition Eq. (7.16) still holds.

It can easily be verified that these equations indeed satisfy the Einstein equations. In particular, the first two Einstein equations Eq. (7.4) and Eq. (7.5) are automatically satisfied, whereas the third equation Eq. (7.6) is satisfied if the parameters  $\mu$  and  $Q$  are fixed by

$$\mu = -\frac{512}{27} g^2 \xi_1^3 b_1^3 + \frac{2\xi_1 (p^1)^2}{3b_1}, \quad (7.23)$$

$$Q = -\frac{256}{27} g^2 \xi_1^4 b_1^4 + \frac{4}{3} \xi_1^2 (p^1)^2. \quad (7.24)$$

Since the scalar field has the same form, the singularities are still at  $r_{s,1} = \frac{4}{3}\xi_1 b_1$  and  $r_{s,0} = -4\xi_1 b_1$ . The solution now depends on the parameters  $b_1$  and  $p^1$ , fixing  $p^0$  by the quantization condition. It can be shown that for certain values of  $b_1$  and  $p^1$  the singularity is hidden behind an event horizon.

Notice that this solution contains two parameters which can be varied. However, as stated at the end of section 7.1.1, we expect a family of solutions to depend on two initial conditions, beside the magnetic charge. It might therefore seem strange to find that this solution only depends on one parameter beside  $p^1$ . Heuristically, if we expand the scalar field for this solution, we find that

$$z = \frac{3\xi_0}{\xi_1} + \frac{\alpha}{r} + \frac{\beta}{r^2} + \dots \quad (7.25)$$

where  $\alpha = -16\xi_0 b_1$  and  $\beta = \alpha^2 \frac{\xi_1}{4\xi_0}$ . Hence, one can expect that a solution with an arbitrary value of  $\beta$  exists. For example, in [50]  $\beta = \kappa\alpha^2$  is found.  $\kappa$  is then an arbitrary real number, which then depends on the additional parameter rather than being fixed to a specific value. Our next aim is to find such a solution.

In [49], the thermodynamics for the spherically symmetric version of this solution were studied. One could perform a similar analysis for the black branes. However, here we have chosen first to look for a more general solution and subsequently analyze the thermodynamics of that solution.

## 7.5 Searching for a new analytical solution

We will first try to find a new analytical solution. The 1/4 BPS deformation was found by imposing the minimal modification as an Ansatz and subsequently substituting it in the equations of motion. Here, we will try a slightly more systematic approach. We will try and relax some of the features of the BPS deformation and subsequently try to solve the equations of motion using this relaxed deformation. In what follows, we will list the attempts we made to find more general solutions. We will set  $g = 1$  by absorbing it in the FI parameters.

### 7.5.1 Small deformations of the known solution

Firstly, we take the known solution and see what happens if we make minor changes. Inspired by the previous section, we wish to find a solution where the  $\beta$  in Eq. (7.25) is not fixed by  $\alpha$ . Therefore we first see what happens if we take the known solution, but with  $X^1$  arbitrary and  $X^0 = a_0 + \frac{b_0}{r}$ , with  $a_0$  and  $b_0$  arbitrary. In this case, the first Einstein equation Eq. (7.4) returns  $X^{1''}(u) = 0$  where  $u = r^{-1}$ , which implies that  $X^1$  is still a harmonic function. We also find that the other Einstein equations yield the parameters in Eq. (7.14). Hence, simply relaxing the form of  $X^1$  and the parameters of  $X^0$  is not enough to find a new solution.

Notice that the first Einstein equation Eq. (7.4) does not depend the function  $U$ . Therefore,

if we relax both  $X^1$  and  $U$  while keeping the form of  $h$  and  $X^0$ , we will still find that  $X^1$  is harmonic. However, the constants appearing in  $z$  could be different. We will return to this possibility later.

Next, let us see what happens if we relax both  $X^1$  and  $X^0$ , keeping  $h$  and  $U$  the same. In this case, the first Einstein equation Eq. (7.4) reduces to

$$3X^0 X^{1''} + X^1 X^{0''} = 0 \quad (7.26)$$

where the prime again denotes differentiation with respect to  $u = 1/r$ . Again, as the first Einstein equation does not depend on  $U$ , this equation should always hold if  $h$  is of the form  $h = e^{\mathcal{K}/2} r$ . The second Einstein equation Eq. (7.5) becomes

$$-6 - cu^2 + 16\xi_0\xi_1 X^0 X^1 + \frac{16}{3}\xi_1^2 (X^1)^2 = 0, \quad (7.27)$$

which we can use to recast the first Einstein equation as a second-order ordinary differential equation in  $X^0$ . This equation is however a rather tedious one and moreover depends on the parameter  $c$  which we did not set to a specific value. As it turns out, the equation is also numerically difficult to solve.

Notice that writing  $z$  in terms of  $X^1$  and  $X^0$  does not seem to make the equations look more elegant. How can we circumvent these sections? The difficulty lies in the fact that  $h$  and  $U$  seem to depend on the specific choice of  $X^1$  and  $X^0$ , rather than on  $z$  itself, because of the specific form of the Kähler potential Eq. (1.14). On the other hand, the sections do not appear explicitly in the equations of motion. By choosing a different  $X^0$ , we obtain a new Kähler potential which is related to the old one by a so-called Kähler transform<sup>7</sup>, under which the metric for  $g_{z\bar{z}}$  is invariant. Therefore the physics should not depend on the specific choice for  $X^0$  and  $X^1$ , but only on  $z$ . In what follows, we will therefore concentrate on finding a new solution  $z$ .

### 7.5.2 A new solution?

We now wish to work in terms of  $z$  rather than the sections  $X^0$  and  $X^1$ . Therefore, we wish to ignore the Kähler potential altogether. In the known solution, we notice that this Kähler potential appears in both  $h$  and  $U$ , but not in the combination  $F = h^2 U^2$ . Therefore, we can avoid the Kähler potential by letting  $h$  and  $z$  be arbitrary functions and choosing  $F$  as in the old solution. Thus,  $F$  is given by

$$F(r) = r^4 + cr^2 - \mu r + Q \quad (7.28)$$

and we want to solve the Einstein equations for  $h$  and  $z$ .

Notice that upon inserting  $F$ , the second Einstein equation Eq. (7.5) becomes algebraic. This means we can use this equation to express  $h$  in terms of  $z$ . Subsequently, we can insert this

<sup>7</sup>This implies that we transform  $\mathcal{K}$  as  $\mathcal{K} \rightarrow \mathcal{K} + f(z) + f(\bar{z})$ , with  $f$  a holomorphic function.

expression for  $h$  in the first Einstein equation, Eq. (7.4), which results in

$$z'' = \frac{\xi_1(-3\xi_0 + 2\xi_1 z)}{-9\xi_0^2 + \xi_1^2 z^2} z'^2 - \frac{2cu}{6 + cu^2} z' + \frac{24cz(3\xi_0 + \xi_1 z)}{(6 + cu^2)^2(-3\xi_0 + \xi_1 z)}. \quad (7.29)$$

The third Einstein equation Eq. (7.6) looks very tedious. Our hope is that solving the above differential equation will also yield a solution to this tedious equation, such that the third equation will only fix the parameters  $\mu$  and  $Q$ , as was the case for the deformed BPS solution.

Next, we attempt to solve this differential equation. For this we will first pick  $\xi_1 = 3\xi_0$ . This specific choice is such that our theory can be embedded in eleven-dimensional supergravity [49] and will greatly simplify our equations. Notice that demanding that  $z$  is asymptotically in the minimum of the potential, i.e. Eq. (7.18), now gives the boundary condition  $z(0) = 1$ . Moreover, in accordance with the expansion Eq. (7.25) we can write the second boundary condition as  $z'(0) = \alpha$ .

At first sight, it seems this approach might fail. Indeed, Eq. (7.29) is a second-order differential equation and we have two initial conditions  $z(0) = 1$  and  $z'(0) = \alpha$ , so the solution seems fixed, such that  $\beta$  is not arbitrary. Let us continue anyway and see what happens. First of all, we will substitute the expansion Eq. (7.25) in the differential equation and expand the result around the AdS boundary. This results in

$$0 = \frac{4c}{3\alpha} + \frac{\alpha}{2} u^{-1} + \frac{(3\alpha^2 - 2\beta)(3\alpha^2 + 8c)}{12\alpha^2} + \mathcal{O}(u). \quad (7.30)$$

From the first term follows immediately that we must fix the value of  $c$  to  $c = -\frac{3\alpha^2}{8}$ . The second term then automatically vanishes, putting no constraint on  $\beta$ .

Inserting the obtained value for  $c$  and shifting to  $\tilde{z} = z - 1$ , such that  $\tilde{z}(0) = 0$ , Eq. (7.29) becomes

$$\tilde{z}(2 + \tilde{z})\tilde{z}'' - (1 + 2\tilde{z})\tilde{z}'^2 - \frac{2u\alpha^2(2 + \tilde{z})\tilde{z}\tilde{z}'}{16 - u^2\alpha^2} + \frac{64\alpha^2(1 + \tilde{z})(2 + \tilde{z})^2}{(16 - u^2\alpha^2)^2} = 0. \quad (7.31)$$

Now notice that at  $u = 0$ , the coefficient in front of  $\tilde{z}''$  vanishes. This implies that the differential equation is singular at that point! What this means, is that the differential equation can admit singular solutions, i.e. solutions that cannot be uniquely fixed by giving initial conditions. As such, uniqueness of solutions does not hold at the point  $u = 0$ , so there can be different solutions through this point with the same value of  $\alpha$ . This is of course great news, as it implies that  $\beta$  is not fixed by the initial conditions.

Solving the differential equation remains nontrivial. However, numerically we are able to find an analytic (singular) solution<sup>8</sup> which beside  $\alpha$  contains another free parameter, which we can write in terms of  $\alpha$  and  $\beta$  using  $z''(0) = 2\beta$ . After a huge amount of simplifications, we find that

---

<sup>8</sup>We used Maple to find this solution. Actually, Maple returns two solutions containing many hyperbolic and inverse hyperbolic functions, which we glued together to one smooth solution.

the solution can be written as<sup>9</sup>

$$z = \frac{-1 - \frac{\alpha}{2}u + \left(\frac{5}{16}\alpha^2 - \frac{1}{2}\beta\right)u^2}{-1 + \frac{\alpha}{2}u - \left(\frac{3}{16}\alpha^2 - \frac{1}{2}\beta\right)u^2}. \quad (7.32)$$

This seems like a more general version of the known deformed BPS solution. Indeed, this solution is retrieved by setting  $\beta = \frac{3\alpha^2}{4}$ . From the second Einstein equation, we can find the corresponding form of  $h$  and thereby also the corresponding  $U$ . In addition, we find that if we define

$$X^1 = \frac{-\sqrt{-1 - \frac{\alpha}{2}u + \left(\frac{5}{16}\alpha^2 - \frac{1}{2}\beta\right)u^2}}{4\xi_0}, \quad X^0 = \frac{-1 + \frac{\alpha}{2}u - \left(\frac{3}{16}\alpha^2 - \frac{1}{2}\beta\right)u^2}{4\xi_0\sqrt{-1 - \frac{\alpha}{2}u + \left(\frac{5}{16}\alpha^2 - \frac{1}{2}\beta\right)u^2}}, \quad (7.33)$$

so that indeed  $z = X^1/X^0$ , we can write the solution  $h$  as

$$h = \frac{e^{-\mathcal{K}/2}}{u} \quad (7.34)$$

and consequently we can write  $U$  as

$$U^2 = e^{\mathcal{K}} \left( \frac{1}{u^2} + c - \mu u + Qu^2 \right). \quad (7.35)$$

Hence,  $U$  and  $h$  have the same form as for the old solution! Notice that this should imply that Eq. (7.26) should also hold, which we verified.

We have however not yet checked the final Einstein equation, Eq. (7.6). Upon imposing this, we hope to find generalized expressions for Eq. (7.23) and Eq. (7.24). We note that since the Einstein equations should hold for any  $u$ , we can consider an asymptotic expansion of the equation near  $u = 0$  and demand that each coefficient in the series vanishes separately. This indeed gives us the expressions for  $\mu$  and  $Q$  that we hoped for, namely

$$\mu = -\frac{\alpha^3}{4} + \frac{\alpha\beta}{2} - \frac{32(p^1)^2\xi_0^2}{\alpha}, \quad (7.36)$$

$$Q = -\frac{15\alpha^4}{256} + \frac{\alpha^2\beta}{4} - \frac{\beta^2}{4} + 12(p^1)^2\xi_0^2 \quad (7.37)$$

which reduce to Eq. (7.23) and Eq. (7.24) for  $\beta = \frac{3}{4}\alpha^2$ .

Checking the next order of the final Einstein equation yields the constraint

$$\beta = \frac{3}{4}\alpha^2 \quad (7.38)$$

which brings us back to the solution which was already known. What does this result, however unfortunate, teach us? Notice that the only assumption from the old solution we held on to was

---

<sup>9</sup>Notice that here we use  $z$  again instead of  $\tilde{z}$ , so that we can easier compare this to the known solution.

the form of  $U$ , after extracting the factor with the Kähler potential. This form must asymptotically behave like  $r^4$ , using that our solution must be asymptotically AdS as well as the fact that  $\mathcal{K}$  approaches a constant at infinity. Thus, imposing this leading order behavior to be followed by a simple power series with three extra terms is already enough to bring us back to the old solution. We have also verified that this is the case when adding another term to  $F$ . I.e., imposing  $F(r) = r^4 + cr^2 - \mu r + Q + \frac{d}{r}$  yielded again  $\beta = \frac{3}{4}\alpha^2$ , as well as  $d = 0$ .

Our next step will be to have a closer look at the asymptotics of the Einstein equations and see if we can immediately draw conclusions, such as the relation between  $\beta$  and  $\alpha$ .

### 7.5.3 Asymptotic solutions

In this subsection we will use series expansions as an asymptotic solutions and see how much we can determine from looking at the asymptotic equations of motion. We will again use the function  $F = U^2 h^2$  and the coordinate  $u = r^{-1}$ . Requiring our solutions to be asymptotically AdS enforces the leading order terms  $F \propto u^{-4}$ ,  $h^2 \propto u^{-2}$  and  $z \propto 1$ . Moreover, using the scaling symmetries mentioned in 7.1.1, we can fix the coefficients in front of the leading order terms of  $F$  and  $h$ . For convenience, we choose them to be equal to those of the old solution. Hence the asymptotic expansions are given by

$$F = \frac{1}{u^4} + \sum_{i=-2}^n f_i u^i, \quad (7.39)$$

$$h^2 = \frac{1}{2\xi_0^2 u^2} + \sum_{i=-1}^n h_i u^i, \quad (7.40)$$

$$z = 1 + \sum_{i=1}^n z_i u^i. \quad (7.41)$$

$$(7.42)$$

In principle we take  $n = \infty$ , although we can only investigate a finite number of terms numerically. Our next step is to put these expansions in the equations of motion Eq. (7.4), Eq. (7.5) and Eq. (7.6) and derive mutual relations between the coefficients.

Notice that for a given  $n$ , the above expansions contain  $3n + 5$  parameters. Our goal is to reduce this as much as possible. To this end, we start by noticing two simple constraints given by the third equation of motion Eq. (7.6). Expanding this equation of motion, the first terms read

$$-4 \frac{\xi_0^2 h_{-1}}{u} + \left( f_{-2} + 4\xi_0^2 (\xi_0^2 h_{-1}^2 - h_0) \right) + \mathcal{O}(u) \quad (7.43)$$

from which we immediately see that  $h_{-1} = 0$  and  $f_{-2} = 4\xi_0^2 h_0$ . We proceed by investigating Eq. (7.4). The first few terms read

$$\left( 2\xi_0^2 h_0 + \frac{3z_1^2}{16} \right) u^4 + \left( 6\xi_0^2 h_1 - \frac{3}{8}(z_1^3 - 2z_1 z_2) \right) u^5 + \mathcal{O}(u^6). \quad (7.44)$$

From this one can see that the leading order term contains  $h_0$ , the next term contains  $h_1$ , and so on. Additionally, the term containing  $h_i$  as the highest coefficient of  $h$  additionally contains coefficients of  $z$  up to  $z_{i+1}$ . Therefore, this equation of motion can be used to express all coefficients  $h_i$  in terms of coefficients  $z_{j \leq i+1}$ , thereby eliminating all  $h$  coefficients. We are left with  $2n + 2$  coefficients.

A similar approach can be used by considering the expansion of the second equation of motion Eq. (7.5). The expansion looks too tedious to write down here. However, it turns out that the leading order contains  $z_3$  as the highest coefficient of  $z$ , the next order  $z_4$ , and so on. Additionally, in the term containing  $z_i$  as highest  $z$  coefficient, coefficients of  $F$  up to  $f_{i-3}$  appear, except for  $f_0$  and  $f_{-1}$ . We can use this equation of motion to eliminate all  $z$  coefficients, except for  $z_1$  and  $z_2$ . The latter correspond to the coefficients  $\alpha$  and  $\beta$  from our previous analysis.

Using a similar approach, it turns out that we use the last equation of motion to solve for all but one coefficient of  $F$ , for example  $f_1$ . Therefore, in the end, *we can express all coefficients in terms of 4 parameters*, namely  $\alpha$ ,  $\beta$ ,  $f_1$  and  $p^1$ . This is one more than we had expected from the discussion in 7.1.1. One possibility is that we can reduce this number even further by considering the boundary conditions at the event horizon.

Furthermore, we note that if we keep  $n$  finite for the expansion of  $F$ , the constraints  $f_{n+1} = 0$  can be used to eliminate  $f_1$ , whereas the other constraints  $f_{i \geq n+2} = 0$  always seem to lead to  $\beta = \frac{3}{4}\alpha^2$ . We have checked this up to only  $n = 4$ , as the computations seem to become too difficult to handle numerically for higher  $n$ . Moreover, after obtaining  $\beta = \frac{3}{4}\alpha^2$ , expressing all the other coefficients of  $F$  in terms of  $\alpha$  yields  $f_i = 0$  for  $i > 2$ , such that  $F$  reduces to the old solution again. We conclude that for any new solution  $F$  must be an infinite series, probably making it hard to find an analytic solution.

In Fig. 7.1, we plotted the solutions corresponding to the asymptotic expansions up to the first seven leading order terms. In Fig. 7.1a, we chose parameters in accordance with the known solution, whereas in Fig. 7.1b we chose different parameters. The important thing to notice is the location of the event horizon, which corresponds to the zero of the black curves in the plot. Typically, at the singularity,  $z$  vanishes or diverges<sup>10</sup>. Therefore, in both plots any singularity seems to be shielded by an event horizon, therefore representing viable black hole solutions. The question is how much we can rely on these plots, being only asymptotic solutions. However, the fact that Fig. 7.1b does not seem to show a configuration of any kind, might suggest that this does correspond to a new black hole solution. It would be interesting to see if we can numerically find the full solution corresponding to such an asymptotic solution. We intend to do so in the very near future.

As a final remark, we realize now that putting the coefficient  $f_{-3}$  to zero has probably not been a justified decision. Initially, we omitted the coefficient since it is absent from the second factor in  $U^2$  in the known solution, see Eq. (7.22). However, there is no reason that multiplication with an arbitrary  $h$  should still lead to a vanishing coefficient  $f_{-3}$ . Although one might be able to eliminate this coefficient with a coordinate transformation, we must be wary of the fact that if

<sup>10</sup>Indeed, this leads to a diverging Kähler potential.



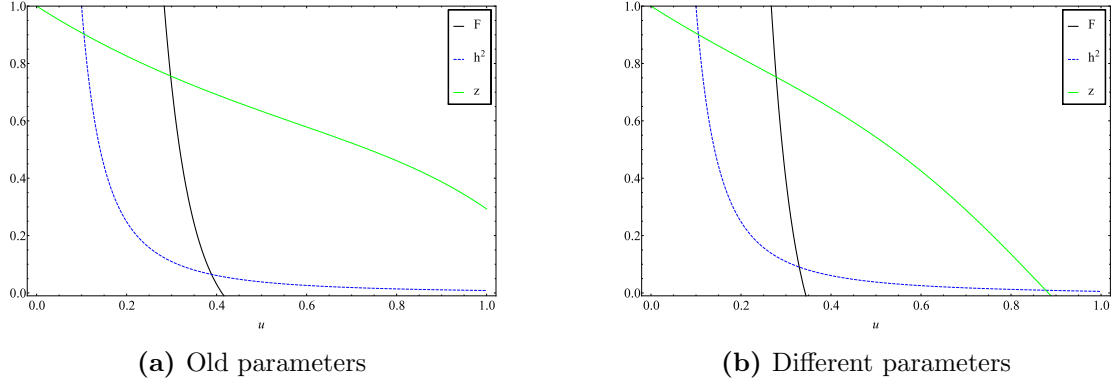


**Figure 7.1:** The solutions for specific values of the coefficients which are in (a) the same as the parameters for the old solution and in (b) different from these parameters. In particular in (a) we chose  $\alpha = -1$ ,  $\beta = \frac{3}{4}$ ,  $f_1 = 0$  and  $p^1 = 1$ , whereas in (b) we picked  $\alpha = -1$ ,  $\beta = \frac{3}{5}$ ,  $f_1 = 1$  and  $p^1 = 1$ . The event horizon is at the root of the black curve. The arbitrary normalization of the fields  $f$  and  $h$  is chosen such that all functions can be seen clearly in the graph.

this is true, then we have been using a very specific set of coordinates. We will continue looking into this in the very near future.

## 7.6 Summary

In this chapter, our goal was to find a generalization of the magnetic  $\text{AdS}_4$  black brane solution that was recently found in [47]. A simple argument counting the degrees of freedom following from the equations of motion suggest that such solutions exist. In particular, inspired by [50], we aimed to find an analytical solution where the coefficient  $\beta$  in the solution Eq. (7.25) is not fixed by  $\alpha$ . However, by trying to relax some of the functions appearing in the known solution, the equations of motion kept leading us back to the old solution.

An asymptotic analysis suggests that solutions will depend on a maximum of four parameters, whereas the known solution has two free parameters. Investigating these asymptotic solutions show that they can exhibit singularities behind an event horizon, making them viable candidates for black hole solutions. It would be interesting to see if we can promote these asymptotic solutions to full solutions. Here the shooting method seems the most obvious approach.

# Conclusion and Outlook

In the first part of this thesis we thoroughly reviewed a variety of black hole phase transitions. The Hawking-Page phase transition served as a starting point. Covering it in detail provided us with the framework that can generally be applied to the study of black hole phase transitions.

Afterwards, we started introducing new elements into the theory and applying the abovementioned framework to the new theory. First of all, we saw how much richer the phase diagram became upon introducing a temporal gauge field in the theory, thereby electrically charging the black hole. We also discussed the influence of the cosmological constant on the phase diagram. The negative value of  $\Lambda$  basically served as a confining potential. As we have seen, it is exactly this confinement which resulted in the rich phase structure we found. This followed from the fact that a Minkowski spacetime confined to a finite spherical cavity yielded comparable phase diagrams.

Furthermore, we mentioned the influence of the black hole topology on the phase diagram. It turned out that black holes with planar or hyperbolic symmetry have a far more trivial phase structure than spherical black holes. This phase structure can be made less trivial by introducing more fields in the theory. As an example, we saw that the addition of a complex scalar field to a charged black brane theory yielded an interesting phase diagram reminding us of a superconductor.

By adding many of the different elements as described above to the theory, we were able to tackle the the  $N = 2$  supergravity theory containing a purely magnetic black brane in four space-time dimensions. We aimed to find a new black brane solution of this kind, generalizing the one that has recently been found. It appeared that finding an analytical generalization of this solution is very difficult and might not even be possible. This also followed from investigating the asymptotics of magnetic black brane solutions. However, these asymptotics also hinted that black solutions exist with different parameters than the ones used in the known solution.

In the immediate future, we will continue investigating these asymptotic solutions, carefully determining exactly how many parameters a more general solution can depend on. At this moment, we expect there exist solutions with at least one more fixed parameter than the known solution. Using the asymptotic solutions, we will try to find full solutions with the shooting method. For this we must also investigate the asymptotic solutions in the near-horizon region, which has not yet been done within this thesis.

It is not yet clear how the new set of parameters will be constrained by demanding the existence of an event horizon that shields the singularity appearing in the solution. This means that if we find a solution, we must make sure that there are no naked singularities. If a new solution is found, it will be interesting to apply the framework used in the first part of this thesis to investigate the phase diagram corresponding to the solution. This can be done by numerically calculating the temperature, which should follow immediately from the metric tensor of the solution, and consequently using this temperature to check the thermal stability. Subsequently, we can find the free energy, for example by integrating the first law, and check which of the new phases will dominate the thermodynamics. In case we do not find a new solution, it would still be interesting to investigate the thermodynamics of the known black brane solution, something which until now has only been done for the spherically symmetric counterpart.

# Appendix A

## Mass in general relativity

In general relativity, mass or energy is a highly nontrivial concept. For example, how do we calculate the mass corresponding to a black hole solution? Let us take the Schwarzschild black hole as an example. This solution describes the gravitational field around a spherically symmetric mass distribution. Usually, one can obtain the mass associated to a field by computing its energy-momentum tensor. However, for the Schwarzschild solution the energy momentum tensor vanishes everywhere! Clearly, the problem is that there is no well-defined notion of a gravitational energy-momentum tensor, because the gravitational field is itself determined by the energy momentum tensor.

Then how do we define the energy of the system? There exist many possibilities for such a definition. Here we consider three of them.

### Komar Mass

The Komar mass [25] is defined for an asymptotically flat spacetime which has a timelike Killing vector field  $K$ , e.g. a stationary spacetime. It uses that fact that there exists a current

$$J^\mu = K_\nu R^{\mu\nu} \tag{A.1}$$

which is conserved, i.e. its covariant divergence  $\nabla_\mu J^\mu$  vanishes. The Komar mass is then defined as the conserved charge associated to this current. Using Stokes' theorem and the Killing equation, this can be written as[1]

$$M_{Komar} = \frac{1}{4\pi} \int_{\partial\Sigma} d^2x \sqrt{\gamma} n_\mu \sigma_\nu \nabla^\mu K^\nu. \tag{A.2}$$

Here,  $\Sigma$  is a spacelike volume with timelike unit normal vector  $n_\mu$ ,  $\sigma_\mu$  is an outward spacelike unit normal vector to  $\partial\Sigma$  and  $\gamma$  is the absolute determinant of the induced metric on  $\partial\Sigma$ . Notice that  $M_{Komar}$  can indeed be written as a surface integral, as stated in section 4.1. The fact that this is a conserved quantity implies that this definition does not depend on the surface  $\partial\Sigma$  chosen, as long as it encloses all of the mass. That is, we cannot deform the surface  $\partial\Sigma$  such that it crosses a region where  $T_{\mu\nu} \neq 0$ .

### ADM Mass

The ADM mass [28], named after R. Arnowitt, S. Deser and C.W. Misner, is derived for asymptotically flat stationary spacetimes. It is derived from the Hamiltonian formulation of general relativity and is given by the charge associated to the time translation invariance of the theory. The ADM mass can be written in terms of the extrinsic curvature  $K$  as

$$M_{ADM} = -\frac{1}{8\pi} \int_{\partial\Sigma} d^2x \sqrt{\gamma} (K - K^0), \quad (\text{A.3})$$

where  $K^0$  is the extrinsic curvature of flat spacetime. The extrinsic curvature can simply be computed with the definition

$$K = h^{\mu\nu} \nabla_\mu n_\nu \quad (\text{A.4})$$

where  $h_{\mu\nu}$  is the induced metric on the volume  $\Sigma$  and  $n_\mu$  is a outward spacelike unit normal vector to  $\partial\Sigma$ .

It can be shown that the Komar mass and the ADM mass coincide for asymptotically flat stationary spacetimes. In this thesis we are however more interested in general relativity with a negative cosmological constant. Although the ADM mass has also been generalized to include such spacetimes, we will discuss another definition designed for asymptotically AdS spacetimes will be discussed next.

### AMD mass

The AMD mass [16] is named after A. Ashtekar, A. Magnon and S. Das<sup>1</sup>. This mass is computed using the Weyl tensor, given by

$$C_{\mu\nu\rho\sigma} = R_{\mu\nu\rho\sigma} + \frac{1}{2} \left( g_{\mu\sigma} R_{\rho\nu} + g_{\nu\rho} R_{\mu\sigma} + \frac{1}{3} R g_{\mu\rho} g_{\nu\sigma} - (\rho \leftrightarrow \sigma) \right), \quad (\text{A.5})$$

and using the conformal metric  $\tilde{g}_{\mu\nu} = \Omega^2 g_{\mu\nu}$  evaluated at the boundary  $r \rightarrow \infty$  of spacetime. Here, the conformal factor  $\Omega$  must vanish at the boundary, whereas its exterior derivative does not vanish. Using this, one defines the quantity

$$\mathcal{E}_{\mu\nu} = L^2 \Omega n^\rho n^\sigma C_{\mu\rho\nu\sigma} \quad (\text{A.6})$$

also defined at the boundary of AdS, with  $n_\mu = \partial_\mu \Omega$ . The AMD mass is then given by

$$M_{AMD} = \frac{L}{8\pi} \oint \mathcal{E}_\mu{}^\nu K^\mu dS_\nu, \quad (\text{A.7})$$

where  $K = \frac{\partial}{\partial t}$  is the timelike Killing vector and the area element is given by  $dS = \sqrt{\gamma} d^2x dt$ .

---

<sup>1</sup>This makes it easy to confuse it with the ADM mass.

To get some more intuition, we now derive the mass given Eq. (6.11) for  $n = 3$  using this formalism. Clearly

$$M_{AMD} = \frac{L}{8\pi} \lim_{r \rightarrow \infty} \int g^{tt} \mathcal{E}_{tt} \frac{r^2}{L^2} d\Sigma_{k,2}. \quad (\text{A.8})$$

We take  $\Omega = L/r$ , such that

$$\begin{aligned} \mathcal{E}_{tt} &= L^2 \frac{L}{r} \frac{L^2}{r^4} (\tilde{g}^{rr})^2 C_{trtr} \\ &= \frac{L}{r} (g^{rr})^2 C_{trtr} \end{aligned} \quad (\text{A.9})$$

where  $g^{rr} = f(r)$  as in Eq. (6.2). By computing the Riemann tensor, it follows that the relevant component of the Weyl tensor is given by

$$C_{trtr} = \frac{1}{r^2} \left( -\frac{2m}{r} + \frac{r^2}{L^2} \right) + \frac{2}{L^2} - \frac{3}{L^2} = -\frac{2m}{r^3}, \quad (\text{A.10})$$

such that upon inserting  $f(r)$  we get

$$\mathcal{E}_{tt} = \frac{-2mL}{r^4} f(r)^2 \quad (\text{A.11})$$

and therefore

$$M_{AMD} = \frac{V_{k,2}}{8\pi L} \lim_{r \rightarrow \infty} \frac{-2mL}{r^2} \left( k - \frac{2m}{r} + \frac{r^2}{L^2} \right) = \frac{mV_{k,2}}{4\pi L^2}, \quad (\text{A.12})$$

which proves Eq. (6.11). Notice that for  $k = 1$ , using  $V_{1,2} = 4\pi L^2$  we indeed get that  $M_{AMD} = m$ . Moreover, notice that the AMD mass vanishes for pure AdS spacetime. It can be shown that the definition of the AMD mass is compatible with the mass obtained from integrating the first law of thermodynamics [48].

## Appendix B

# Calculation of thermodynamic potentials

In this thesis we have given the form of many differences in thermodynamic potentials corresponding to particular black hole solutions. Most of these can be obtained by evaluating the on-shell action, remembering to match the asymptotics (e.g. the temperature or electrostatic potential) of the solutions. However, in doing so we must make sure that the action we use is consistent with the thermodynamic ensemble. This means we must make sure that the boundary conditions corresponding to the variational principle coincide with the boundary conditions imposed by the thermodynamic ensemble.

Consider the Einstein-Hilbert-Maxwell action with a negative cosmological constant Eq. (3.1) as an example. Upon varying  $A_\mu$ , the variation of the action is easily shown to read

$$\delta S = \frac{1}{4\pi} \left( - \int_M d^4x \partial_\mu (\sqrt{g} F^{\mu\nu}) \delta A_\nu + \int_{\partial M} d^3x \sqrt{\gamma} F^{\mu\nu} n_\mu \delta A_\nu \right) \quad (\text{B.1})$$

where  $\gamma$  is the determinant of the induced metric and  $n_\mu$  is the outward spacelike normal vector to  $\partial M$ . From this it follows that if we fix  $A_\mu$  at  $r = \infty$ , the variational principle yields the correct equation of motion. Hence this corresponds to the grand canonical ensemble.

If we wish to calculate the on-shell action in the canonical ensemble, we must add a boundary term to the action given by [13]

$$S_{\partial M} = -\frac{1}{4\pi} \int_{\partial M} d^3x \sqrt{\gamma} F^{\mu\nu} n_\mu \delta A_\nu. \quad (\text{B.2})$$

In this way, one obtains that in the case of a temporal gauge field  $A = A dt$ , the boundary term in the variation of the action  $S + S_{\partial M}$  becomes proportional to  $\delta(F^{\mu 0} n_\mu)$  which using Gauss' vanishes if the charge vanishes.

Note that in principle, there is also a boundary term to make sure that to obtain the Einstein

Equations, we only need to fix the metric  $g_{\mu\nu}$  on the boundary, rather than any derivatives of  $g_{\mu\nu}$ . This is the Gibbons-Hawking-York boundary term. However, when comparing two asymptotically anti-de Sitter spacetimes, the contributions of this boundary term will cancel.

When dealing with additional fields, one also gets additional parameters defining the thermodynamic ensemble, and therefore also additional boundary conditions. For example, when adding the scalar field to the theory as in 5, one must choose whether one fixes the parameter  $\alpha$  or  $\beta$  in Eq. (5.30) on the boundary. This yields an extra boundary action, which is needed to derive Eq. (5.33). In this particular case, because we put  $\alpha = 0$ , the boundary action is the same regardless of which boundary condition is chosen. It is however nonzero and one must actually take it into account to cancel a divergence in the on-shell action. For the exact form of the boundary term, see [38].

After introducing the right boundary terms, the calculation of the action proceeds in a similar way as in chapter 2. Another way of calculating the thermodynamic potential is by using their definitions, for example  $F = M - TS$  for the Helmholtz free energy. This can be shown to give the same result as an on-shell action calculation when using the AMD formalism from appendix A to calculate the mass.



# Bibliography

- [1] S.M. Carroll *Spacetime and Geometry: An Introduction to General Relativity*, ISBN: 0-80530-8732-3, Addison Wesley (2004)
- [2] J. M Maldacena, *The Large N Limit of Superconformal Field Theories and Supergravity*, Adv. Theor. Math. Phys. **2**, 231-252 (1998)
- [3] O. Aharony, S.S. Gubser, J. Maldacena, H. Ooguri and Y. Oz, *Large N Field Theories, String Theory and Gravity*, Phys. Rept. **323**,183-386 (2000)
- [4] J.D. Bekenstein, *Black Holes and Entropy*, Phys. Rev. D **7**, 2333 (1973)
- [5] S.W. Hawking, *Particle creation by black holes*, Comm. Math. Phys. Volume 43, **3**, 199-220 (1975)
- [6] D.Z. Freedman and A. Van Proeyen, *Supergravity*, ISBN: 978-05211-9401-3, Cambridge University Press (2012)
- [7] S.W. Hawking and D.N. Page, *Thermodynamics of Black Holes in Anti-de Sitter Space*, Commun. Math. Phys. **87**, 577-588 (1983)
- [8] D.M. Witt and K. Schleich, *A simple proof of Birkhoff's theorem for cosmological constant*, J.Math.Phys. **51**, 112502 (2010)
- [9] H.T.C. Stoof, K.B. Gubbels and D.B.M. Dickerscheid, *Ultracold Quantum Fields*, ISBN: 13 978-1-4020-8762-2, Springer (2009)
- [10] G.Gibbons and M. Perry, *Black holes and thermal Green functions*, Proc. R. Soc. Lond. A. **358**, 467-494 (1978)
- [11] J.D. Brown, G.L. Comer, E.A. Martinez, J. Melmed, B.F. Whiting and J.W. York Jr., *Thermodynamic ensembles and gravitation*, Class. Quantum Grav. **7**, 1433-1444 (1990)
- [12] C. Rovelli and M. Smerlak, *Thermal time and Tolman-Ehrenfest effect: "temperature as the speed of time"*, Class. Quantum Grav. **28** 075007 (2011)
- [13] A. Chamblin, R. Emparan, C. V. Johnson and R.C. Meyers, *Charged AdS Black Holes and Catastrophic Holography*, Phys.Rev. **D60**, 064018 (1999)
- [14] A. Chamblin, R. Emparan, C. V. Johnson and R.C. Meyers, *Holography, Thermodynamics and Fluctuations of Charged AdS Black Holes*, Phys.Rev. D **60**, 104026 (1999)

- [15] L.F. Abbott and S.Deser, *Stability of Gravity with a Cosmological Constant*, Nucl. Phys. B **195**, 76-96 (1982)
- [16] A. Ashtekar and A. Magnon, *Asymptotically anti-de Sitter space-times*, Class. Quantum Grav. **1**, L39-L44 (1984)
- [17] A. Ashtekar and S. Das, *Asymptotically Anti-de Sitter Space-times: Conserved Quantities*, Class. Quantum Grav. **17**, L17-L30 (2000)
- [18] S.W. Hawking, G.T. Horowitz and S.F. Ross, *Entropy, area, and black hole pairs*, Phys. Rev. D **51**, 4302-4314 (1995)
- [19] S. Das, A. Dasgupta and P. Ramadevi, *Can Extremal Black Holes Have Non-Zero Entropy?* Mod. Phys. Lett. A **12**, 3067-3080, 1996
- [20] S.W. Hawking, *Black Hole Explosions?*, Nature **248**, 30-31 (1974)
- [21] E. Hackmann and C. Lämmerzahl, *Geodesic equation in Schwarzschild-(anti-)de Sitter space-times: Analytical solutions and applications*, Phys. Rev. D **78**, 024035 (2008)
- [22] J.W. York Jr., *Black-hole thermodynamics and the Euclidean Einstein action*, Phys. Rev. D **33**, 2092-2099 (1986)
- [23] H.W. Braden, J.D. Brown, B.F. Whiting and J.W. York Jr., *Charged black hole in a grand canonical ensemble*, Phys. Rev. D **42**, 3376-3385 (1990)
- [24] J.L. Jaramillo and E. Gourgoulhon, *Mass and Angular Momentum in General Relativity*, Fundam. Theor. Phys. **162**, 87-124 (2011)
- [25] A. Komar, *Positive-Definite Energy Density and Global Consequences for General Relativity*, Phys. Rev. **129**, 1873-1876 (1963)
- [26] J.D. Brown and J.W. York Jr., *Quasilocal energy and conserved charges derived from the gravitational action*, Phys. Rev. D **47**, 1407-1419 (1993)
- [27] J.D. Brown, J. Creighton and R.B. Mann, *Temperature, Energy, and Heat Capacity of Asymptotically Anti-de Sitter Black Holes*, Phys. Rev. D **50**, 6394-6403 (1994)
- [28] R. Arnowitt, S. Deser and C.W. Misner, *Dynamical Structure and Definition of Energy in General Relativity*, Phys. Rev. **116**, 1322-1330 (1959)
- [29] S. Hollands, A. Ishibashi and D. Marolf, *Comparison between various notions of conserved charges in asymptotically AdS-spacetimes*, Class. Quant. Grav. **22**, 2881-2920 (2005)
- [30] V.V.P. Frolov and I.D. Novikov, *Black hole physics: basic concepts and new developments*, Vol 96, ISBN: 0-7923-5145-2, Springer (1998)
- [31] C.S. Peça and J.P.S. Lemos, *Thermodynamics of Reissner-Nordström-anti-de Sitter black holes in the grand canonical ensemble*, Phys.Rev. D **59**, 124007 (1999)
- [32] A.P. Lundgren, *Charged Black Hole in a Canonical Ensemble*, Phys.Rev. D **77**, 044014 (2006)

- [33] S. Carlip and S. Vaidya, *Phase Transitions and Critical Behavior for Charged Black Holes*, Class. Quant. Grav. **20**, 3827-3838 (2003)
- [34] S.A. Hartnoll, C.P. Herzog and G.T. Horowitz, *Building an AdS/CFT superconductor*, Phys. Rev. Lett. **101**, 031601 (2008)
- [35] S. W. Hawking and G. F. R. Ellis, *The Large Scale Structure of Space-Time*, ISBN: 0 521 09906-4, Cambridge University Press (1973)
- [36] S.A. Hartnoll, *Lectures on holographic methods for condensed matter physics*, Class. Quant. Grav. **26**, 224002 (2009)
- [37] B. Sprenger, *On Lifshitz rotating black holes and black branes in light of AdS/CFT*, Master thesis, [http://web.science.uu.nl/ITF/Teaching/2011/2012/Brigitte Sprenger.pdf](http://web.science.uu.nl/ITF/Teaching/2011/2012/Brigitte%20Sprenger.pdf) (2012)
- [38] S.A. Hartnoll, C.P. Herzog and G.T. Horowitz, *Holographic Superconductors*, JHEP **0812**, 015 (2008)
- [39] G.T. Horowitz, *Introduction to Holographic Superconductors*, Lecture Notes in Physics **828**, 313-347, 2011
- [40] G.T. Horowitz and M.M. Roberts, *Zero Temperature Limit of Holographic Superconductors*, JHEP **0911**, 015 (2009)
- [41] S.S. Gubser and S.S. Pufu, *The gravity dual of a p-wave superconductor*, JHEP **0811**, 033 (2008)
- [42] C. Charmousis, *From Gravity to Thermal Gauge Theories: The AdS/CFT Correspondence, chapter 1: Introduction to Anti de Sitter Black Holes*, ISBN: 978-3-642-04863-0, Springer (2011)
- [43] R.-G. Cai and A. Wang, *Thermodynamics and stability of hyperbolic charged black holes*, Phys. Rev. D **70**, 064013 (2004)
- [44] R. Emparan, *AdS/CFT Duals of Topological Black Holes and the Entropy of Zero-Energy States*, JHEP **9906**, 036 (1999)
- [45] R.C. Meyers, J. Rao and S. Sugishita, *Holographic holes in higher dimensions*, JHEP **1406**, 044 (2014)
- [46] D. Birmingham, *Topological Black Holes in Anti-de Sitter Space*, Class. Quant. Grav. **16**, 1197-1205 (1999)
- [47] C. Toldo and S. Vandoren, *Static nonextremal AdS<sub>4</sub> black hole solutions*, arXiv: 1207.3014 (2012)
- [48] K.Hristov, C. Toldo and S. Vandoren, *Black branes in AdS: BPS bounds and asymptotic charges*, Contribution to the proceedings of the "XVII European Workshop on String Theory 2011" (2011)
- [49] K.Hristov, C. Toldo and S. Vandoren, *Phase transitions of magnetic AdS<sub>4</sub> black holes with scalar hair*, Phys. Rev. D **88**, 026019 (2013)

- [50] T. Hertog and G.T. Horowitz, *Designer Gravity and Field Theory Effective Potentials*, Phys. Rev. Lett. **94**, 22130 (2005)

# Acknowledgements

I would like to thank my supervisor Stefan, my physics partner in crime Erik, Jorgo and Alex for being *μαλακας*, Rob for keeping my math skills sharp, Stef for being Stef, Henk for giving me a PhD position, my parents for paying my tuition fees, all the PhDs and professors who lent me their coffee cards and all the people I am forgetting now.